MULTISCALE NUMERICAL METHODS FOR SOME TYPES OF PARABOLIC EQUATIONS

A Dissertation

by

DUKJIN NAM

Submitted to the Office of Graduate Studies of
Texas A&M University
in partial fulfillment of the requirements for the degree of

DOCTOR OF PHILOSOPHY

August 2008

Major Subject: Mathematics

MULTISCALE NUMERICAL METHODS FOR SOME TYPES OF PARABOLIC EQUATIONS

A Dissertation

by

DUKJIN NAM

Submitted to the Office of Graduate Studies of
Texas A&M University
in partial fulfillment of the requirements for the degree of

DOCTOR OF PHILOSOPHY

Approved by:

Chair of Committee,	Yalchin Efendiev
Committee Members,	Raytcho Lazarov
	Bojan Popov
	Akhil Datta-Gupta
Head of Department,	Albert Boggess

August 2008

Major Subject: Mathematics

ABSTRACT

Multiscale Numerical Methods for Some Types of Parabolic Equations. (August 2008)

Dukjin Nam, B.S., Hanyang University, Korea;

M.S., Hanyang University, Korea

Chair of Advisory Committee: Dr. Yalchin Efendiev

In this dissertation we study multiscale numerical methods for nonlinear parabolic equations, turbulent diffusion problems, and high contrast parabolic equations. We focus on designing and analysis of multiscale methods which can capture the effects of the small scale locally.

At first, we study numerical homogenization of nonlinear parabolic equations in periodic cases. We examine the convergence of the numerical homogenization procedure formulated within the framework of the multiscale finite element method. The goal of the second problem is to develop efficient multiscale numerical techniques for solving turbulent diffusion equations governed by celluar flows. The solution near the separatrices can be approximated by the solution of a system of one dimensional heat equations on the graph. We study numerical implementation for this asymptotic approach, and spectral methods and finite difference scheme on exponential grids are used in solving coupled heat equations. The third problem we study is linear parabolic equations in strongly channelized media. We concentrate on showing that the solution depends on the steady state solution smoothly.

As for the first problem, we obtain quantitive estimates for the convergence of the correctors and some parts of truncation error. These explicit estimates show us the sources of the resonance errors. We perform numerical implementations for the asymptotic approach in the second problem. We find that finite difference scheme

with exponential grids are easy to implement and give us more accurate solutions while spectral methods have difficulties finding the constant states without major reformulation. Under some assumption, we justify rigorously the formal asymptotic expansion using a special coordinate system and asymptotic analysis with respect to high contrast for the third problem.

To my parents and my brother

ACKNOWLEDGMENTS

First of all, I am deeply grateful to Dr. Yalchin Efendiev, my advisor, for his kind support and patience for my slow improvement in doing research throughout my Ph.D. study. Without his guidance, this dissertation would not have been completed.

In addition, I would like to extend my thanks to Dr. Raytcho Lazarov, Dr. Bojan Popov, and Dr. Akhil Datta-Gupta for their helpful comments and reviews with regard to my research results. I also would like to thank Dr. Alexei Novikov and Dr. Yuliya Gorb for their valuable suggestions and help.

I thank Dr. Jay Walton, Dr. Thomas Schlumprecht, Dr. Paulo Lima-Filho, Ms. Stewart Monique, and all other staff in the Department of Mathematics for their appropriate support.

I thank all of you who gave me love and help during my study at Texas A&M University. It is a blessing for me to have met many of kind and friendly colleagues, especially Taejong Kim, Woonjung Choi, Beng Seong Ong, Kyounghwa Bae, Youngdeug Ko, and Seungil Kim.

I wish to express my hearty appreciation to all of my family, parents and brother, for their encouragement and support throughout the years and I could not have done it without their support.

Finally, I thank God for everything.

TABLE OF CONTENTS

CHAPTER Page

I INTRODUCTION 1

II NUMERICAL HOMOGENIZATION FOR NONLINEAR PARABOLIC EQUATIONS IN PERIODIC MEDIA 6

A. Preliminaries 6
B. Analysis of Numerical Homogenization 10
C. Correctors 37
D. Numerical examples 52

III MULTISCALE NUMERICAL METHODS FOR TURBULENT DIFFUSION EQUATIONS 67

A. Background 67
1. Asymptotic computational approach 70
a. The two-cell case 70
b. The general multiple-cell case 73
B. Numerical discretization techniques 75
1. Spectral methods 75
a. Preliminaries 75
b. Galerkin approach 77
c. Collocation approach 88
2. Finite difference methods on exponential grids 90
a. Two-cell problem 91
b. Four-cell problem 93
C. Numerical results 95
1. Truncated region approach 99

IV EFFICIENT MULTISCALE METHODS FOR PARABOLIC EQUATIONS IN HIGH CONTRAST MEDIA 104

V CONCLUSIONS AND FUTURE WORK 111

REFERENCES 113

VITA 117

LIST OF TABLES

TABLE Page

I L_2-norms of the difference between initial and solution functions on $[4M\pi, 4(M+1)\pi](M = 0, 1, 2, 3)$ 95

LIST OF FIGURES

FIGURE Page

1 The strip S_ε in $K \times [t_n, t_{n+1}]$ 20

2 Left figure: The solutions are averaged over the spatial domain. Middle figure: The solutions are averaged in horizontal direction. Right figure: The solutions are averaged in vertical direction. $\delta = 0.1, \varepsilon = 0.1$ 55

3 Left figure: The solutions are averaged over the spatial domain. Middle figure: The solutions are averaged in horizontal direction. Right figure: The solutions are averaged in vertical direction. $\delta = 0.2, \varepsilon = 0.1$ 56

4 Left figure: The solutions are averaged over the spatial domain. Middle figure: The solutions are averaged in horizontal direction. Right figure: The solutions are averaged in vertical direction. $\delta = 0.3, \varepsilon = 0.1$ 56

5 Left figure: The solutions are averaged over the spatial domain. Middle figure: The solutions are averaged in horizontal direction. Right figure: The solutions are averaged in vertical direction. $\delta = 0.4, \varepsilon = 0.1$ 57

6 Left figure: The solutions are averaged over the spatial domain. Middle figure: The solutions are averaged in horizontal direction. Right figure: The solutions are averaged in vertical direction. $\delta = 0.5, \varepsilon = 0.1$ 57

7 Left figure: The solutions are averaged over the spatial domain. Middle figure: The solutions are averaged in horizontal direction. Right figure: The solutions are averaged in vertical direction. $\delta = 0.4, \varepsilon = 0.05$ 58

FIGURE Page

8 Left figure: The solutions are averaged over the spatial domain. Middle figure: The solutions are averaged in horizontal direction. Right figure: The solutions are averaged in vertical direction. $\delta = 0.5, \varepsilon = 0.05$ 58

9 Left figure: The solutions are averaged over the spatial domain. Right figure: The solutions are averaged in vertical direction. $k(x/\varepsilon, t/\varepsilon^2) = (\sin(2\pi x/\varepsilon) + \cos(2\pi y/\varepsilon) + 3)$. 60

10 Left figure: The solutions are averaged over the spatial domain. Right figure: The solutions are averaged in vertical direction. $k(x/\varepsilon, t/\varepsilon^2) = (\sin(2\pi x/\varepsilon) + \cos(2\pi y/\varepsilon) + 3)(\cos(t/\varepsilon^2) + 2)$. 60

11 Left figure: The solutions are averaged over the spatial domain. Right figure: The solutions are averaged in vertical direction. $k(x/\varepsilon, t/\varepsilon^2) = \frac{2+1.8\sin(2\pi x/\varepsilon)}{2+1.8\cos(2\pi y/\varepsilon)} + \frac{2+1.8\sin(2\pi y/\varepsilon)}{2+1.8\cos(2\pi x/\varepsilon)} + 3$. 61

12 Left figure: The solutions are averaged over the spatial domain. Right figure: The solutions are averaged in vertical direction. $k(x/\varepsilon, t/\varepsilon^2) = \left(\frac{2+1.8\sin(2\pi x/\varepsilon)}{2+1.8\cos(2\pi y/\varepsilon)} + \frac{2+1.8\sin(2\pi y/\varepsilon)}{2+1.8\cos(2\pi x/\varepsilon)} + 3\right)(\cos(t/\varepsilon^2) + 2)$. . . 61

13 Left figure: The solutions are averaged over the spatial domain. Right figure: The solutions are averaged in vertical direction. $k(x/\varepsilon, t/\varepsilon^2) = (\sin(2\pi x/\varepsilon) + \cos(2\pi y/\varepsilon) + 3)$. 62

14 Left figure: The solutions are averaged over the spatial domain. Right figure: The solutions are averaged in vertical direction. $k(x/\varepsilon, t/\varepsilon^2) = (\sin(2\pi x/\varepsilon) + \cos(2\pi y/\varepsilon) + 3)(\cos(t/\varepsilon^2) + 2)$. 63

15 Left figure: The solutions are averaged over the spatial domain. Right figure: The solutions are averaged in vertical direction. $k(x/\varepsilon, t/\varepsilon^2) = \frac{2+1.8\sin(2\pi x/\varepsilon)}{2+1.8\cos(2\pi y/\varepsilon)} + \frac{2+1.8\sin(2\pi y/\varepsilon)}{2+1.8\cos(2\pi x/\varepsilon)} + 3$. 64

16 Left figure: The solutions are averaged over the spatial domain. Right figure: The solutions are averaged in vertical direction. $k(x/\varepsilon, t/\varepsilon^2) = \left(\frac{2+1.8\sin(2\pi x/\varepsilon)}{2+1.8\cos(2\pi y/\varepsilon)} + \frac{2+1.8\sin(2\pi y/\varepsilon)}{2+1.8\cos(2\pi x/\varepsilon)} + 3\right)(\cos(t/\varepsilon^2) + 2)$. . . 64

17 Left figure: The solutions are averaged over the whole spatial domain. Right figure: The solutions are averaged in vertical direction. $i = 1$ and $k(x/\varepsilon, t/\varepsilon^2) = (\sin(2\pi x/\varepsilon) + \cos(2\pi y/\varepsilon) + 3)$. . . . 65

FIGURE Page

18 Left figure: The solutions are averaged over the whole spatial domain. Right figure: The solutions are averaged in vertical direction. $i = 1$ and $k(x/\varepsilon, t/\varepsilon^2) = (\sin(2\pi x/\varepsilon) + \cos(2\pi y/\varepsilon) + 3)(\cos(t/\varepsilon^2) + 2)$. 65

19 Left figure: The solutions are averaged over the whole spatial domain. Right figure: The solutions are averaged in vertical direction. $i = 1$ and $k(x/\varepsilon, t/\varepsilon^2) = \left(\frac{2+1.8\sin(2\pi x/\varepsilon)}{2+1.8\cos(2\pi y/\varepsilon)} + \frac{2+1.8\sin(2\pi y/\varepsilon)}{2+1.8\cos(2\pi x/\varepsilon)} + 3\right)$. 66

20 Left figure: The solutions are averaged over the whole spatial domain. Right figure: The solutions are averaged in vertical direction. $i = 1$ and $k(\frac{x}{\varepsilon}, \frac{t}{\varepsilon^2}) = \left(\frac{2+1.8\sin(2\pi x/\varepsilon)}{2+1.8\cos(2\pi y/\varepsilon)} + \frac{2+1.8\sin(2\pi y/\varepsilon)}{2+1.8\cos(2\pi x/\varepsilon)} + 3\right)\left(\cos(\frac{t}{\varepsilon^2}) + 2\right)$. 66

21 The two-cell problem (left) and the gluing procedure (right). 71

22 The velocity profile (left) and the graph (right). 73

23 Two cell problem 83

24 Four cell problem 93

25 Initial and final curve of periodic solution 96

26 Periodic solution (left) and reconstructed solution of Childress problem (right). 96

27 Periodic solution at $t = 0$ and $t = 3\pi$ (left), and comparison of initial curve from periodic solution with curve from 2-D solution (right). 97

28 Periodic solution u_1 (left) and u_2 (right) at $\theta = 0$ 98

29 Comparison of periodic solution with curve from 2-D solution 98

30 Periodic solution at $t = 0$ and $t = 3\pi$ (left) and at $t = \pi$ (right) . . . 100

31 Periodic solution (negative and positive parts) at $t = \frac{3\pi}{2}$ 100

32 Periodic solution (negative and positive parts) at $t = \frac{5\pi}{2}$ 101

33 Periodic solution (negative and positive parts) at $t = 3\pi$ 101

34 Comparison of periodic solution with curve from exact solution . . . 102

FIGURE Page

35 Approximating solutions by truncated region approach 103

36 High flow channel 104

CHAPTER I

INTRODUCTION

The purpose of this dissertation is to develop and analyze effective numerical methods for multiscale phenomena. Multiscale phenomena are involved in many areas, such as oil and gas science, earth atmospheric science, plasma physics, and so on. Analyzing and simulating directly these phenomena are difficult due to a wide range of scales. Consequently, in order to perform analysis and simulation of multiscale problems, it has been considered to use several ways, such as singular perturbation methods [6], asymptotic analysis, upscaling, homogenization, and so on. In this dissertation, we focus on developing numerical methods for the problems for porous media simulations and turbulent flows.

Our methods use homogenization theory to study the limiting behavior of the solution, as the microscopic scale tends to zero. The main idea of numerical homogenization procedure is to obtain the numerical solution of large-scale equations including all the effects of small-scales. Recently, many numerical methods for multiscale problems have been proposed. Among them, a multiscale finite element method (MsFEM) for elliptic linear problems was designed and discussed in [20]. This method is one of the numerical homogenization techniques for the problems which contain different spatial scales. It can capture the small-scale details by using oscillatory basis functions in finite element methods. This idea is naturally generalized to nonlinear elliptic problems, which is proposed and analyzed in [9], by considering a multiscale map from the coarse grid space to the underlying fine grid space, instead of using

---

The dissertation model is SIAM Journal on Numerical Analysis.

the basis functions. It was also applied to a numerical homogenization of nonlinear random parabolic equations [10]. Furthermore, numerical correctors for the solution of nonlinear parabolic equations is constructed to obtain the convergence of gradients of the solutions for our numerical scheme.

In Chapter II we analyze MsFEM for nonlinear parabolic problems, which is proposed in [9], in periodic media. Previous studies were limited to more general cases and did not study scale interaction issues properly. In particular, explicit convergence rates cannot be obtained for problems investigated in [10] due to general assumptions on heterogeneities. We study the convergence of the numerical homogenization procedure formulated within the framework of the generalized MsFEM for periodic case. The numerical homogenization procedure proposed in the paper uses general finite element procedure and solves local problems that are further coupled in the global formulation. We introduce appropriate correctors to approximate the solutions of the local problems, where the correctors are periodic with respect to the fast variables in both space and time. The local problems are formulated in the domains with selected boundary and initial conditions. Our goal is to obtain the convergence for the numerical homogenization procedure. Estimates for corrector approximations are obtained in the Section B of Chapter II. Once the estimate for the correctors is found, we can obtain the convergence of the numerical homogenization using comparison principles, compactness arguments, and discrete Meyers type estimates. Note that the numerical homogenization provides us an approximation for the homogenized solution. To obtain the approximation for oscillatory solutions, we introduce numerical correctors and find the estimates for the convergence of the numerical correctors.

In Chapter III, we focus on developing efficient numerical techniques for turbulent diffusion transport governed by cellular flows. According to the asymptotic approach proposed in [24], the full problem can be reduced to a system of one-dimensional

heat equations on a graph. We present the procedure to solve the system of heat equations using spectral methods and finite difference methods on exponential grids. Spectral methods, e.g. Galerkin approach [18, 28] and collocation method, are considered to solve heat equations over the unbounded domain. The Laguerre and Hermite functions are used as basis elements in the Galerkin formulation. Although the computational cost of the spectral approach is usually inexpensive and the method is fast, it is not easy for the spectral method to find the constant to which the solution of the heat equation tends at infinity. We note that these basis elements vanish at infinity and the Hermite functions are either even or odd. Hence we consider the decomposition of the approximate solution by even, odd, and constant parts. Since the basis functions are defined over the whole domain, it is difficult to manipulate processes effectively, described in Section A.1 of Chapter III, restricting the function over the positive and negative half intervals, and gluing the restrictions together. Instead, finite difference methods on the non-uniform exponential grids are performed to capture the constant for each cell. Note that the Laguerre and Hermite functions decay exponentially and it is expensive to use finite difference scheme with uniform grid points over unbounded domain. Thus, we develop the finite difference approach on the exponential grids.

We perform numerical tests to find the periodic solution of the reduced asymptotic problem for each case where a square domain has some number of cells. Our numerical results demonstrate that our approach is working efficiently. Furthermore, in one-cell case, we reconstruct the solution from the periodic solution over the some restricted region of the domain of the full problem.

In Chapter IV, MsFEM was modified to solve some types of problems, for instance, for the porous media with channelized features. A modified MsFEM was proposed and discussed in [8] to use a global information in constructing finite el-

ement basis functions. In Chapter IV we perform some analysis for the modified MsFEM for a simple and symmetric channelized porous media.

We consider 2-D model of the advection-diffusion problem in a bounded domain. We are interested in the case of small molecular diffusivity ε or large Péclet number Pe, where the Péclet number indicates the relative dominance between advection and diffusion in the transport. This problem was studied in previous findings, such as numerical studies [1, 3, 5, 17, 25] (where not all of them were focused on large Péclet number) and physical and the mathematical studies [27, 30]. In particular, [15, 16, 19, 23] are concerned with finding bounds on the effective diffusivity. In [27, 30] the boundary layer analysis is used to show the asymptotic behavior of the effective diffusivity in the special case of symmetric square cells. The effective diffusivity was studied in [15, 16] by using variational principles instead. It has been recently generalized to non-square periodic cells using probabilistic techniques [23]. Uniform estimate for the effective diffusivity in the periodic cellular flows was derived and justified in [19].

It was proved in [24] that there is a constant outside the boundary layer of the width $O(\sqrt{\varepsilon})$, to which the solution converges in each cell without any assumptions on periodicity or symmetry for the flow. Next, the "water-pipe network" problem was introduced reducing the domain on the boundary layer and shown that the solution of the "water-pipe network" problem can approximate the solution of the original problem in L_∞ norm. Finally, the reduced Childress asymptotic approach finding a periodic solution of a system of one-dimensional heat equations on a graph was studied, which was based on the analysis of [4]. Furthermore, the asymptotic approach for the one-cell case over a square domain was discussed in [15]. It was proven in [24] that the solution of asymptotic approach approximates the solution of the "water-pipe" model.

This dissertation is organized as follows. In Chapter II, we collect some basic facts that are used later. We introduce MsFEM for nonlinear parabolic problems and perform the analysis of MsFEM. Next, we present the corrector results. In Chapter III, we introduce the main problem related to advection-diffusion equation in the limit of small diffusion coefficients. The summary for an asymptotic computational approach proposed in [24] is presented as background. We discuss the numerical discretization techniques to implement the asymptotic approach. Some numerical results are presented. In Chapter IV, the analysis of the modified MsFEM for high contrast parabolic equations is presented. Finally, Chapter V provides some conclusions and future works.

CHAPTER II

NUMERICAL HOMOGENIZATION FOR NONLINEAR PARABOLIC EQUATIONS IN PERIODIC MEDIA

A. Preliminaries

In this chapter, we introduce the numerical homogenization method for the nonlinear parabolic equations in a periodic media and study the convergence of the method.

Let $\Omega \in \mathbb{R}^d$ be a bounded open set with Lipschitz boundary [2]. Let Y be a unit square $(0,1)^d$ in $\mathbb{R}^d$ and T_0 be a unit interval $(0,1)$ in $\mathbb{R}$. We consider the nonlinear parabolic problem

$$D_t u_\varepsilon - \operatorname{div}(a(x/\varepsilon^\beta, t/\varepsilon^\alpha, u_\varepsilon, D_x u_\varepsilon)) + a_0(x/\varepsilon^\beta, t/\varepsilon^\alpha, u_\varepsilon, Du_\varepsilon) = f \quad \text{in } \Omega \times (0,T), \tag{2.1}$$

with initial condition $u_\varepsilon(x,0) = u_0(x)$ and boundary condition $u_\varepsilon(x,t) = 0$ on $\partial\Omega \times (0,T)$. Here $T > 0$ is a fixed time, and ε^α and ε^β represent the microscopic scales in time and length, respectively. The operators a and a_0 are satisfying the following assumptions from $\mathbb{R}^d \times \mathbb{R} \times \mathbb{R} \times \mathbb{R}^d$ into $\mathbb{R}^d$ and $\mathbb{R}$, respectively.

A1 *polynomial growth*:

$$|a(\cdot,\cdot,\eta,\xi)| + |a_0(\cdot,\cdot,\eta,\xi)| \le C(1 + |\eta|^{p-1} + |\xi|^{p-1}),$$

for every $\eta \in \mathbb{R}$ and $\xi \in \mathbb{R}^d$.

A2 *monotonicity with respect to* ξ:

$$(a(\cdot,\cdot,\eta,\xi_1) - a(\cdot,\cdot,\eta,\xi_2),\ \xi_1 - \xi_2) \ge C|\xi_1 - \xi_2|^p,$$

for every $\eta \in \mathbb{R}$ and $\xi_1, \xi_2 \in \mathbb{R}^d$.

A3 *coercivity*:

$$(a(\cdot,\cdot,\eta,\xi),\ \xi) + a_0(\cdot,\cdot,\eta,\xi)\ \eta \geq C|\xi|^p,$$

for every $\eta \in \mathbb{R}$ and $\xi \in \mathbb{R}^d$.

A4 *continuity*: For each $\eta_1, \eta_2 \in \mathbb{R}$ and $\xi_1, \xi_2 \in \mathbb{R}^d$

$$\begin{aligned}|a(\cdot,\eta_1,\xi_1) - a(\cdot,\eta_2,\xi_2)| \leq\ & C(1+|\eta_i|^{p-1}+|\xi_i|^{p-1})\nu(|\eta_1-\eta_2|)\\ & +C(1+|\eta_i|^{p-1-s}+|\xi_i|^{p-1-s})|\xi_1-\xi_2|^s,\end{aligned}$$

where $\nu(r)$ is the modulus of continuity, i.e., $\nu(r)$ is continuous in $\mathbb{R}_+$ such that

$$\nu(0)=0,\ \nu(r)=1 \text{ for } r\geq 1,\ \text{and } \nu(r)>0 \text{ for } r>0,$$

and $s>0$ with $s \in (0, \min\{p-1, 1\}]$.

From now on, we assume that

$$p = q = 2, \tag{2.2}$$

and $s = p-1$ throughout this chapter. In addition, let C, $\tilde{C}$ and c denote generic positive constants in this dissertation and q be the number defined by $1/p + 1/q = 1$.

Now, we consider the homogenization of the problem (2.1) with $u_\varepsilon \in L^p(0,T;$ $W_0^{1,p}(\Omega))$. It was proved in [26] that u_ε converges to u weakly in $L^p(0,T;W_0^{1,p}(\Omega))$ as $\varepsilon \to 0$, where u is the solution of the homogenized problem

$$D_t u - \operatorname{div}(a^*(u, D_x u)) + a_0^*(u, D_x u) = f, \tag{2.3}$$

where $a^*(\eta,\xi)$ and $a_0^*(\eta,\xi)$ are defined by

$$a^*(\eta,\xi) = \int_{T_0}\int_Y a(y,\tau,\eta,\xi + D_y N_{\eta,\xi}(y))dyd\tau,$$

$$a_0^*(\eta,\xi) = \int_{T_0}\int_Y a_0(y,\tau,\eta,\xi + D_y N_{\eta,\xi}(y))dyd\tau,$$

and $N_{\eta,\xi}$ is a solution of the following problem for each case:

- self-similar case ($\alpha = 2\beta$),

$$D_t N_{\eta,\xi} - \mathrm{div}(a(y,\tau,\eta,\xi + D_y N_{\eta,\xi}(y))) = 0, \tag{2.4}$$

- non-self-similar case ($\alpha < 2\beta$),

$$-\mathrm{div}(a(y,\tau,\eta,\xi + D_y N_{\eta,\xi}(y))) = 0, \tag{2.5}$$

- non-self-similar case ($\alpha > 2\beta$),

$$-\mathrm{div}(\bar{a}(y,\eta,\xi + D_y N_{\eta,\xi}(y))) = 0. \tag{2.6}$$

  Here

$$\bar{a}(y,\eta,\xi + D_y N_{\eta,\xi}) = \langle a(y,\tau,\eta,\xi + D_y N_{\eta,\xi})\rangle_\tau,$$

  where $\langle u\rangle_\tau$ is the mean value of u with respect to the variable τ

Note that the calculation of a^* and a_0^* depends on the ratio between α and β [10].

We consider a standard finite element space S^h over a coarse triangulation $\mathcal{T}_h$ of Ω. In other words, S^h consists of the functions $v_h \in C^0(\bar{\Omega})$ such that the restriction of v_h is linear over each triangle $K \in \mathcal{T}_h$ with $diam(K) \leq Ch_x$. Furthermore, we consider $0 = t_0 < t_1 < \cdots < t_{m-1} < t_m = T$ and $\max(t_i - t_{i-1}) = h_t$.

For fixed $p \in [2,\infty)$ we let $\mathcal{U}_K = L^p(t_n, t_{n+1}; L^p(K))$ and $\mathcal{V}_K = L^p(t_n, t_{n+1}; W^{1,p}(K))$ with its dual space denoted by $\mathcal{V}_K^*$. The duality pairing on $\mathcal{V}_K^* \times \mathcal{V}_K$ is defined by

$$\langle f, g\rangle = \int_{t_n}^{t_{n+1}} f(t)\, g(t)\, dt.$$

The numerical homogenization procedure is defined in the following way. For

each linear function v_0 over K, we solve

$$\begin{aligned} D_t v_\varepsilon - \mathrm{div}(a(x/\varepsilon^\beta, t/\varepsilon^\alpha, \eta^{v_0}, D_x v_\varepsilon)) &= 0 \text{ in } K \times (t_n, t_{n+1}), \\ v_\varepsilon(t = t_n) &= v_0, \\ v_\varepsilon \,|_{\partial K} &= v_0, \end{aligned}$$

where $\eta^{v_0} = \frac{1}{|K|}\int_K v_0 dx$. Then the homogenized flux can be approximated by

$$a^*(\eta^{v_0}, D_x v_0) = \int_{t_n}^{t_{n+1}} \int_K a(x/\varepsilon^\beta, t/\varepsilon^\alpha, \eta^{v_0}, D_x v_\varepsilon) dx\, dt,$$

$$a_0^*(\eta^{v_0}, D_x v_0) = \int_{t_n}^{t_{n+1}} \int_K a_0(x/\varepsilon^\beta, t/\varepsilon^\alpha, \eta^{v_0}, D_x v_\varepsilon) dx\, dt.$$

We introduce the multiscale mapping $E^{MsFEM} : S^h \to V_\varepsilon^h$ in the following way. For each $v_h \in S^h$ there exists $v_\varepsilon^h = E^{MsFEM} v_h$ satisfying

$$\begin{aligned} D_t v_\varepsilon^h - \mathrm{div}(a(x/\varepsilon^\beta, t/\varepsilon^\alpha, \eta^{v_h}, D_x v_\varepsilon^h)) &= 0 \text{ in } K \times [t_n, t_{n+1}], \\ v_\varepsilon^h(t = t_n) &= v_h, \\ v_\varepsilon^h \,|_{\partial K} &= v_h, \end{aligned} \tag{2.7}$$

where $\eta^{v_h} = \frac{1}{|K|}\int_K v_h dx$ for each K. Then multiscale finite element formulation for the nonlinear parabolic equations is defined in the following way. Find $u_h(t) \in S^h$ such that

$$\int_{t_n}^{t_{n+1}} \int_\Omega D_t u_h w_h dx\, dt + \langle A_\varepsilon^h u_h, w_h \rangle = \int_{t_n}^{t_{n+1}} \int_\Omega f w_h dx\, dt \quad \text{for all } w_h \in S^h, \tag{2.8}$$

where $\langle A_\varepsilon^h u_h, w_h \rangle$ is defined by

$$\begin{aligned} \langle A_\varepsilon^h u_h, w_h \rangle = \sum_{K \in \mathcal{T}_h} \int_{t_n}^{t_{n+1}} \int_K & (a(x/\varepsilon^\beta, t/\varepsilon^\alpha, \eta^{u_h}, D_x u_\varepsilon^h), D_x w_h) \\ & + a_0(x/\varepsilon^\beta, t/\varepsilon^\alpha, \eta^{u_h}, D_x u_\varepsilon^h) w_h) dx\, dt, \end{aligned} \tag{2.9}$$

where u_ε^h is the solution of (2.7) and $\eta^{u_h} = \frac{1}{|K|}\int_K u_h dx$. Here, the methods for time-discretization of the formulation (2.8) can be performed in either implicit or explicit

way. For example, an implicit scheme can be implemented in the following way.

$$\int_\Omega (u_h(t_{n+1}) - u_h(t_n))w_h dx + \langle A_\varepsilon^h u_h, w_h\rangle = \int_{t_n}^{t_{n+1}}\int_\Omega f w_h dx\, dt \quad \text{for all } w_h \in S^h,$$

where $u_h(x, t_{n+1})$ is taken in computing the term $\langle A_\varepsilon^h u_h, w_h\rangle$ (see (2.9)). On the other hand, for the explicit scheme $u_h(x, t_n)$ is taken within $\langle A_\varepsilon^h u_h, w_h\rangle$ (see (2.9)).

B. Analysis of Numerical Homogenization

In this section, we investigate the convergence of the numerical homogenization procedure formulated in the previous section. We begin with an estimate for the solution of the local problem (2.7), and obtain a comparison principle. After introducing a numerical corrector, we present estimates for the corrector. We derive the corrector estimate which is one of our main results. We use the idea described in [22] (see page 28 in [22]) to prove this corrector result. By the comparison principle, the corrector result can be estimated by addition of two terms, and we obtain explicit estimates for those two terms. Next, we show the coercivity property for A_ε^h, and finally the convergence property will be given by showing that truncation error tends to zero. We note that this is the first work where resonance errors are quantitatively estimated. Now we start to examine the convergence.

Lemma II.1. *Let v_ε be the solution of*

$$\begin{aligned} D_t v_\varepsilon - \operatorname{div}(a(x/\varepsilon^\beta, t/\varepsilon^\alpha, \eta, D_x v_\varepsilon)) &= 0 \text{ in } K \times (t_n, t_{n+1}), \\ v_\varepsilon(t = t_n) &= v_0, \\ v_\varepsilon\,|_{\partial K} &= v_0, \end{aligned}$$

where v_0 is a linear function and η is a constant in K. Then we have the following

estimate

$$\int_{t_n}^{t_{n+1}}\int_K |D_x v_\varepsilon|^p dx\, dt \le C(|K\times[t_n,t_{n+1}]| + \|\eta\|_{\mathcal{U}_K}^p + \|D_x v_0\|_{\mathcal{U}_K}^p),$$

where C is independent of ε, h, and v_0.

Proof. Let $\tilde{v}_\varepsilon = v_\varepsilon - v_0$. Then

$$D_t(\tilde{v}_\varepsilon + v_0) - \mathrm{div}(a(x/\varepsilon^\beta, t/\varepsilon^\alpha, \eta, D_x(\tilde{v}_\varepsilon + v_0))) = 0.$$

Since v_0 is linear over K, $D_x v_0 = \xi$, where ξ is a constant. And hence $D_t v_0 = 0$. Thus we get

$$\begin{aligned} D_t\tilde{v}_\varepsilon - \mathrm{div}(a(x/\varepsilon^\beta, t/\varepsilon^\alpha, \eta, D_x\tilde{v}_\varepsilon + \xi)) &= 0 \text{ in } K\times(t_n,t_{n+1}),\\ \tilde{v}_\varepsilon(t=t_n) &= 0,\\ \tilde{v}_\varepsilon\,|_{\partial K} &= 0. \end{aligned}$$

Multiplying by $\tilde{v}_\varepsilon$ on both sides and integrating by parts give us

$$\int_{t_n}^{t_{n+1}}\int_K D_t\tilde{v}_\varepsilon\cdot\tilde{v}_\varepsilon dx\, dt + \int_{t_n}^{t_{n+1}}\int_K (a(x/\varepsilon^\beta, t/\varepsilon^\alpha, \eta, D_x\tilde{v}_\varepsilon+\xi), D_x\tilde{v}_\varepsilon) dx\, dt = 0.$$

Adding the same number on both sides makes

$$\begin{aligned} &\frac{1}{2}\int_{t_n}^{t_{n+1}}\int_K D_t\,|\tilde{v}_\varepsilon|^2\, dx\, dt + \int_{t_n}^{t_{n+1}}\int_K (a(x/\varepsilon^\beta, t/\varepsilon^\alpha, \eta, D_x\tilde{v}_\varepsilon+\xi), \xi + D_x\tilde{v}_\varepsilon) dx\, dt\\ &= \int_{t_n}^{t_{n+1}}\int_K (a(x/\varepsilon^\beta, t/\varepsilon^\alpha, \eta, D_x\tilde{v}_\varepsilon+\xi), \xi) dx\, dt. \end{aligned}$$

From the initial condition for $\tilde{v}_\varepsilon$ at $t = t_n$ we obtain

$$\begin{aligned} &\frac{1}{2}\int_K |\tilde{v}_\varepsilon(x,t_{n+1})|^2 dx + \int_{t_n}^{t_{n+1}}\int_K (a(x/\varepsilon^\beta, t/\varepsilon^\alpha, \eta, D_x\tilde{v}_\varepsilon+\xi), \xi + D_x\tilde{v}_\varepsilon) dx\, dt\\ &= \int_{t_n}^{t_{n+1}}\int_K (a(x/\varepsilon^\beta, t/\varepsilon^\alpha, \eta, D_x\tilde{v}_\varepsilon+\xi), \xi) dx\, dt. \end{aligned}$$

Since the first term is non-negative and by the coercivity assumption **A3** of the

operator, we have the following inequality:

$$\begin{aligned}\int_{t_n}^{t_{n+1}}\int_K |D_x v_\varepsilon|^p dx\,dt &\le C\int_{t_n}^{t_{n+1}}\int_K (a(x/\varepsilon^\beta, t/\varepsilon^\alpha, \eta, D_x\tilde{v}_\varepsilon+\xi),\xi)dx\,dt\\ &= C\int_{t_n}^{t_{n+1}}\int_K (a(x/\varepsilon^\beta, t/\varepsilon^\alpha, \eta, D_x\tilde{v}_\varepsilon+\xi), D_x v_0)dx\,dt\\ &\le C\int_{t_n}^{t_{n+1}}\int_K (1+|\eta|^{p-1}+|D_x v_\varepsilon|^{p-1})|D_x v_0|dx\,dt.\end{aligned}$$

By Hölder's inequality with $r_1 = q$ and $r_2 = p$ and Young's inequality appropriately, the latter is at most

$$\begin{aligned}& C\left\{\int_{t_n}^{t_{n+1}}\int_K (1+|\eta|^p+|D_x v_\varepsilon|^p)dx\,dt\right\}^{1/q}\left\{\int_{t_n}^{t_{n+1}}\int_K |D_x v_0|^p dx\,dt\right\}^{1/p}\\ \le\ & \frac{C\delta}{q}\int_{t_n}^{t_{n+1}}\int_K (1+|\eta|^p+|D_x v_\varepsilon|^p)dx\,dt + \frac{C}{p\delta}\|D_x v_0\|^p_{\mathcal{U}_K}.\end{aligned}$$

When we choose $\delta > 0$ so that $\frac{C\delta}{q} \le \frac{1}{2}$, then the term including $|D_x v_\varepsilon|^p$ can be moved to the left hand side. So we get the following estimate:

$$\int_{t_n}^{t_{n+1}}\int_K |D_x v_\varepsilon|^p dx\,dt \le C(|K\times[t_n,t_{n+1}]| + \|\eta\|^p_{\mathcal{U}_K} + \|D_x v_0\|^p_{\mathcal{U}_K}).$$

□

Further we have the following comparison principle which will be used in proving our main results.

Lemma II.2. *Suppose v_ε is the solution of the equation*

$$\begin{aligned} D_t v_\varepsilon - \operatorname{div}(a(x/\varepsilon^\beta, t/\varepsilon^\alpha, \eta, D_x v_\varepsilon)) &= 0,\\ v_\varepsilon(t=t_n) &= v_0,\\ v_\varepsilon|_{\partial K} &= v_0(t),\end{aligned} \tag{2.10}$$

and w_ε is a solution of the equation

$$\begin{aligned} D_t w_\varepsilon - \mathrm{div}(a(x/\varepsilon^\beta, t/\varepsilon^\alpha, \eta, D_x w_\varepsilon)) &= 0, \\ w_\varepsilon(t = t_n) &= w_0, \\ w_\varepsilon|_{\partial K} &= w_0(t). \end{aligned} \tag{2.11}$$

Then we obtain

$$\|w_\varepsilon - v_\varepsilon\|^p_{\mathcal{V}_K} \le C\|D_x(w_0 - v_0)\|^{p/(p-s)}_{\mathcal{U}_K} + \tilde{C}\|D_t(v_0 - w_0)\|^q_{\mathcal{V}_K^*}, \tag{2.12}$$

where $C = C_0(|K \times [t_n, t_{n+1}]| + \|\eta\|^p_{\mathcal{U}_K} + \|D_x v_0\|^p_{\mathcal{U}_K} + \|D_x w_0\|^p_{\mathcal{U}_K})^{(p-s-1)/(p-s)}$.

Proof. Let $\tilde{v}_\varepsilon = v_\varepsilon - v_0$ and $\tilde{w}_\varepsilon = w_\varepsilon - w_0$. Then the equations (2.10) and (2.11) become

$$\begin{aligned} D_t \tilde{v}_\varepsilon - \mathrm{div}(a(x/\varepsilon^\beta, t/\varepsilon^\alpha, \eta, D_x \tilde{v}_\varepsilon + D_x v_0)) &= -D_t v_0, \\ \tilde{v}_\varepsilon &= 0 \text{ at } t = t_n, \\ \tilde{v}_\varepsilon|_{\partial K} &= 0, \end{aligned}$$

$$\begin{aligned} D_t \tilde{w}_\varepsilon - \mathrm{div}(a(x/\varepsilon^\beta, t/\varepsilon^\alpha, \eta, D_x \tilde{w}_\varepsilon + D_x w_0)) &= -D_t w_0, \\ \tilde{w}_\varepsilon &= 0 \text{ at } t = t_n, \\ \tilde{w}_\varepsilon|_{\partial K} &= 0, \end{aligned}$$

where $-D_t v_0$ and $-D_t w_0$ belong to $\mathcal{V}_K^*$. Since the norm $\|D_x u\|_{L^p}$ is equivalent to

$\|u\|_{W^{1,p}}$ on $W_0^{1,p}$ and by monotonicity, we have

$$
\begin{aligned}
&\|w_\varepsilon - v_\varepsilon\|^p_{\mathcal{V}_K} \\
&\le C\int_{t_n}^{t_{n+1}}\int_K (a(x/\varepsilon^\beta, t/\varepsilon^\alpha, \eta, D_x w_\varepsilon) - a(x/\varepsilon^\beta, t/\varepsilon^\alpha, \eta, D_x v_\varepsilon), D_x w_\varepsilon - D_x v_\varepsilon)dx\,dt \\
&= C\int_{t_n}^{t_{n+1}}\int_K (a(x/\varepsilon^\beta, t/\varepsilon^\alpha, \eta, D_x w_\varepsilon) - a(x/\varepsilon^\beta, t/\varepsilon^\alpha, \eta, D_x v_\varepsilon), \\
&\qquad\qquad D_x\tilde{w}_\varepsilon + D_x w_0 - D_x\tilde{v}_\varepsilon - D_x v_0)dx\,dt \\
&= C\int_{t_n}^{t_{n+1}}\int_K (a(x/\varepsilon^\beta, t/\varepsilon^\alpha, \eta, D_x w_\varepsilon) - a(x/\varepsilon^\beta, t/\varepsilon^\alpha, \eta, D_x v_\varepsilon), D_x\tilde{w}_\varepsilon - D_x\tilde{v}_\varepsilon)dx\,dt \\
&\quad + C\int_{t_n}^{t_{n+1}}\int_K (a(x/\varepsilon^\beta, t/\varepsilon^\alpha, \eta, D_x w_\varepsilon) - a(x/\varepsilon^\beta, t/\varepsilon^\alpha, \eta, D_x v_\varepsilon), D_x w_0 - D_x v_0)dx\,dt \\
&= C\int_{t_n}^{t_{n+1}}\int_K (a(x/\varepsilon^\beta, t/\varepsilon^\alpha, \eta, D_x w_\varepsilon) - a(x/\varepsilon^\beta, t/\varepsilon^\alpha, \eta, D_x v_\varepsilon), D_x w_0 - D_x v_0)dx\,dt \\
&\quad + C\int_{t_n}^{t_{n+1}}\int_{\partial K} (a(x/\varepsilon^\beta, t/\varepsilon^\alpha, \eta, D_x w_\varepsilon) - a(x/\varepsilon^\beta, t/\varepsilon^\alpha, \eta, D_x v_\varepsilon))\cdot \mathbf{n}\ (\tilde{w}_\varepsilon - \tilde{v}_\varepsilon)dS\,dt \\
&\quad - C\int_{t_n}^{t_{n+1}}\int_K (\mathrm{div}(a(x/\varepsilon^\beta, t/\varepsilon^\alpha, \eta, D_x w_\varepsilon)) - \mathrm{div}(a(x/\varepsilon^\beta, t/\varepsilon^\alpha, \eta, D_x v_\varepsilon))) \\
&\qquad\qquad (\tilde{w}_\varepsilon - \tilde{v}_\varepsilon)dx\,dt.
\end{aligned}
$$

Since $\tilde{v}_\varepsilon$ and $\tilde{w}_\varepsilon$ are zero on the boundary of K, the second term of the last expression will be zero. From the given equations we get $D_t w_\varepsilon = D_t\tilde{w}_\varepsilon + D_t w_0$ and $D_t v_\varepsilon = D_t\tilde{v}_\varepsilon + D_t v_0$. Thus the last expression becomes

$$
\begin{aligned}
&C\int_{t_n}^{t_{n+1}}\int_K (a(x/\varepsilon^\beta, t/\varepsilon^\alpha, \eta, D_x w_\varepsilon) - a(x/\varepsilon^\beta, t/\varepsilon^\alpha, \eta, D_x v_\varepsilon), D_x w_0 - D_x v_0)dx\,dt \\
&-C\int_{t_n}^{t_{n+1}}\int_K D_t(\tilde{w}_\varepsilon - \tilde{v}_\varepsilon)\cdot(\tilde{w}_\varepsilon - \tilde{v}_\varepsilon)dx\,dt \\
&+C\int_{t_n}^{t_{n+1}}\int_K (-D_t w_0 + D_t v_0)(\tilde{w}_\varepsilon - \tilde{v}_\varepsilon)dx\,dt.
\end{aligned}
$$

Since $D_t(\tilde{w}_\varepsilon - \tilde{v}_\varepsilon)\cdot(\tilde{w}_\varepsilon - \tilde{v}_\varepsilon) = \frac{1}{2}D_t|(\tilde{w}_\varepsilon - \tilde{v}_\varepsilon)|^2$ and when we apply the initial conditions for $\tilde{w}_\varepsilon$ and $\tilde{v}_\varepsilon$, the second term is non-negative, and hence by disregarding the second

term, the above expression is at most

$$
\begin{aligned}
& C\int_{t_n}^{t_{n+1}}\int_K (a(x/\varepsilon^\beta, t/\varepsilon^\alpha, \eta, D_x w_\varepsilon) - a(x/\varepsilon^\beta, t/\varepsilon^\alpha, \eta, D_x v_\varepsilon), D_x w_0 - D_x v_0) dx\, dt \\
& \quad + C\int_{t_n}^{t_{n+1}}\int_K (-D_t w_0 + D_t v_0)(\tilde{w}_\varepsilon - \tilde{v}_\varepsilon) dx\, dt \\
\le\ & C\int_{t_n}^{t_{n+1}}\int_K (1 + |\eta|^{p-1-s} + |D_x w_\varepsilon|^{p-1-s} + |D_x v_\varepsilon|^{p-1-s}) |D_x(w_\varepsilon - v_\varepsilon)|^s \\
& \qquad\qquad |D_x(w_0 - v_0)| dx\, dt \qquad (2.13) \\
& \quad + C\int_{t_n}^{t_{n+1}}\int_K (-D_t w_0 + D_t v_0)(\tilde{w}_\varepsilon - \tilde{v}_\varepsilon) dx\, dt. \qquad (2.14)
\end{aligned}
$$

After applying Hölder's inequality with $r_1 = \frac{p}{p-1-s}$, $r_2 = \frac{p}{s}$, and $r_3 = p$, we have the following bound for (2.13) in the last expression:

$$
\begin{aligned}
& C\left\{\int_{t_n}^{t_{n+1}}\int_K (1 + |\eta|^p + |D_x w_\varepsilon|^p + |D_x v_\varepsilon|^p) dx\, dt\right\}^{(p-1-s)/p} \\
& \quad \times \left\{\int_{t_n}^{t_{n+1}}\int_K |D_x(w_\varepsilon - v_\varepsilon)|^p dx\, dt\right\}^{s/p} \times \left\{\int_{t_n}^{t_{n+1}}\int_K |D_x(w_0 - v_0)|^p dx\, dt\right\}^{1/p} \\
\le\ & C\frac{p-s}{\delta p}(|K \times [t_n, t_{n+1}]| + \|\eta\|_{\mathcal{U}_K}^p + \|D_x w_\varepsilon\|_{\mathcal{U}_K}^p + \|D_x v_\varepsilon\|_{\mathcal{U}_K}^p)^{\frac{p-1-s}{p-s}} \\
& \quad \times \|D_x(v_0 - w_0)\|_{\mathcal{U}_K}^{\frac{p}{p-s}} \ +\ C\frac{\delta s}{p}\|D_x(w_\varepsilon - v_\varepsilon)\|_{\mathcal{U}_K}^p \\
\le\ & C\frac{p-s}{\delta p}(|K \times [t_n, t_{n+1}]| + \|\eta\|_{\mathcal{U}_K}^p + \|D_x w_\varepsilon\|_{\mathcal{U}_K}^p + \|D_x v_\varepsilon\|_{\mathcal{U}_K}^p)^{\frac{p-1-s}{p-s}} \\
& \quad \times \|D_x(v_0 - w_0)\|_{\mathcal{U}_K}^{\frac{p}{p-s}} \ +\ C\frac{\delta s}{p}\|w_\varepsilon - v_\varepsilon\|_{\mathcal{V}_K}^p.
\end{aligned}
$$

By Lemma 3.1 and choosing $\delta > 0$ appropriately, we have

$$
\begin{aligned}
\|v_\varepsilon - w_\varepsilon\|_{\mathcal{V}_K}^p \ \le\ & C(|K \times [t_n, t_{n+1}]| + \|\eta\|_{\mathcal{U}_K}^p + \|D_x v_0\|_{\mathcal{U}_K}^p + \|D_x w_0\|_{\mathcal{U}_K}^p)^{\frac{p-s-1}{p-s}} \\
& \times \|D_x(v_0 - w_0)\|_{\mathcal{U}_K}^{p/(p-s)} + C\int_{t_n}^{t_{n+1}}\int_K (-D_t w_0 + D_t v_0)(\tilde{w}_\varepsilon - \tilde{v}_\varepsilon) dx\, dt.
\end{aligned}
$$

By Hölder's inequality with $r_1 = q$ and $r_2 = p$ and Young's inequality appropriately,

the last term is

$$\begin{aligned} C\int_{t_n}^{t_{n+1}}\int_K (-D_t w_0 + D_t v_0)(\tilde{w}_\varepsilon - \tilde{v}_\varepsilon)dx\,dt &\le C\|D_t w_0 - D_t v_0\|_{\mathcal{V}_K^*}\|\tilde{w}_\varepsilon - \tilde{v}_\varepsilon\|_{\mathcal{V}_K} \\ &\le C_\delta \|D_t(w_0 - v_0)\|_{\mathcal{V}_K^*}^q + C\delta\|\tilde{w}_\varepsilon - \tilde{v}_\varepsilon\|_{\mathcal{V}_K}^p. \end{aligned}$$

The comparison principle (2.12) is obtained from this inequality by choosing $\delta > 0$ appropriately. □

Now we introduce a numerical corrector. For $\eta \in \mathbb{R}$ and $\xi \in \mathbb{R}^d$ let us define a corrector P by

$$P_{\eta,\xi}(y) = \xi + D_y N^\mu_{\eta,\xi}(y),$$

where $N^\mu_{\eta,\xi}$ is a zero mean periodic solution of

$$\mu D_\tau N^\mu_{\eta,\xi} - \mathrm{div}_y(a(y,\tau,\eta,\xi + D_y N^\mu_{\eta,\xi}(y))) = 0,$$

for some constant μ. Then we obtain the following estimation for the corrector P.

Lemma II.3. *For every $\eta \in \mathbb{R}$ and $\xi \in \mathbb{R}^d$ we have*

$$\|P_{\eta,\xi}\|^p_{L^p(T_{0,\varepsilon};L^p(Y_\varepsilon))} \le C(1 + |\eta|^p + |\xi|^p)|Y_\varepsilon \times T_{0,\varepsilon}|,$$

where Y_ε is a period of size ε^β in space and $T_{0,\varepsilon}$ is a period of size ε^α in time, i.e., $Y_\varepsilon = \varepsilon^\beta Y$ and $T_{0,\varepsilon} = \varepsilon^\alpha T_0$.

Proof. By monotonicity we have

$$
\begin{aligned}
&\|P_{\eta,\xi}\|^p_{L^p(T_{0,\varepsilon};L^p(Y_\varepsilon))}\\
&= \int_{T_{0,\varepsilon}}\int_{Y_\varepsilon} |P_{\eta,\xi}-0|^p dx\,dt\\
&\le C\int_{T_{0,\varepsilon}}\int_{Y_\varepsilon} (a(x/\varepsilon^\beta,t/\varepsilon^\alpha,\eta,P_{\eta,\xi})-a(x/\varepsilon^\beta,t/\varepsilon^\alpha,\eta,0),P_{\eta,\xi}-0)\\
&= C\int_{T_{0,\varepsilon}}\int_{Y_\varepsilon} (a(x/\varepsilon^\beta,t/\varepsilon^\alpha,\eta,P_{\eta,\xi}),P_{\eta,\xi})dx\,dt - C\int_{T_{0,\varepsilon}}\int_{Y_\varepsilon} (a(x/\varepsilon^\beta,t/\varepsilon^\alpha,\eta,0),P_{\eta,\xi})dx\,dt\\
&= C\int_{T_{0,\varepsilon}}\int_{Y_\varepsilon} (a(x/\varepsilon^\beta,t/\varepsilon^\alpha,\eta,\xi+D_yN),\xi)dx\,dt\\
&\quad +C\int_{T_{0,\varepsilon}}\int_{Y_\varepsilon} (a(x/\varepsilon^\beta,t/\varepsilon^\alpha,\eta,\xi+D_yN),D_yN)dx\,dt\\
&\quad -C\int_{T_{0,\varepsilon}}\int_{Y_\varepsilon} (a(x/\varepsilon^\beta,t/\varepsilon^\alpha,\eta,0),P_{\eta,\xi})dx\,dt\\
&= C\int_{T_{0,\varepsilon}}\int_{Y_\varepsilon} (a(x/\varepsilon^\beta,t/\varepsilon^\alpha,\eta,P_{\eta,\xi}),\xi)dxdt - C\int_{T_{0,\varepsilon}}\int_{Y_\varepsilon} (a(x/\varepsilon^\beta,t/\varepsilon^\alpha,\eta,0),P_{\eta,\xi})dxdt\\
&\le C\int_{T_{0,\varepsilon}}\int_{Y_\varepsilon} (1+|\eta|^{p-1}+|P_{\eta,\xi}|^{p-1})|\xi|dx\,dt + C\int_{T_{0,\varepsilon}}\int_{Y_\varepsilon} (1+|\eta|^{p-1})|P_{\eta,\xi}|dx\,dt. \qquad (2.15)
\end{aligned}
$$

By Hölder's inequality with $r_1 = q$ and $r_2 = p$ and Young's inequality appropriately, the last expression (2.15) is bounded by

$$
\begin{aligned}
&C\left\{\int_{T_{0,\varepsilon}}\int_{Y_\varepsilon}(1+|\eta|^p+|P_{\eta,\xi}|^p)dx\,dt\right\}^{1/q}\left\{\int_{T_{0,\varepsilon}}\int_{Y_\varepsilon}|\xi|^p dx\,dt\right\}^{1/p}\\
&\quad +C\left\{\int_{T_{0,\varepsilon}}\int_{Y_\varepsilon}(1+|\eta|^p)dx\,dt\right\}^{1/q}\left\{\int_{T_{0,\varepsilon}}\int_{Y_\varepsilon}|P_{\eta,\xi}|^p dx\,dt\right\}^{1/p}\\
\le\ & \frac{C\delta}{q}\int_{T_{0,\varepsilon}}\int_{Y_\varepsilon}(1+|\eta|^p+|P_{\eta,\xi}|^p)dx\,dt + \frac{C}{\delta p}\int_{T_{0,\varepsilon}}\int_{Y_\varepsilon}|\xi|^p dx\,dt\\
&+\frac{C}{\delta q}\int_{T_{0,\varepsilon}}\int_{Y_\varepsilon}(1+|\eta|^p)dx\,dt + \frac{C\delta}{p}\int_{T_{0,\varepsilon}}\int_{Y_\varepsilon}|P_{\eta,\xi}|^p dx\,dt.
\end{aligned}
$$

Choosing $\delta > 0$ appropriately, we get the following estimate:

$$\begin{aligned} \|P_{\eta,\xi}\|^p_{L^p(T_{0,\varepsilon};L^p(Y_\varepsilon))} &\leq C\int_{T_{0,\varepsilon}}\int_{Y_\varepsilon}(1+|\eta|^p+|\xi|^p)dx\,dt \\ &\leq C(1+|\eta|^p+|\xi|^p)|Y_\varepsilon \times T_{0,\varepsilon}|. \end{aligned}$$

□

We have the following corollary.

Corollary II.4. *For every $\eta \in \mathbb{R}$ and $\xi \in \mathbb{R}^d$ we have*

$$\|D_y N^\mu_{\eta,\xi}\|^p_{L^p(T_{0,\varepsilon};L^p(Y_\varepsilon))} \leq C(1+|\eta|^p+|\xi|^p)|Y_\varepsilon \times T_{0,\varepsilon}|,$$

$$\|N^\mu_{\eta,\xi}\|^p_{L^p(T_{0,\varepsilon};L^p(Y_\varepsilon))} \leq C(1+|\eta|^p+|\xi|^p)|Y_\varepsilon \times T_{0,\varepsilon}|.$$

In the previous section, we discussed that the homogenization of parabolic equations depends on the relation between α and β. The solution N can be obtained by solving different types of equations (2.4), (2.5), and (2.6) for each case. Furthermore, we have the following convergence properties.

Lemma II.5. *Let us consider the ε-dependent auxiliary equations*

$$\mu D_\tau N^\varepsilon - \operatorname{div} a(y,\tau,\eta,\xi+D_y N^\varepsilon) = 0, \tag{2.16}$$

where $\mu = \varepsilon^{2\beta-\alpha}$. Then the solution N^ε of (2.16) converges to the solution N of the auxiliary problems (2.4), (2.5), and (2.6), respectively, satisfying

$$\int_{T_0}\int_Y |D_y N^\varepsilon - D_y N|^p dx\,dt \to 0,$$

as ε tends to zero.

The above lemma was proved in [26] for each case. One of our main results is the following corrector result.

Theorem II.6. *Let v_h be bounded in $\mathcal{V}_\Omega = L^p(t_n, t_{n+1}; W_0^{1,p}(\Omega))$ and let v_ε^h satisfy*

$$\begin{aligned} D_t v_\varepsilon^h - \operatorname{div}(a(x/\varepsilon^\beta, t/\varepsilon^\alpha, \eta^{v_h}, D_x v_\varepsilon^h)) &= 0 \quad \text{in } K \times [t_n, t_{n+1}), \\ v_\varepsilon^h &= v_h \quad \text{on } \partial K, \\ v_\varepsilon^h(t = t_n) &= v_h. \end{aligned}$$

Then

$$\int_{t_n}^{t_{n+1}} \int_\Omega |D_x v_\varepsilon^h - P|^p dx\, dt \le C \left(\frac{\varepsilon^\beta}{h}\right) (|\Omega \times [t_n, t_{n+1}]| + \|v_h\|_{\mathcal{U}_\Omega}^p + \|D_x v_h\|_{\mathcal{U}_\Omega}^p), \quad (2.17)$$

where $\mathcal{U}_\Omega = L^p(t_n, t_{n+1}; L^p(\Omega))$ and h is chosen so that $h = h_x = h_t$. Here

$$P_{\eta^{v_h}, D_x v_h} = D_x v_h + \varepsilon^\beta D_x N^\varepsilon_{\eta^{v_h}, D_x v_h}(x/\varepsilon^\beta, t/\varepsilon^\alpha),$$

where $N^\varepsilon_{\eta^{v_h}, D_x v_h}$ is a zero mean periodic function satisfying the following:

$$\mu D_\tau N - \operatorname{div}_y(a(y, \tau, \eta^{v_h}, D_x v_h + D_y N)) = 0,$$

where $\eta^{v_h} = \frac{1}{|K|} \int_K v_h\, dx$ and $\mu = \varepsilon^{2\beta - \alpha}$.

Proof. Let $v_\varepsilon^h = v_h + \varepsilon^\beta N + \theta_\varepsilon(x, t)$ and $w_\varepsilon^h = v_h + \varepsilon^\beta N$. Then $D_t w_\varepsilon^h = \frac{\varepsilon^\beta}{\varepsilon^\alpha} D_\tau N(y, \tau)$ and $D_x w_\varepsilon^h = D_x v_h + D_y N(y, \tau) = \xi + D_y N(y, \tau)$. In other words, $D_\tau N = \frac{\varepsilon^\alpha}{\varepsilon^\beta} D_t w_\varepsilon^h$ and $\xi + D_y N = D_x w_\varepsilon^h$. Thus we get

$$\mu \frac{\varepsilon^\alpha}{\varepsilon^{2\beta}} D_t w_\varepsilon^h - \operatorname{div}_x(a(x/\varepsilon^\beta, t/\varepsilon^\alpha, \eta^{v_h}, D_x w_\varepsilon^h)) = 0,$$

which is same as $D_t w_\varepsilon^h - \operatorname{div}_x(a(x/\varepsilon^\beta, t/\varepsilon^\alpha, \eta^{v_h}, D_x w_\varepsilon^h)) = 0$. Thus w_ε^h satisfies the

following boundary value problem:

$$\begin{aligned} D_t w_\varepsilon^h - \mathrm{div}(a(x/\varepsilon^\beta, t/\varepsilon^\alpha, \eta^{v_h}, D_x w_\varepsilon^h)) &= 0 \text{ in } K, \\ w_\varepsilon^h &= v_h + \varepsilon^\beta \tilde{N}_{\eta^{v_h}, D_x v_h}(x,t) \text{ on } \partial K, \\ w_\varepsilon^h(t=t_n) &= v_h + \varepsilon^\beta \tilde{N}_{\eta^{v_h}, D_x v_h}(x,t_n), \end{aligned}$$

with $\tilde{N}_{\eta^{v_h}, D_x v_h} = N_{\eta^{v_h}, D_x v_h}\, \varphi(x,t)$, where $\varphi \in C_0^\infty$ such that $\varphi(x,t) = 1$ on a strip of width δ_1 adjacent to ∂K for all t with $t_n < t < t_{n+1}$, $\varphi(x,t) = 1$ on K for every t with $t_n < t < t_n + \delta_2$, and 0 elsewhere (see Figure 1). We denote this strip by S_ε. By Lemma II.2,

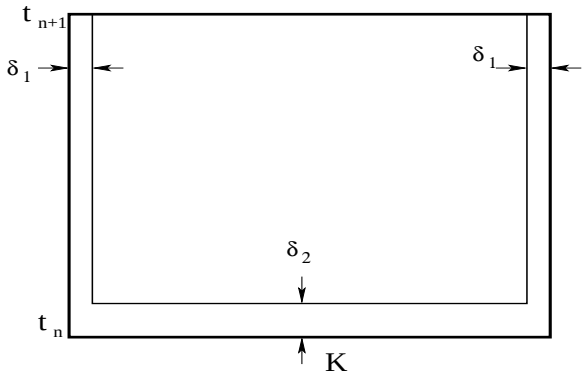

Fig. 1. The strip S_ε in $K \times [t_n, t_{n+1}]$

$$\begin{aligned} & \int_{t_n}^{t_{n+1}} \int_K |D_x v_\varepsilon^h - P|^p dx\, dt \\ \leq\ & C \| v_\varepsilon^h - w_\varepsilon^h \|_{\mathcal{V}_K}^p \\ \leq\ & C \| D_x (v_h - v_h - \varepsilon^\beta \tilde{N}_{\eta^{v_h}, D_x v_h}) \|_{\mathcal{U}_K}^{p/(p-s)} + C \| D_t (v_h - v_h - \varepsilon^\beta \tilde{N}_{\eta^{v_h}, D_x v_h}) \|_{\mathcal{V}_K^*}^q \\ \leq\ & C \| \varepsilon^\beta D_x \tilde{N}_{\eta^{v_h}, D_x v_h} \|_{\mathcal{U}_K}^{p/(p-s)} + C \| \varepsilon^\beta D_t \tilde{N}_{\eta^{v_h}, D_x v_h} \|_{\mathcal{V}_K^*}^q \end{aligned} \tag{2.18}$$

We will show the convergence of the last two terms in (2.18) separately.

Step 1. First we study $\|\varepsilon^\beta D_x \tilde{N}_{\eta^{v_h}, D_x v_h}\|^p_{\mathcal{U}_K}$. Let $J_\varepsilon^{K\times[t_n,t_{n+1}]} = \{i \in \mathbb{Z}^{d+1} : (Y_\varepsilon \times T_{0,\varepsilon})^i \cap (K \times [t_n, t_{n+1}]) \neq \emptyset, (Y_\varepsilon \times T_{0,\varepsilon})^i \setminus (K \times [t_n, t_{n+1}]) \neq \emptyset\}$, where $(Y_\varepsilon \times T_{0,\varepsilon})^i = i + Y_\varepsilon \times T_{0,\varepsilon}$ is the translation of $Y_\varepsilon \times T_{0,\varepsilon}$. Let $F_\varepsilon^{K\times[t_n,t_{n+1}]} = \bigcup_{i\in J_\varepsilon^{K\times[t_n,t_{n+1}]}} (Y_\varepsilon \times T_{0,\varepsilon})^i$ be the union of the periods which intersect with the boundary of the domain. Then

$$\begin{aligned}
\|\varepsilon^\beta D_x \tilde{N}_{\eta^{v_h}, D_x v_h}\|^p_{\mathcal{U}_K} &= \varepsilon^{\beta p} \int_{t_n}^{t_{n+1}} \int_K |D_x(N_{\eta^{v_h}, D_x v_h}\, \varphi)|^p dx\, dt \\
&\leq \varepsilon^{\beta p} \sum_{i\in J_\varepsilon^{K\times[t_n,t_{n+1}]}} \int_{(Y_\varepsilon\times T_{0,\varepsilon})^i} |D_x(N_{\eta^{v_h}, D_x v_h}\, \varphi)|^p dx\, dt \\
&\leq C\varepsilon^{\beta p} \sum_i \int_{(Y_\varepsilon\times T_{0,\varepsilon})^i} (|D_x N|^p |\varphi|^p + |N|^p |D_x\varphi|^p) dx\, dt.
\end{aligned}$$

Since $|D_x\varphi| \leq C/\delta_1$ and by Corollary II.4, we obtain

$$\begin{aligned}
&\|\varepsilon^\beta D_x \tilde{N}_{\eta^{v_h}, D_x v_h}\|^p_{\mathcal{U}_K} \\
\leq\ & C\varepsilon^{\beta p} \left(1 + \frac{1}{\delta_1^p}\right) \sum_i \int_{(Y_\varepsilon\times T_{0,\varepsilon})^i} (|D_x N|^p + |N|^p) dx\, dt \\
\leq\ & C\varepsilon^{\beta p} \left(1 + \frac{1}{\delta_1^p}\right) \sum_i (1 + |\eta^{v_h}|^p + |D_x v_h|^p) |(Y_\varepsilon \times T_{0,\varepsilon})^i| \\
\leq\ & C \left(\frac{\varepsilon^\beta}{\delta_1}\right)^p \frac{h_x^d h_t}{h_x^d h_t} (1 + |\eta^{v_h}|^p + |D_x v_h|^p)(h_x^{d-1}\delta_1 h_t + h_x^d \delta_2) \\
\leq\ & C \left(\frac{\varepsilon^\beta}{\delta_1}\right)^p \left(\frac{\delta_1}{h_x} + \frac{\delta_2}{h_t}\right) (|K \times [t_n, t_{n+1}]| + \|\eta^{v_h}\|^p_{\mathcal{U}_K} + \|D_x v_h\|^p_{\mathcal{U}_K}).
\end{aligned}$$

Step 2. Next, we show that $\|\varepsilon^\beta D_t \tilde{N}_{\eta^{v_h}, D_x v_h}\|^q_{\mathcal{V}_K^*} \to 0$ as $\varepsilon \to 0$. Indeed,

$$\begin{aligned}
\|\varepsilon^\beta D_t \tilde{N}_{\eta^{v_h}, D_x v_h}\|^q_{\mathcal{V}_K^*} &= \int_{t_n}^{t_{n+1}} \|\varepsilon^\beta D_t \tilde{N}\|^q_{W^{-1,q}(K)} dt \\
&= \int_{t_n}^{t_{n+1}} \sup_{\psi \in W_0^{1,p}(K)} \frac{\left\langle \varepsilon^\beta D_t \tilde{N}, \psi \right\rangle^q}{\|\psi\|^q_{1,p}} dt \\
&= \int_{t_n}^{t_{n+1}} \sup_{\psi \in W_0^{1,p}(K)} \frac{\left\langle \varepsilon^\beta (D_t N)\varphi + \varepsilon^\beta N D_t \varphi, \psi \right\rangle^q}{\|\psi\|^q_{1,p}} dt \\
&= \int_{t_n}^{t_{n+1}} \sup_{\psi \in W_0^{1,p}(K)} \frac{\left(\int_K \varepsilon^\beta (D_t N)\varphi\psi dx + \int_K \varepsilon^\beta N (D_t \varphi)\psi dx\right)^q}{\|\psi\|^q_{1,p}} dt \\
&\leq \int_{t_n}^{t_{n+1}} \sup_{\psi \in W_0^{1,p}(K)} \frac{2^{q-1}\left(\int_K \varepsilon^\beta (D_t N)\varphi\psi dx\right)^q}{\|\psi\|^q_{1,p}} dt \qquad (2.19) \\
&\quad + \int_{t_n}^{t_{n+1}} \sup_{\psi \in W_0^{1,p}(K)} \frac{2^{q-1}\left(\int_K \varepsilon^\beta N (D_t \varphi)\psi dx\right)^q}{\|\psi\|^q_{1,p}} dt. \qquad (2.20)
\end{aligned}$$

The estimation for the last expression will be split up into two parts (2.19) and (2.20).

Step 2.1. First, we estimate the inside of supremum. To keep calculation simple, we will not carry time integration for now. The inside of the supremum in (2.19) is

$$\left\{\int_K (D_t N)\varphi\psi\right\}^q = \left\{\int_K \operatorname{div}(a(x/\varepsilon^\beta, t/\varepsilon^\alpha, \eta^{v_h}, D_x v_h + D_x \varepsilon^\beta N))\varphi\psi dx\right\}^q.$$

Since $\psi \in W_0^{1,p}(K)$, the integration by parts gives us

$$\begin{aligned}
&\left\{\int_K (a(x/\varepsilon^\beta, t/\varepsilon^\alpha, \eta^{v_h}, D_x v_h + D_x \varepsilon^\beta N), D_x(\varphi\psi))dx\right\}^q \\
&\leq C\left\{\int_K (a(x/\varepsilon^\beta, t/\varepsilon^\alpha, \eta^{v_h}, D_x v_h + D_x \varepsilon^\beta N), (D_x\varphi)\psi)dx\right\}^q \qquad (2.21) \\
&\quad + C\left\{\int_K (a(x/\varepsilon^\beta, t/\varepsilon^\alpha, \eta^{v_h}, D_x v_h + D_x \varepsilon^\beta N), \varphi(D_x\psi))dx\right\}^q. \qquad (2.22)
\end{aligned}$$

Now let $I_\varepsilon^K = \{i \in \mathbb{Z}^d : Y_\varepsilon^i \subseteq K\} \cup J_\varepsilon^K$ with $J_\varepsilon^K = \{i \in \mathbb{Z}^d : Y_\varepsilon^i \cap K \neq \emptyset, Y_\varepsilon^i \setminus K \neq \emptyset\}$ and $I_\varepsilon^{[t_n, t_{n+1}]} = \{j \in \mathbb{Z} : T_{0,\varepsilon}^j \subseteq [t_n, t_{n+1}]\} \cup J_\varepsilon^{[t_n, t_{n+1}]}$ with $J_\varepsilon^{[t_n, t_{n+1}]} = \{j \in \mathbb{Z} :$

$T^j_{0,\varepsilon} \cap [t_n, t_{n+1}] \neq \emptyset, T^j_{0,\varepsilon} \setminus [t_n, t_{n+1}] \neq \emptyset\}$. Then (2.21) is bounded by

$$C \left\{ \sum_{i \in I^K_\varepsilon} \int_{Y^i_\varepsilon} (a(x/\varepsilon^\beta, t/\varepsilon^\alpha, \eta^{v_h}, D_x v_h + D_x \varepsilon^\beta N), (D_x \varphi)\psi) dx \right\}^q$$
$$\leq C \left\{ \sum_{i \in I^K_\varepsilon} \int_{Y^i_\varepsilon} (1 + |\eta^{v_h}|^{p-1} + |D_x v_h + D_x \varepsilon^\beta N|^{p-1}) |D_x \varphi| |\psi| dx \right\}^q . \quad (2.23)$$

Since $|D_x \varphi| \leq C/\delta_1$ and φ is nonzero near the boundary of K, the right hand side of (2.23) does not exceed

$$\frac{C}{\delta_1^q} \left\{ \sum_{i \in J^K_\varepsilon} \int_{Y^i_\varepsilon} (1 + |\eta^{v_h}|^{p-1} + |D_x v_h + D_x \varepsilon^\beta N|^{p-1}) |\psi| dx \right\}^q$$
$$\leq \frac{C}{\delta_1^q} \sum_{i \in J^K_\varepsilon} \left\{ \int_{Y^i_\varepsilon} (1 + |\eta^{v_h}|^{p-1} + |D_x v_h + D_x \varepsilon^\beta N|^{p-1}) |\psi| dx \right\}^q .$$

By Hölder's inequality with $r_1 = q$ and $r_2 = p$, we obtain an estimate for (2.21)

$$C \left\{ \int_K (a(x/\varepsilon^\beta, t/\varepsilon^\alpha, \eta^{v_h}, D_x v_h + D_x \varepsilon^\beta N), (D_x \varphi)\psi) dx \right\}^q$$
$$\leq \frac{C}{\delta_1^q} \sum_{i \in J^K_\varepsilon} \left\{ \int_{Y^i_\varepsilon} (1 + |\eta^{v_h}|^p + |D_x v_h + D_x \varepsilon^\beta N|^p) dx \right\} \left\{ \int_{Y^i_\varepsilon} |\psi|^p dx \right\}^{q/p}$$
$$\leq \frac{C}{\delta_1^q} \sum_{i \in J^K_\varepsilon} \left\{ \int_{Y^i_\varepsilon} (1 + |\eta^{v_h}|^p + |D_x v_h + D_x \varepsilon^\beta N|^p) dx \right\} \|\psi\|^q_{1,p}.$$

On the other hand, (2.22) can be estimated similarly

$$C \left\{ \sum_{i \in I^K_\varepsilon} \int_{Y^i_\varepsilon} (a(x/\varepsilon^\beta, t/\varepsilon^\alpha, \eta^{v_h}, D_x v_h + D_x \varepsilon^\beta N), \varphi(D_x \psi)) dx \right\}^q$$
$$\leq C \left\{ \sum_{i \in I^K_\varepsilon} \int_{Y^i_\varepsilon} (1 + |\eta^{v_h}|^{p-1} + |D_x v_h + D_x \varepsilon^\beta N|^{p-1}) |\varphi| |D_x \psi| dx \right\}^q .$$

Since $|\varphi| \le 1$, we have

$$\le C \left\{ \sum_{i \in J_\varepsilon^K} \int_{Y_\varepsilon^i} (1 + |\eta^{v_h}|^{p-1} + |D_x v_h + D_x \varepsilon^\beta N|^{p-1}) |D_x \psi| dx \right\}^q$$
$$\le C \sum_{i \in J_\varepsilon^K} \left\{ \int_{Y_\varepsilon^i} (1 + |\eta^{v_h}|^{p-1} + |D_x v_h + D_x \varepsilon^\beta N|^{p-1}) |D_x \psi| dx \right\}^q.$$

By Hölder's inequality with $r_1 = q$ and $r_2 = p$ again,

$$\begin{aligned} (2.22) \quad &\le C \sum_{i \in J_\varepsilon^K} \left\{ \int_{Y_\varepsilon^i} (1 + |\eta^{v_h}|^p + |D_x v_h + D_x \varepsilon^\beta N|^p) dx \right\} \left\{ \int_{Y_\varepsilon^i} |D_x \psi|^p dx \right\}^{q/p} \\ &\le C \sum_{i \in J_\varepsilon^K} \left\{ \int_{Y_\varepsilon^i} (1 + |\eta^{v_h}|^p + |D_x v_h + D_x \varepsilon^\beta N|^p) dx \right\} \|\psi\|_{1,p}^q. \end{aligned}$$

Thus, (2.19) is estimated by

$$\int_{t_n}^{t_{n+1}} \sup_{\psi \in W_0^{1,p}(K)} \frac{2^{q-1} \left(\int_K \varepsilon^\beta (D_t N) \varphi \psi dx \right)^q}{\|\psi\|_{1,p}^q} dt$$
$$\le C \int_{t_n}^{t_{n+1}} \sup_{\psi \in W_0^{1,p}(K)} \varepsilon^{\beta q} \left(\frac{1}{\delta_1^q} + 1 \right) \sum_{i \in J_\varepsilon^K} \left\{ \int_{Y_\varepsilon^i} (1 + |\eta^{v_h}|^p + |D_x v_h + D_x \varepsilon^\beta N|^p) dx \right\} \times \frac{\|\psi\|_{1,p}^q}{\|\psi\|_{1,p}^q} dt$$
$$\le C \int_{t_n}^{t_{n+1}} \varepsilon^{\beta q} \left(\frac{1}{\delta_1^q} + 1 \right) \sum_{i \in J_\varepsilon^K} \left\{ \int_{Y_\varepsilon^i} (1 + |\eta^{v_h}|^p + |D_x v_h + D_x \varepsilon^\beta N|^p) dx \right\} dt$$
$$\le C \varepsilon^{\beta q} \left(\frac{1}{\delta_1^q} + 1 \right) \sum_{j \in I_\varepsilon^{[t_n, t_{n+1}]}} \sum_{i \in J_\varepsilon^K} \int_{T_{0,\varepsilon}^j} \int_{Y_\varepsilon^i} (1 + |\eta^{v_h}|^p + |D_x v_h|^p + |D_y N|^p) dx \, dt.$$

Corollary II.4 implies the estimate for (2.19)

$$\begin{aligned}
&\int_{t_n}^{t_{n+1}} \sup_{\psi\in W_0^{1,p}(K)} \frac{2^{q-1}\left(\int_K \varepsilon^\beta (D_t N)\varphi\psi dx\right)^q}{\|\psi\|_{1,p}^q} dt \\
&\le C\varepsilon^{\beta q}\left(\frac{1}{\delta_1^q}+1\right)(1+|\eta^{v_h}|^p+|D_x v_h|^p) \sum_{i\in J_\varepsilon^{K\times[t_n,t_{n+1}]}} |(Y_\varepsilon\times T_{0,\varepsilon})^i| \\
&\le C\left(\frac{\varepsilon^\beta}{\delta_1}\right)^q (1+|\eta^{v_h}|^p+|D_x v_h|^p) \sum_{i\in J_\varepsilon^{K\times[t_n,t_{n+1}]}} |(Y_\varepsilon\times T_{0,\varepsilon})^i| \\
&\le C\left(\frac{\varepsilon^\beta}{\delta_1}\right)^q \frac{h_x^d h_t}{h_x^d h_t}(1+|\eta^{v_h}|^p+|D_x v_h|^p)(h_x^{d-1}\delta_1 h_t + h_x^d\delta_2) \\
&\le C\left(\frac{\varepsilon^\beta}{\delta_1}\right)^q \left(\frac{\delta_1}{h_x}+\frac{\delta_2}{h_t}\right)(|K\times[t_n,t_{n+1}]| + \|\eta^{v_h}\|_{\mathcal{U}_K}^p + \|D_x v_h\|_{\mathcal{U}_K}^p).
\end{aligned}$$

Step 2.2. Now let us move on finding an estimation for the other term (2.20). Note that we assumed $p=q=2$ in the previous section (see (2.2)). (2.20) becomes

$$\begin{aligned}
&C\int_{t_n}^{t_{n+1}} \varepsilon^{\beta q} \sup_{\psi\in W_0^{1,p}(K)} \frac{\{\int_K N(D_t\varphi)\psi dx\}^q}{\|\psi\|_{1,p}^q} dt \\
&\le C \sum_{j\in I_\varepsilon^{[t_n,t_{n+1}]}} \int_{T_{0,\varepsilon}^i} \varepsilon^{\beta q} \sup_{\psi\in W_0^{1,p}(K)} \frac{\{\sum_{i\in I_\varepsilon^K}\int_{Y_\varepsilon^i} N(D_t\varphi)\psi dx\}^q}{\|\psi\|_{1,p}^q} dt.
\end{aligned}$$

Since $|D_t\varphi|\le C/\delta_2$ and by Schwarz inequality, we have

$$\begin{aligned}
&C\int_{t_n}^{t_{n+1}} \varepsilon^{\beta q} \sup_{\psi\in W_0^{1,p}(K)} \frac{\{\int_K N(D_t\varphi)\psi dx\}^q}{\|\psi\|_{1,p}^q} dt \\
&\le C\left(\frac{\varepsilon^\beta}{\delta_2}\right)^q \sum_{j\in I_\varepsilon^{[t_n,t_{n+1}]}} \int_{T_{0,\varepsilon}^i} \sup_{\psi\in W_0^{1,p}(K)} \frac{\{\sum_{i\in J_\varepsilon^K}\int_{Y_\varepsilon^i} |N||\psi| dx\}^q}{\|\psi\|_{1,p}^q} dt \\
&\le C\left(\frac{\varepsilon^\beta}{\delta_2}\right)^2 \sum_{j\in I_\varepsilon^{[t_n,t_{n+1}]}} \int_{T_{0,\varepsilon}^i} \sup_{\psi\in W_0^{1,2}(K)} \frac{\{\sum_{i\in J_\varepsilon^K}\{\int_{Y_\varepsilon^i}|N|^2 dx\}\{\int_{Y_\varepsilon^i}|\psi|^2 dx\}}{\|\psi\|_{1,2}^2} dt.
\end{aligned}$$

By Corollary II.4, we obtain an estimate for (2.20)

$$
\begin{aligned}
& C\int_{t_n}^{t_{n+1}} \varepsilon^{\beta q} \sup_{\psi\in W_0^{1,p}(K)} \frac{\{\int_K N(D_t\varphi)\psi dx\}^q}{\|\psi\|_{1,p}^q} dt \\
& \le C\left(\frac{\varepsilon^\beta}{\delta_2}\right)^2 \sum_{j\in I_\varepsilon^{[t_n,t_{n+1}]}} \sum_{i\in J_\varepsilon^K} \int_{T_{0,\varepsilon}^j}\int_{Y_\varepsilon^i} |N|^2 dx\, dt \\
& \le C\left(\frac{\varepsilon^\beta}{\delta_2}\right)^2 \sum_{i\in J_\varepsilon^{K\times[t_n,t_{n+1}]}} \int_{(Y_\varepsilon\times T_{0,\varepsilon})^i} |N|^2 dx\, dt \\
& \le C\left(\frac{\varepsilon^\beta}{\delta_2}\right)^2 \sum_{i\in J_\varepsilon^{K\times[t_n,t_{n+1}]}} (1+|\eta^{v_h}|^2+|D_x v_h|^2)|(Y_\varepsilon\times T_{0,\varepsilon})^i| \\
& \le C\left(\frac{\varepsilon^\beta}{\delta_2}\right)^2 \frac{h_x^d h_t}{h_x^d h_t}(1+|\eta^{v_h}|^2+|D_x v_h|^2)(h_x^{d-1}h_t\delta_1 + h_x^d\delta_2) \\
& \le C\left(\frac{\varepsilon^\beta}{\delta_2}\right)^2 \left(\frac{\delta_1}{h_x}+\frac{\delta_2}{h_t}\right)(|K\times[t_n,t_{n+1}]| + \|\eta^{v_h}\|_{\mathcal{U}_K}^2 + \|D_x v_h\|_{\mathcal{U}_K}^2).
\end{aligned}
$$

Step 3. By taking the results from the Step 1 and Step 2 into account with the assumption $s = p-1$, we have

$$
\begin{aligned}
& \int_{t_n}^{t_{n+1}}\int_K |D_x v_\varepsilon^h - P|^2 dx\, dt \\
\le\ & C\left(\frac{\varepsilon^\beta}{\delta_1}\right)^{2/(2-s)} \left(\frac{\delta_1}{h_x}+\frac{\delta_2}{h_t}\right)^{1/(2-s)} (|K\times[t_n,t_{n+1}]| + \|\eta^{v_h}\|_{\mathcal{U}_K}^2 + \|D_x v_h\|_{\mathcal{U}_K}^2)^{1/(2-s)} \\
& + C\left(\frac{\varepsilon^\beta}{\delta_1}\right)^2 \left(\frac{\delta_1}{h_x}+\frac{\delta_2}{h_t}\right)(|K\times[t_n,t_{n+1}]| + \|\eta^{v_h}\|_{\mathcal{U}_K}^2 + \|D_x v_h\|_{\mathcal{U}_K}^2) \\
& + C\left(\frac{\varepsilon^\beta}{\delta_2}\right)^2 \left(\frac{\delta_1}{h_x}+\frac{\delta_2}{h_t}\right)(|K\times[t_n,t_{n+1}]| + \|\eta^{v_h}\|_{\mathcal{U}_K}^2 + \|D_x v_h\|_{\mathcal{U}_K}^2) \\
=\ & C\left(\frac{\varepsilon^{2\beta}}{\delta_1^2}+\frac{\varepsilon^{2\beta}}{\delta_2^2}\right)\left(\frac{\delta_1}{h_x}+\frac{\delta_2}{h_t}\right)(|K\times[t_n,t_{n+1}]| + \|\eta^{v_h}\|_{\mathcal{U}_K}^2 + \|D_x v_h\|_{\mathcal{U}_K}^2) \\
=\ & C\varepsilon^{2\beta}\left(\frac{1}{\delta_1^2}+\frac{1}{\delta_2^2}\right)\left(\frac{\delta_1}{h_x}+\frac{\delta_2}{h_t}\right)(|K\times[t_n,t_{n+1}]| + \|\eta^{v_h}\|_{\mathcal{U}_K}^2 + \|D_x v_h\|_{\mathcal{U}_K}^2).
\end{aligned}
$$

Here we choose $\delta_1 = \delta_2 = \varepsilon^\beta$ and $h_x = h_t = h$. Then we obtain the following estimate:

$$
\|D_x v_\varepsilon^h - P\|_{\mathcal{U}_K}^2 \le C\frac{\varepsilon^\beta}{h}(|K\times[t_n,t_{n+1}]| + \|\eta^{v_h}\|_{\mathcal{U}_K}^2 + \|D_x v_h\|_{\mathcal{U}_K}^2).
$$

Note that Jensen's inequality implies

$$\|\eta^{v_h}\|_{L^p(K)} \leq C\|v_h\|_{L^p(K)}.$$

Finally, summing over all $K \in \mathcal{T}_h$, we have

$$\begin{aligned}\int_{t_n}^{t_{n+1}}\int_\Omega |D_x v_\varepsilon^h - P|^2 dx\, dt &= \sum_K \int_{t_n}^{t_{n+1}}\int_K |D_x v_\varepsilon^h - P|^2 dx\, dt \\ &\leq C\frac{\varepsilon^\beta}{h}\sum_K (|K\times[t_n,t_{n+1}]| + \|v_h\|^2_{\mathcal{U}_K} + \|D_x v_h\|^2_{\mathcal{U}_K}) \\ &= C\frac{\varepsilon^\beta}{h}(|\Omega\times[t_n,t_{n+1}]| + \|v_h\|^2_{\mathcal{U}_\Omega} + \|D_x v_h\|^2_{\mathcal{U}_\Omega}).\end{aligned}$$

□

We have the following coercive property for the operator A_ε^h.

Theorem II.7. *There exists a constant $C > 0$ such that for each $v_h \in S^h$*

$$\langle A_\varepsilon^h v_h, v_h\rangle \geq C\|D_x v_h\|^p_{\mathcal{U}_\Omega} - c_1 h_x \sum_K \int_{t_n}^{t_{n+1}}\int_K (1 + |\eta^{v_h}|^p) dx\, dt,$$

for sufficiently small h_x.

Proof.

$$\begin{aligned}\langle A_\varepsilon^h v_h, v_h\rangle &= \sum_{K\in\mathcal{T}_h}\int_{t_n}^{t_{n+1}}\int_K ((a(x/\varepsilon^\beta, t/\varepsilon^\alpha, \eta^{v_h}, D_x v_\varepsilon^h), D_x v_h) \\ &\qquad + a_0(x/\varepsilon^\beta, t/\varepsilon^\alpha, \eta^{v_h}, D_x v_\varepsilon^h) v_h) dx\, dt \\ &= \sum_K \int_{t_n}^{t_{n+1}}\int_K ((a(x/\varepsilon^\beta, t/\varepsilon^\alpha, \eta^{v_h}, D_x v_\varepsilon^h), D_x v_h) \\ &\qquad + a_0(x/\varepsilon^\beta, t/\varepsilon^\alpha, \eta^{v_h}, D_x v_\varepsilon^h)\eta^{v_h}) dx\, dt \qquad (2.24) \\ &\quad + \sum_K \int_{t_n}^{t_{n+1}}\int_K a_0(x/\varepsilon^\beta, t/\varepsilon^\alpha, \eta^{v_h}, D_x v_\varepsilon^h)(v_h - \eta^{v_h}) dx\, dt. \qquad (2.25)\end{aligned}$$

Let $\tilde{v}_\varepsilon^h = v_\varepsilon^h - v_h$, where $v_\varepsilon^h = E^{MsFEM} v_h$. Then $\tilde{v}_\varepsilon^h \in L^p(t_n, t_{n+1}; W_0^{1,p}(K))$ satisfies

$$D_t \tilde{v}_\varepsilon^h - \mathrm{div}(a(x/\varepsilon^\beta, t/\varepsilon^\alpha, \eta^{v_h}, D_x \tilde{v}_\varepsilon^h + D_x v_h)) = 0.$$

Multiplying by $\tilde{v}_\varepsilon^h$ on both sides and integrating them by parts imply

$$\begin{aligned}
&\tilde{v}_\varepsilon^h D_t \tilde{v}_\varepsilon^h - \operatorname{div}(a(x/\varepsilon^\beta, t/\varepsilon^\alpha, \eta^{v_h}, D_x\tilde{v}_\varepsilon^h + D_x v_h))\tilde{v}_\varepsilon^h = 0\\
&\int_{t_n}^{t_{n+1}}\int_K \tilde{v}_\varepsilon^h D_t \tilde{v}_\varepsilon^h dx\,dt + \int_{t_n}^{t_{n+1}}\int_K (a(x/\varepsilon^\beta, t/\varepsilon^\alpha, \eta^{v_h}, D_x\tilde{v}_\varepsilon^h + D_x v_h), D_x\tilde{v}_\varepsilon^h)dx\,dt = 0\\
&\int_{t_n}^{t_{n+1}}\int_K \frac{1}{2} D_t|\tilde{v}_\varepsilon^h|^2 dx\,dt + \int_{t_n}^{t_{n+1}}\int_K (a(x/\varepsilon^\beta, t/\varepsilon^\alpha, \eta^{v_h}, D_x\tilde{v}_\varepsilon^h + D_x v_h), D_x\tilde{v}_\varepsilon^h)dx\,dt = 0.
\end{aligned}$$

From the initial condition for $\tilde{v}_\varepsilon^h$ at $t = t_n$ we obtain

$$\frac{1}{2}\int_K |\tilde{v}_\varepsilon^h(t_{n+1})|^2 dx = -\int_{t_n}^{t_{n+1}}\int_K (a(x/\varepsilon^\beta, t/\varepsilon^\alpha, \eta^{v_h}, D_x\tilde{v}_\varepsilon^h + D_x v_h), D_x\tilde{v}_\varepsilon^h)dx\,dt.$$

The first term (2.24) becomes

$$\begin{aligned}
&\sum_K \int_{t_n}^{t_{n+1}}\int_K ((a(x/\varepsilon^\beta, t/\varepsilon^\alpha, \eta^{v_h}, D_x\tilde{v}_\varepsilon^h + D_x v_h), D_x v_h + D_x\tilde{v}_\varepsilon^h)\\
&\qquad\qquad + a_0(x/\varepsilon^\beta, t/\varepsilon^\alpha, \eta^{v_h}, D_x\tilde{v}_\varepsilon^h D_x v_h)\eta^{v_h})dx\,dt\\
&\quad - \sum_K \int_{t_n}^{t_{n+1}}\int_K (a(x/\varepsilon^\beta, t/\varepsilon^\alpha, \eta^{v_h}, D_x\tilde{v}_\varepsilon^h + D_x v_h), D_x\tilde{v}_\varepsilon^h)dx\,dt\\
\geq\ & C\sum_K \int_{t_n}^{t_{n+1}}\int_K |D_x v_h + D_x\tilde{v}_\varepsilon^h|^p dx\,dt + \frac{1}{2}\sum_K \int_K |\tilde{v}_{\varepsilon,h}(t = t_{n+1})|^2 dx\\
\geq\ & C\sum_K \int_{t_n}^{t_{n+1}}\int_K |D_x v_h + D_x\tilde{v}_\varepsilon^h|^p dx\,dt.
\end{aligned}$$

The fact that $|v_h - \eta^{v_h}| \leq Ch_x|D_x v_h|$ in each K implies an estimate for the second term (2.25)

$$\begin{aligned}
&|\sum_K \int_{t_n}^{t_{n+1}}\int_K a_0(x/\varepsilon^\beta, t/\varepsilon^\alpha, \eta^{v_h}, D_x v_\varepsilon^h)(v_h - \eta^{v_h})dx\,dt|\\
&\leq Ch_x \sum_K \int_{t_n}^{t_{n+1}}\int_K a_0(x/\varepsilon^\beta, t/\varepsilon^\alpha, \eta^{v_h}, D_x v_\varepsilon^h)|D_x v_h|dx\,dt\\
&\leq Ch_x \sum_K \int_{t_n}^{t_{n+1}}\int_K (1 + |\eta^{v_h}|^{p-1} + |D_x v_\varepsilon^h|^{p-1})|D_x v_h|dx\,dt.
\end{aligned}$$

Hölder's inequality with $r_1 = q$ and $r_2 = p$ and Young's inequality give us the further

estimates for (2.25)

$$
\begin{aligned}
&|\sum_K \int_{t_n}^{t_{n+1}}\int_K a_0(x/\varepsilon^\beta, t/\varepsilon^\alpha, \eta^{v_h}, D_x v_\varepsilon^h)(v_h - \eta^{v_h})dx\,dt| \\
&\le Ch_x \sum_K \left\{\int_{t_n}^{t_{n+1}}\int_K (1+|\eta^{v_h}|^p + |D_x v_\varepsilon^h|^p)dx\,dt\right\}^{1/q} \left\{\int_{t_n}^{t_{n+1}}\int_K |D_x v_h|^p dx\,dt\right\}^{1/p} \\
&\le Ch_x \sum_K \left(\frac{1}{q}\int_{t_n}^{t_{n+1}}\int_K (1+|\eta^{v_h}|^p + |D_x v_\varepsilon^h|^p)dx\,dt + \frac{1}{p}\int_{t_n}^{t_{n+1}}\int_K |D_x v_h|^p dx\,dt\right) \\
&\le Ch_x \sum_K \int_{t_n}^{t_{n+1}}\int_K (1+|\eta^{v_h}|^p + |D_x v_\varepsilon^h|^p + |D_x v_h|^p)dx\,dt.
\end{aligned}
$$

Thus, we have

$$
\begin{aligned}
\langle A_\varepsilon^h v_h, v_h\rangle &\ge c\sum_K \int_{t_n}^{t_{n+1}}\int_K |D_x v_\varepsilon^h|^p dx\,dt \\
&\quad -c_1 h_x \sum_K \int_{t_n}^{t_{n+1}}\int_K (1+|\eta^{v_h}|^p + |D_x v_\varepsilon^h|^p + |D_x v_h|^p)dx\,dt \\
&= (c - c_1 h_x)\sum_K \int_{t_n}^{t_{n+1}}\int_K |D_x v_\varepsilon^h|^p dx\,dt \\
&\quad -c_1 h_x \sum_K \int_{t_n}^{t_{n+1}}\int_K (1+|\eta^{v_h}|^p + |D_x v_h|^p)dx\,dt.
\end{aligned}
$$

Denote $\hat{K}$ a reference triangle such that $diam(\hat{K}) = O(1)$, $y = x/h_x$, and $\hat{v}_\varepsilon^h = v_\varepsilon^h(yh_x)$. Then applying the trace inequality $\|u\|_{L^p(\partial K)} \le \|D_x u\|_{L^p(K)}$ and the fact $\|D_x u\|_{L^p(Q)} \ge C\|u - f(u)\|_{W^{1,p}(Q)}$, where Q is a Lipschitz domain and $f(u)$ can be

chosen to be the average of u on ∂Q, we can obtain

$$\begin{aligned}
\int_{t_n}^{t_{n+1}}\int_K |D_x v_\varepsilon^h|^p dx\,dt &= \frac{h_x^d}{h_x^p}\int_{t_n}^{t_{n+1}}\int_{\hat{K}} |D_y \hat{v}_\varepsilon^h|^p dy\,dt \\
&\geq c\frac{h_x^d}{h_x^p}\int_{t_n}^{t_{n+1}} \|\hat{v}_\varepsilon^h - \tilde{\eta}^{v_h}\|_{W^{1,p}(\hat{K})} dt \\
&\geq c\frac{h_x^d}{h_x^p}\int_{t_n}^{t_{n+1}}\int_{\partial\hat{K}} |v_h - \tilde{\eta}^{v_h}|^p dy_l\,dt \\
&= c\frac{h_x^d}{h_x^p}\int_{t_n}^{t_{n+1}}\int_{\partial\hat{K}} |(D_y v_h, y - y_0)|^p dy_l\,dt \\
&= c\int_{t_n}^{t_{n+1}} h_x^d |D_x v_h|^p \int_{\partial\hat{K}} |(e_{D_y v_h}, y - y_0)|^p dy_l\,dt.
\end{aligned}$$

Here $\tilde{\eta}^{v_h} = \frac{1}{|\partial\hat{K}|}\int_{\partial\hat{K}} v_h dy_l$ and $v_h = \tilde{\eta}^{v_h} + (D_y v_h, y - y_0)$, where $y_0 = \frac{1}{|\partial\hat{K}|}\int_{\partial\hat{K}} y dy_l$. It was proved in [9] that $\int_{\partial\hat{K}} |(e_{D_y v_h}, y - y_0)|^p dy_l$ is bounded below independent of $D_y v_h$. Hence we have

$$\begin{aligned}
\int_{t_n}^{t_{n+1}}\int_K |D_x v_\varepsilon^h|^p dx\,dt &\geq cc_0\int_{t_n}^{t_{n+1}} h_x^d |D_x v_h|^p dt \\
&= C\int_{t_n}^{t_{n+1}}\int_K |D_x v_h|^p dx\,dt.
\end{aligned}$$

Finally, we obtain

$$\begin{aligned}
\langle A_\varepsilon^h v_h, v_h\rangle &\geq (c - c_1 h_x) C\sum_K \int_{t_n}^{t_{n+1}}\int_K |D_x v_h|^p dx\,dt \\
&\quad - c_1 h_x \sum_K \int_{t_n}^{t_{n+1}}\int_K (1 + |\eta^{v_h}|^p + |D_x v_h|^p) dx\,dt \\
&\geq C\|D_x v_h\|_{\mathcal{U}_\Omega}^p - c_1 h_x \sum_K \int_{t_n}^{t_{n+1}}\int_K (1 + |\eta^{v_h}|^p) dx\,dt,
\end{aligned}$$

for sufficiently small $h_x > 0$. □

Next theorem is one of the our main results which shows the convergence of the solution of the numerical homogenization procedure. We note that the proof assumes that $p = q = 2$.

Theorem II.8. *Suppose $v_h(t), w_h(t) \in S^h$ where $D_x v_h$ is uniformly bounded in $L^p(t_n, t_{n+1}; L^{p+\lambda}(\Omega))$ for some $\lambda > 0$ and $D_x w_h$ is uniformly bounded in $L^p(t_n, t_{n+1}; L^p(\Omega))$. Let A^* be the homogenized operator defined by*

$$\langle A^* v_h, w_h \rangle = \sum_{K \in \mathcal{T}_h} \int_{t_n}^{t_{n+1}} \int_K ((a^*(v_h, D_x v_h), D_x w_h) + a_0^*(v_h, D_x v_h) w_h) dx\, dt$$

for every $v_h(t), w_h(t) \in S^h$. Then we have

$$\lim_{\varepsilon \to 0} \langle A_\varepsilon^h v_h - A^* v_h, w_h \rangle = 0. \tag{2.26}$$

Proof. Given $v_h(t) \in S^h$, we define the corrector P by

$$P = D_x v_h + D_y N^\varepsilon_{\eta^{v_h}, D_x v_h}(y, \tau),$$

where $N^\varepsilon_{\eta^{v_h}, D_x v_h}$ is defined in Theorem II.6. Then we have

$$\begin{aligned}
&\langle A_\varepsilon^h v_h - A^* v_h, w_h \rangle \\
&= \sum_{K \in \mathcal{T}_h} \int_{t_n}^{t_{n+1}} \int_K (a(x/\varepsilon^\beta, t/\varepsilon^\alpha, \eta^{v_h}, D_x v_\varepsilon^h), D_x w_h) - (a^*(v_h, D_x v_h), D_x w_h) dx\, dt \quad (2.27)\\
&\quad + \sum_{K \in \mathcal{T}_h} \int_{t_n}^{t_{n+1}} \int_K (a_0(x/\varepsilon^\beta, t/\varepsilon^\alpha, \eta^{v_h}, D_x v_\varepsilon^h) - a_0^*(v_h, D_x v_h)) w_h\, dx\, dt. \quad (2.28)
\end{aligned}$$

Adding and subtracting same quantities gives us that (2.27) can be split into three terms

$$\begin{aligned}
\sum_{K \in \mathcal{T}_h} \Bigg\{ &\int_{t_n}^{t_{n+1}} \int_K (a(x/\varepsilon^\beta, t/\varepsilon^\alpha, \eta^{v_h}, D_x v_\varepsilon^h) - a(x/\varepsilon^\beta, t/\varepsilon^\alpha, \eta^{v_h}, P), D_x w_h) dx\, dt \quad (2.29)\\
&+ \int_{t_n}^{t_{n+1}} \int_K (a(x/\varepsilon^\beta, t/\varepsilon^\alpha, \eta^{v_h}, P) - a^*(\eta^{v_h}, D_x v_h), D_x w_h) dx\, dt \quad (2.30)\\
&+ \int_{t_n}^{t_{n+1}} \int_K (a^*(\eta^{v_h}, D_x v_h) - a^*(v_h, D_x v_h), D_x w_h) dx\, dt \Bigg\}. \quad (2.31)
\end{aligned}$$

Similarly, we split (2.28) by

$$\sum_{K\in\mathcal{T}_h}\Big\{\int_{t_n}^{t_{n+1}}\!\!\int_K (a_0(x/\varepsilon^\beta,t/\varepsilon^\alpha,\eta^{v_h},D_xv_\varepsilon^h)-a_0(x/\varepsilon^\beta,t/\varepsilon^\alpha,\eta^{v_h},P))D_xw_h dx\,dt \quad (2.32)$$

$$+\int_{t_n}^{t_{n+1}}\!\!\int_K (a_0(x/\varepsilon^\beta,t/\varepsilon^\alpha,\eta^{v_h},P)-a_0^*(\eta^{v_h},D_xv_h))D_xw_h dx\,dt \quad (2.33)$$

$$+\int_{t_n}^{t_{n+1}}\!\!\int_K (a_0^*(\eta^{v_h},D_xv_h)-a_0^*(v_h,D_xv_h))D_xw_h dx\,dt\Big\}. \quad (2.34)$$

By the continuity assumption **A4** for the operator $a(\cdot,\cdot,\eta,\xi)$ and applying Hölder's inequality, the inside of the first sum (2.29) can be estimated

$$\begin{aligned}
&\int_{t_n}^{t_{n+1}}\!\!\int_K (a(x/\varepsilon^\beta,t/\varepsilon^\alpha,\eta^{v_h},D_xv_\varepsilon^h)-a(x/\varepsilon^\beta,t/\varepsilon^\alpha,\eta^{v_h},P),D_xw_h)dx\,dt\\
&\le c\int_{t_n}^{t_{n+1}}\!\!\int_K |D_xv_\varepsilon^h-P|^s(1+|\eta^{v_h}|^{p-1-s}+|D_xv_\varepsilon^h|^{p-1-s}+|P|^{p-1-s})|D_xw_h|dx\,dt\\
&\le c\Big\{\int_{t_n}^{t_{n+1}}\!\!\int_K |D_xv_\varepsilon^h-P|^p dx\,dt\Big\}^{s/p}\Big\{\int_{t_n}^{t_{n+1}}\!\!\int_K |D_xw_h|^p dx\,dt\Big\}^{1/p}\\
&\quad\times\Big\{\int_{t_n}^{t_{n+1}}\!\!\int_K (1+|\eta^{v_h}|^{p-1-s}+|D_xv_\varepsilon^h|^{p-1-s}+|P|^{p-1-s})^{p/(p-1-s)}dx\,dt\Big\}^{(p-1-s)/p}.
\end{aligned}$$

The last term is bounded above by

$$\begin{aligned}
&c\left(\int_{t_n}^{t_{n+1}}\!\!\int_K (1+|\eta^{v_h}|^p+|D_xv_\varepsilon^h|^p+|P|^p)dx\,dt\right)^{(p-1-s)/p}\\
=\;&c\left(\int_{t_n}^{t_{n+1}}\!\!\int_K (1+|\eta^{v_h}|^p)dx\,dt+\int_{t_n}^{t_{n+1}}\!\!\int_K |D_xv_\varepsilon^h|^p dx\,dt+\int_{t_n}^{t_{n+1}}\!\!\int_K |P|^p)dx\,dt\right)^{(p-1-s)/p}\\
\le\;& c\big\{|K\times[t_n,t_{n+1}]|+\|\eta^{v_h}\|_{\mathcal{U}_K}^p+C(|K\times[t_n,t_{n+1}]|+\|\eta^{v_h}\|_{\mathcal{U}_K}^p+\|D_xv_h\|_{\mathcal{U}_K}^p)\\
&\qquad+C(|K\times[t_n,t_{n+1}]|+\|\eta^{v_h}\|_{\mathcal{U}_K}^p+\|D_xv_h\|_{\mathcal{U}_K}^p)\big\}^{(p-1-s)/p}\\
\le\;& C(|K\times[t_n,t_{n+1}]|+\|v_h\|_{\mathcal{U}_K}^p+\|D_xv_h\|_{\mathcal{U}_K}^p)^{(p-1-s)/p}. \qquad (2.35)
\end{aligned}$$

Summing up those estimates (2.35) over all $K\in\mathcal{T}_h$ and by Theorem II.6, we have

the following estimate for (2.29)

$$\begin{aligned}
&\sum_K \int_{t_n}^{t_{n+1}} \int_K (a(x/\varepsilon^\beta, t/\varepsilon^\alpha, \eta^{v_h}, D_x v_\varepsilon^h) - a(x/\varepsilon^\beta, t/\varepsilon^\alpha, \eta^{v_h}, P), D_x w_h) dx\, dt \\
&\le C \left(\frac{\varepsilon^\beta}{h} (|\Omega \times [t_n, t_{n+1}]| + \|v_h\|_{\mathcal{U}_\Omega}^p + \|D_x v_h\|_{\mathcal{U}_\Omega}^p) \right)^{s/p} \\
&\quad \times \left(|\Omega \times [t_n, t_{n+1}]| + \|v_h\|_{\mathcal{U}_\Omega}^p + \|D_x v_h\|_{\mathcal{U}_\Omega}^p \right)^{(p-1-s)/p} \times \|D_x w_h\|_{\mathcal{U}_\Omega} \\
&\le C \left(\frac{\varepsilon^\beta}{h} \right)^{s/p} \left(|\Omega \times [t_n, t_{n+1}]| + \|v_h\|_{\mathcal{U}_\Omega}^p + \|D_x v_h\|_{\mathcal{U}_\Omega}^p \right)^q \|D_x w_h\|_{\mathcal{U}_\Omega},
\end{aligned}$$

which implies that the last inequality tends to zero as ε approaches zero.

In order to estimate the second sum (2.30), let $I_\varepsilon^{K\times[t_n,t_{n+1}]} = \{i \in \mathbb{Z}^{d+1} : (Y_\varepsilon \times T_{0,\varepsilon})^i \subset (K \times [t_n, t_{n+1}])\}$ and $J_\varepsilon^{K\times[t_n,t_{n+1}]} = \{i \in \mathbb{Z}^{d+1} : (Y_\varepsilon \times T_{0,\varepsilon})^i \cap (K \times [t_n, t_{n+1}]) \neq \emptyset, (Y_\varepsilon \times T_{0,\varepsilon})^i \setminus (K \times [t_n, t_{n+1}]) \neq \emptyset\}$. Let $E_\varepsilon^{K\times[t_n,t_{n+1}]} = \bigcup_{i \in I_\varepsilon^{K\times[t_n,t_{n+1}]}} (Y_\varepsilon \times T_{0,\varepsilon})^i$ and $F_\varepsilon^{K\times[t_n,t_{n+1}]} = \bigcup_{i \in J_\varepsilon^{K\times[t_n,t_{n+1}]}} (Y_\varepsilon \times T_{0,\varepsilon})^i$. By the definition of homogenized fluxes and the fact that $D_x w_h$ is constant in K, the second sum (2.30) can be expressed by

$$\begin{aligned}
&\sum_K \int_{t_n}^{t_{n+1}} \int_K (a(x/\varepsilon^\beta, t/\varepsilon^\alpha, \eta^{v_h}, P) - a^*(\eta^{v_h}, D_x v_h), D_x w_h) dx\, dt \\
= &\sum_K \sum_{i \in I_\varepsilon^{K\times[t_n,t_{n+1}]}} \int_{(Y_\varepsilon \times T_{0,\varepsilon})^i} (a(x/\varepsilon^\beta, t/\varepsilon^\alpha, \eta^{v_h}, P) - a^*(\eta^{v_h}, D_x v_h), D_x w_h) dx\, dt \\
&+ \sum_K \int_{K \setminus E_\varepsilon^{K\times[t_n,t_{n+1}]}} (a(x/\varepsilon^\beta, t/\varepsilon^\alpha, \eta^{v_h}, P) - a^*(\eta^{v_h}, D_x v_h), D_x w_h) dx\, dt \\
\le &\sum_K \sum_{i \in I_\varepsilon^{K\times[t_n,t_{n+1}]}} \int_{(Y_\varepsilon \times T_{0,\varepsilon})^i} (a(x/\varepsilon^\beta, t/\varepsilon^\alpha, \eta^{v_h}, D_x v_h + D_y N^\varepsilon_{\eta^{v_h}, D_x v_h}) \\
&\qquad - a(x/\varepsilon^\beta, t/\varepsilon^\alpha, \eta^{v_h}, D_x v_h + D_y N_{\eta^{v_h}, D_x v_h}), D_x w_h) dx\, dt \quad (2.36) \\
&+ \sum_K \int_{F_\varepsilon^{K\times[t_n,t_{n+1}]}} |(a(x/\varepsilon^\beta, t/\varepsilon^\alpha, \eta^{v_h}, P) - a^*(\eta^{v_h}, D_x v_h), D_x w_h)| dx\, dt. \quad (2.37)
\end{aligned}$$

Note that (2.36) becomes zero if $\alpha = 2\beta$, i.e., $\mu = \varepsilon^{2\beta-\alpha} = 1$. By the continuity assumption **A4** and Hölder's inequality with $r_1 = \frac{p}{p-1-s}$, $r_2 = \frac{p}{s}$, and $r_3 = p$, we get

an estimate for (2.36)

$$\begin{aligned}
&\sum_K \sum_{i\in I_\varepsilon^{K\times[t_n,t_{n+1}]}} \int_{(Y_\varepsilon\times T_{0,\varepsilon})^i} (a(x/\varepsilon^\beta, t/\varepsilon^\alpha, \eta^{v_h}, D_x v_h + D_y N^\varepsilon_{\eta^{v_h}, D_x v_h}) \\
&\qquad\qquad -a(x/\varepsilon^\beta, t/\varepsilon^\alpha, \eta^{v_h}, D_x v_h + D_y N_{\eta^{v_h}, D_x v_h}), D_x w_h) dx\, dt \\
\le &\sum_K \sum_i \int_{(Y_\varepsilon\times T_{0,\varepsilon})^i} \big(1+|\eta^{v_h}|^{p-1-s} + |D_x v_h + D_y N^\varepsilon_{\eta^{v_h}, D_x v_h}|^{p-1-s} + |D_x v_h + D_y N_{\eta^{v_h}, D_x v_h}|^{p-1-s}\big) \\
&\qquad\qquad \times |D_y N^\varepsilon_{\eta^{v_h}, D_x v_h} - D_y N_{\eta^{v_h}, D_x v_h}|^s \ |D_x w_h|\, dx\, dt \\
\le &C\left\{\sum_K \sum_i \int_{(Y_\varepsilon\times T_{0,\varepsilon})^i} \big(1+|\eta^{v_h}|^p + |D_x v_h + D_y N^\varepsilon_{\eta^{v_h}, D_x v_h}|^p + |D_x v_h + D_y N_{\eta^{v_h}, D_x v_h}|^p\big) dx dt\right\}^{\frac{p-1-s}{p}} \\
&\times \left\{\sum_K \sum_i \int_{(Y_\varepsilon\times T_{0,\varepsilon})^i} |D_y N^\varepsilon_{\eta^{v_h}, D_x v_h} - D_y N_{\eta^{v_h}, D_x v_h}|^p dx dt\right\}^{\frac{s}{p}} \left\{\sum_K \sum_i \int_{(Y_\varepsilon\times T_{0,\varepsilon})^i} |D_x w_h|^p dx dt\right\}^{\frac{1}{p}}.
\end{aligned}$$

By Lemma II.3, the above estimate does not exceed the followings

$$\begin{aligned}
&C\left\{\sum_K \sum_i (1+|\eta^{v_h}|^p + |D_x v_h|^p) |(Y_\varepsilon\times T_{0,\varepsilon})^i|\right\}^{\frac{p-1-s}{p}} \left\{\sum_K \sum_i |D_x w_h|^p |(Y_\varepsilon\times T_{0,\varepsilon})^i|\right\}^{\frac{1}{p}} \\
&\quad\times \left\{\sum_K \sum_i \int_{(Y_\varepsilon\times T_{0,\varepsilon})^i} |D_y N^\varepsilon_{\eta^{v_h}, D_x v_h} - D_y N_{\eta^{v_h}, D_x v_h}|^p dx\, dt\right\}^{\frac{s}{p}} \\
\le\ &C\left\{\sum_K (1+|\eta^{v_h}|^p + |D_x v_h|^p) |K\times[t_n, t_{n+1}]|\right\}^{\frac{p-1-s}{p}} \left\{\sum_K |D_x w_h|^p |K\times[t_n, t_{n+1}]|\right\}^{\frac{1}{p}} \\
&\quad\times \left\{\sum_K \sum_i \int_{(Y_\varepsilon\times T_{0,\varepsilon})^i} |D_y N^\varepsilon_{\eta^{v_h}, D_x v_h} - D_y N_{\eta^{v_h}, D_x v_h}|^p dx\, dt\right\}^{\frac{s}{p}} \\
\le\ &C\left(|\Omega\times[t_n, t_{n+1}]| + \|v_h\|^p_{\mathcal{U}_\Omega} + \|D_x v_h\|^p_{\mathcal{U}_\Omega}\right)^{\frac{p-1-s}{p}} \left(\|D_x w_h\|^p_{\mathcal{U}_\Omega}\right)^{\frac{1}{p}} \\
&\quad\times \left\{\sum_K \sum_i \int_{(Y_\varepsilon\times T_{0,\varepsilon})^i} |D_y N^\varepsilon_{\eta^{v_h}, D_x v_h} - D_y N_{\eta^{v_h}, D_x v_h}|^p dx\, dt\right\}^{\frac{s}{p}},
\end{aligned}$$

which tends to zero as $\varepsilon \to 0$ by Lemma II.5.

On the other hand, by Hölder's inequality and Lemma II.3, the second sum (2.37) is estimated by

$$
\begin{aligned}
&\sum_K \sum_{i\in J_\varepsilon^{K\times[t_n,t_{n+1}]}} \int_{(Y_\varepsilon\times T_{0,\varepsilon})^i} (|(a(x/\varepsilon^\beta, t/\varepsilon^\alpha, \eta^{v_h}, P), D_x w_h)| + |(a^*(\eta^{v_h}, D_x v_h), D_x w_h)|) dxdt \\
&\le C \sum_K \sum_i \int_{(Y_\varepsilon\times T_{0,\varepsilon})^i} (1+|\eta^{v_h}|^{p-1}+|P|^{p-1})|D_x w_h| + (1+|\eta^{v_h}|^{p-1}+|D_x v_h|^{p-1})|D_x w_h| dxdt \\
&\le C \sum_K \sum_i \int_{(Y_\varepsilon\times T_{0,\varepsilon})^i} (1+|\eta^{v_h}|^{p-1}+|P|^{p-1}+|D_x v_h|^{p-1})|D_x w_h| dx\, dt \\
&\le C \left(\sum_K \sum_i \int_{(Y_\varepsilon\times T_{0,\varepsilon})^i} (1+|\eta^{v_h}|^{p}+|P|^{p}+|D_x v_h|^{p}) dxdt \right)^{\frac{1}{q}} \left(\sum_K \sum_i \int_{(Y_\varepsilon\times T_{0,\varepsilon})^i} |D_x w_h|^p dxdt \right)^{\frac{1}{p}} \\
&\le C \left(\sum_K \sum_i (1+|\eta^{v_h}|^{p}+|D_x v_h|^{p}) |(Y_\varepsilon\times T_{0,\varepsilon})^i| \right)^{\frac{1}{q}} \left(\sum_K \sum_i |D_x w_h|^p \, |(Y_\varepsilon\times T_{0,\varepsilon})^i| \right)^{\frac{1}{p}} \\
&\le C \left(\sum_K |K\times[t_n,t_{n+1}]| \, (1+|\eta^{v_h}|^{p}+|D_x v_h|^{p}) \frac{|F_\varepsilon^{K\times[t_n,t_{n+1}]}|}{|K\times[t_n,t_{n+1}]|} \right)^{\frac{1}{q}} \\
&\qquad \times \left(\sum_K |K\times[t_n,t_{n+1}]| \, |D_x w_h|^p \frac{|F_\varepsilon^{K\times[t_n,t_{n+1}]}|}{|K\times[t_n,t_{n+1}]|} \right)^{\frac{1}{p}} \\
&\le C \max_K \left(\frac{|F_\varepsilon^{K\times[t_n,t_{n+1}]}|}{|K\times[t_n,t_{n+1}]|} \right)^{\frac{1}{q}+\frac{1}{p}} \left(|\Omega\times[t_n,t_{n+1}]| + \|v_h\|_{\mathcal{U}_\Omega}^p + \|D_x v_h\|_{\mathcal{U}_\Omega}^p \right)^{\frac{1}{q}} \left(\|D_x w_h\|_{\mathcal{U}_\Omega}^p \right)^{\frac{1}{p}} \\
&\le C \left(\frac{\varepsilon^\beta}{h} \right) \left(|\Omega\times[t_n,t_{n+1}]| + \|v_h\|_{\mathcal{U}_\Omega}^p + \|D_x v_h\|_{\mathcal{U}_\Omega}^p \right)^{\frac{1}{q}} \|D_x w_h\|_{\mathcal{U}_\Omega}^p .
\end{aligned}
$$

From the analogous fourth assumption **A4** for the homogenized fluxes and by Hölder inequality, we have the following estimate for the third term (2.31)

$$
\begin{aligned}
(2.31) &\le C \int_{t_n}^{t_{n+1}} \int_K (1+|\eta^{v_h}|^{p-1}+|D_x v_h|^{p-1}+|v_h|^{p-1}) \, \nu(|\eta^{v_h}-v_h|) \, |D_x w_h| dx\, dt \\
&\le C \left(\int_{t_n}^{t_{n+1}} \int_K (1+|\eta^{v_h}|^{p}+|D_x v_h|^{p}+|v_h|^{p}) \, \nu(|\eta^{v_h}-v_h|)^q dx\, dt \right)^{1/q} \|D_x w_h\|_{\mathcal{U}_K} .
\end{aligned}
$$

Hence we sum up those estimates over all $K \in \mathcal{T}_h$

$$C\left(\int_{t_n}^{t_{n+1}}\int_{\Omega}(1+|\eta^{v_h}|^p+|D_xv_h|^p+|v_h|^p)\,\nu(|\eta^{v_h}-v_h|)^q dx\,dt\right)^{1/q}\|D_xw_h\|_{\mathcal{U}_\Omega}$$
$$\leq C\left(\int_{t_n}^{t_{n+1}}\int_{\Omega}(1+|v_h|^p+|D_xv_h|^p+|v_h|^p)\,\nu(|\eta^{v_h}-v_h|)^q dx\,dt\right)^{1/q}\|D_xw_h\|_{\mathcal{U}_\Omega}.$$

Since $D_xv_h \in L^p(t_n,t_{n+1};L^{p+\lambda}(\Omega))$, $D_xw_h \in L^p(t_n,t_{n+1};L^p(\Omega))$ and $\eta^{v_h}-v_h$ converges to zero in $L^p(t_n,t_{n+1};L^p(\Omega))$, the summation of the estimates for (2.31) over all K vanishes as ε goes to zero.

We can get the estimates for the terms (2.32), (2.33), and (2.34) in a similar way. □

We note that Theorem II.8 implies the operator A^* is type M [12], in other words, if u_h converges to u weakly in $\mathcal{V}_\Omega$, A^*u_h converges to g weakly in $\mathcal{V}_\Omega^*$, and $\langle A^*u_h,u_h\rangle$ converges to $\langle g,u\rangle$, then $A^*u=g$. Finally our main result follows from the Bardos-Brezis theorem (see [29] p. 128).

Theorem II.9. *Let u be the solution of the homogenized equation (2.3) and u_h is a MsFEM solution given by (2.8). Then we have*

$$\lim_{\varepsilon\to 0}\|u_h-u\|_{\mathcal{V}_\Omega}=0,$$

where $h=h(\varepsilon)\gg\varepsilon$ and $h\to 0$ as $\varepsilon\to 0$.

Remark II.10. In [12], it is proved that D_xu_h is uniformly bounded in $L^p(t_n,t_{n+1};L^{p+\lambda}(\Omega))$ for some $\lambda>0$.

In conclusion, first, we were able to obtain explicit corrector estimates for monotone operators in terms of $\frac{\varepsilon}{h}$. This is not known before for the nonlinear parabolic equations and gives us quantitative estimate of the convergence. Second, we were able to quantify parts of the truncation errors $\langle A_\varepsilon^h v_h - A^*v_h, w_h\rangle$ in (2.26). More pre-

cisely, we obtained explicit estimates for (2.29) and (2.37). Both of these estimates show the existence of resonance errors appearing in the form of $\frac{\varepsilon^\beta}{h}$. We note that the resonance errors from (2.29) are due to linear boundary condition imposed on local problems. Because the actual solution is not linear along coarse grid boundaries, this mismatch results in resonance errors. The resonance errors from (2.37) are due to the fact that the coarse grid block does not contain integer number of periods. These types of resonance errors are also observed in linear problems [20].

C. Correctors

In this section we study the convergence of a class of correctors for the monotone parabolic operator [7, 31]. In order to extend the results in [31] to our case, we will follow the similar approaches and notations in [31]. Furthermore, we focus on the case of $\alpha = 2\beta$ in the homogenization of parabolic equations. The main result we will present is proved in the following way. At first, we present some properties for correctors, for instance, estimates for correctors and difference of two correctors over a period. The main result is proved by applying the monotonicity assumption **A2** and splitting into two terms after adding and subtracting same quantities. Furthermore, the first term can be expanded into four different terms. By showing each of the four terms converges to same quantity, we verify the first term tends to zero. We apply Hölder's inequality and Young's inequality with appropriate constant to prove the second term approaches to zero.

Let us begin with introducing the $Y \times T_0$-periodic function

$$P(y, \tau, \eta, \xi) = P_{\eta,\xi} = \xi + D_y N_{\eta,\xi}(y, \tau), \tag{2.38}$$

defined on $\mathbb{R}^d \times \mathbb{R} \times \mathbb{R}^d \times \mathbb{R}$. We define the piecewise constant function M_ε by

$$(M_\varepsilon \varphi)(x,t) = \sum_{i \in I_\varepsilon} \sum_{j \in J_\varepsilon} 1_{Y_\varepsilon^i}(x)\ 1_{T_{0,\varepsilon}^j}(t)\ \frac{1}{|Y_\varepsilon^i \times T_{0,\varepsilon}^j|} \int_{T_{0,\varepsilon}^j} \int_{Y_\varepsilon^i} \varphi(y,\tau) dy d\tau, \tag{2.39}$$

where $I_\varepsilon = \{i \in \mathbb{Z}^d : Y_\varepsilon^i \subseteq \Omega\}$ and $J_\varepsilon = \{j \in \mathbb{Z} : T_{0,\varepsilon}^j \subseteq (0,T)\}$, and 1_A is the characteristic function of a set A. Then we have the property that $M_\varepsilon \varphi$ converges to φ in $\mathcal{U} = L^p(0,T;L^p(\Omega))$ [31].

Here is the main result in this section, which is proved for $\alpha = 2\beta$.

Theorem II.11. $\| P(\frac{x}{\varepsilon}, \frac{t}{\varepsilon^2}, M_\varepsilon u, M_\varepsilon D_x u) - D_x u_\varepsilon \|_{L^p(0,T;L^p(\Omega))} \to 0$ *as* $\varepsilon \to 0$*, where* u *is the solution of the homogenized equation (2.3).*

Before we prove this main result, we present some properties for correctors defined in (2.38). We recall that it was shown in Lemma II.3 that for any $\eta \in \mathbb{R}$ and $\xi \in \mathbb{R}^d$, we had $\|P_{\eta,\xi}\|^p_{L^p(T_{0,\varepsilon};L^p(Y_\varepsilon))} \le C(1 + |\eta|^p + |\xi|^p)|Y_\varepsilon \times T_{0,\varepsilon}|$. In addition, the following property for the correctors will be used in proving the next lemma.

Lemma II.12. *For every* $\eta_1, \eta_2 \in \mathbb{R}$ *and* $\xi_1, \xi_2 \in \mathbb{R}^d$ *we have*

$$\begin{aligned} & \|P(\cdot,\cdot,\eta_1,\xi_1) - P(\cdot,\cdot,\eta_2,\xi_2)\|^p_{L^p(T_{0,\varepsilon};L^p(Y_\varepsilon))} \\ \le\ & C(1 + |\eta_i|^p + |\xi_i|^p)^{\frac{p-1-s}{p-s}} |\xi_1 - \xi_2|^{\frac{p}{p-s}} |Y_\varepsilon \times T_{0,\varepsilon}| \\ & + C \int_{T_{0,\varepsilon}} \int_{Y_\varepsilon} (1 + |\eta_i|^p + |\xi_i|^p) \nu(|\eta_1 - \eta_2|)^q dx\, dt. \end{aligned}$$

Proof. By the monotonicity assumption **A2** of the operator and adding and subtract-

ing same quantities, we obtain the following estimates

$$
\begin{aligned}
&\|P(\cdot,\cdot,\eta_1,\xi_1)-P(\cdot,\cdot,\eta_2,\xi_2)\|^p_{L^p(T_{0,\varepsilon};L^p(Y_\varepsilon))}\\
&=\int_{T_{0,\varepsilon}}\int_{Y_\varepsilon}\left|P(\tfrac{x}{\varepsilon},\tfrac{t}{\varepsilon^2},\eta_1,\xi_1)-P(\tfrac{x}{\varepsilon},\tfrac{t}{\varepsilon^2},\eta_2,\xi_2)\right|^p dx\,dt\\
&\le C\int_{T_{0,\varepsilon}}\int_{Y_\varepsilon}(a(\tfrac{x}{\varepsilon},\tfrac{t}{\varepsilon^2},\eta_1,P_{\eta_1,\xi_1})-a(\tfrac{x}{\varepsilon},\tfrac{t}{\varepsilon^2},\eta_1,P_{\eta_2,\xi_2}),P_{\eta_1,\xi_1}-P_{\eta_2,\xi_2})dx\,dt\\
&=C\int_{T_{0,\varepsilon}}\int_{Y_\varepsilon}(a(\tfrac{x}{\varepsilon},\tfrac{t}{\varepsilon^2},\eta_1,P_{\eta_1,\xi_1})-a(\tfrac{x}{\varepsilon},\tfrac{t}{\varepsilon^2},\eta_2,P_{\eta_2,\xi_2}),P_{\eta_1,\xi_1}-P_{\eta_2,\xi_2})dx\,dt\\
&\quad+C\int_{T_{0,\varepsilon}}\int_{Y_\varepsilon}(a(\tfrac{x}{\varepsilon},\tfrac{t}{\varepsilon^2},\eta_2,P_{\eta_2,\xi_2})-a(\tfrac{x}{\varepsilon},\tfrac{t}{\varepsilon^2},\eta_1,P_{\eta_2,\xi_2}),P_{\eta_1,\xi_1}-P_{\eta_2,\xi_2})dx\,dt.
\end{aligned}
$$

Due to the periodicity of $P(\cdot,\cdot,\eta,\xi)=\xi+D_yN_{\eta,\xi}$ and continuity assumption **A4**, we get further estimates

$$
\begin{aligned}
&\|P(\cdot,\cdot,\eta_1,\xi_1)-P(\cdot,\cdot,\eta_2,\xi_2)\|^p_{L^p(T_{0,\varepsilon};L^p(Y_\varepsilon))}\\
&\le C\int_{T_{0,\varepsilon}}\int_{Y_\varepsilon}(a(\tfrac{x}{\varepsilon},\tfrac{t}{\varepsilon^2},\eta_1,P_{\eta_1,\xi_1})-a(\tfrac{x}{\varepsilon},\tfrac{t}{\varepsilon^2},\eta_2,P_{\eta_2,\xi_2}),\xi_1-\xi_2)dx\,dt\\
&\quad+C\int_{T_{0,\varepsilon}}\int_{Y_\varepsilon}(a(\tfrac{x}{\varepsilon},\tfrac{t}{\varepsilon^2},\eta_2,P_{\eta_2,\xi_2})-a(\tfrac{x}{\varepsilon},\tfrac{t}{\varepsilon^2},\eta_1,P_{\eta_2,\xi_2}),P_{\eta_1,\xi_1}-P_{\eta_2,\xi_2})dx\,dt\\
&\le C\int_{T_{0,\varepsilon}}\int_{Y_\varepsilon}(1+|\eta_1|^{p-1-s}+|\eta_2|^{p-1-s}+|P_{\eta_1,\xi_1}|^{p-1-s}+|P_{\eta_2,\xi_2}|^{p-1-s})|P_{\eta_1,\xi_1}-P_{\eta_2,\xi_2}|^s|\xi_1-\xi_2|dxdt\\
&\quad+C\int_{T_{0,\varepsilon}}\int_{Y_\varepsilon}(1+|\eta_1|^{p-1}+|\eta_2|^{p-1}+|P_{\eta_1,\xi_1}|^{p-1}+|P_{\eta_2,\xi_2}|^{p-1})\nu(|\eta_1-\eta_2|)|P_{\eta_1,\xi_1}-P_{\eta_2,\xi_2}|dxdt. \qquad (2.40)
\end{aligned}
$$

By Hölder's inequality with $r_1=q$ and $r_2=p$ and Young's inequality appropriately, the second term of (2.40) is at most

$$
\begin{aligned}
&C\left\{\int_{T_{0,\varepsilon}}\int_{Y_\varepsilon}\left(1+|\eta_1|^{p-1}+|\eta_2|^{p-1}+|P_{\eta_1,\xi_1}|^{p-1}+|P_{\eta_2,\xi_2}|^{p-1}\right)^q\nu(|\eta_1-\eta_2|)^q dx\,dt\right\}^{\frac{1}{q}}\\
&\quad\times\left\{\int_{T_{0,\varepsilon}}\int_{Y_\varepsilon}\left|P\left(\tfrac{x}{\varepsilon},\tfrac{t}{\varepsilon^2},\eta_1,\xi_1\right)-P\left(\tfrac{x}{\varepsilon},\tfrac{t}{\varepsilon^2},\eta_2,\xi_2\right)\right|^p dx\,dt\right\}^{\frac{1}{p}}\\
&\le\frac{C}{q\delta}\int_{T_{0,\varepsilon}}\int_{Y_\varepsilon}(1+|\eta_1|^p+|\eta_2|^p+|P_{\eta_1,\xi_1}|^p+|P_{\eta_2,\xi_2}|^p)\,\nu(|\eta_1|-|\eta_2|)^q dx\,dt\\
&\quad+\frac{C\delta}{p}\int_{T_{0,\varepsilon}}\int_{Y_\varepsilon}|P_{\eta_1,\xi_1}-P_{\eta_2,\xi_2}|^p\,dx\,dt.
\end{aligned}
$$

By Hölder's inequality again with $r_1 = p/(p-1-s)$, $r_2 = p/s$, and $r_3 = p$, the first term of (2.40) is at most

$$
\begin{aligned}
&C\left\{\int_{T_{0,\varepsilon}}\int_{Y_\varepsilon}(1+|\eta_1|^p+|\eta_2|^p+|P(\cdot,\cdot,\eta_1,\xi_1)|^p+|P(\cdot,\cdot,\eta_2,\xi_2)|^p)\,dx\,dt\right\}^{\frac{p-1-s}{p}}\\
&\quad\times\left\{\int_{T_{0,\varepsilon}}\int_{Y_\varepsilon}|P(\tfrac{x}{\varepsilon},\tfrac{t}{\varepsilon^2},\eta_1,\xi_1)-P(\tfrac{x}{\varepsilon},\tfrac{t}{\varepsilon^2},\eta_2,\xi_2)|^p dx\,dt\right\}^{\frac{s}{p}}\left\{\int_{T_{0,\varepsilon}}\int_{Y_\varepsilon}|\xi_1-\xi_2|^p dx\,dt\right\}^{\frac{1}{p}}\\
&\le C\,(1+|\eta_1|^p+|\eta_2|^p+|\xi_1|^p+|\xi_2|^p)^{\frac{p-1-s}{p}}\ \ \|P_{\eta_1,\xi_1}-P_{\eta_2,\xi_2}\|^s\,\|\xi_1-\xi_2\|\\
&\le \frac{C(p-s)}{p\delta}(1+|\eta_1|^p+|\eta_2|^p+|\xi_1|^p+|\xi_2|^p)^{\frac{p-1-s}{p-s}}\,\|\xi_1-\xi_2\|^{\frac{p}{p-s}}+\frac{Cs\delta}{p}\|P_{\eta_1,\xi_1}-P_{\eta_2,\xi_2}\|^p.
\end{aligned}
$$

Here the last inequality holds by Young's inequality. Therefore, by taking the results from the above estimates into account, we obtain the conclusion. □

We have another technical property for the correctors. We will use the following sets in this lemma. At first, for each $0 \le k \le m$, let Ω_k and $(0,T)_k$ be proper subsets of Ω and $(0,T)$, respectively, satisfying $|\partial\Omega_k| = |\partial(0,T)_k| = 0$ and $(\Omega_k \cap \Omega_l) \times ((0,T)_k \cap (0,T)_l) = \emptyset$ for $k \neq l$. Furthermore, we have the sets $I_\varepsilon^k = \{i \in I_\varepsilon : Y_\varepsilon^i \subset \Omega_k\}$, $J_\varepsilon^k = \{j \in J_\varepsilon : T_{0,\varepsilon}^j \subset (0,T)_k\}$, $\tilde{I}_\varepsilon^k = \{i \in I_\varepsilon : Y_\varepsilon^i \cap \Omega_k \neq \emptyset,\ Y_\varepsilon^i \setminus \Omega_k \neq \emptyset\}$, $\tilde{J}_\varepsilon^k = \{j \in J_\varepsilon : T_{0,\varepsilon}^j \cap (0,T)_k \neq \emptyset,\ T_\varepsilon^j \setminus (0,T)_k \neq \emptyset\}$, $E_\varepsilon^{ijk} = \bigcup \overline{Y}_\varepsilon^i \times \overline{T}_{0,\varepsilon}^j$ with $i \in I_\varepsilon^k, j \in J_\varepsilon^k$, $\tilde{E}_\varepsilon^{ijk} = \bigcup \overline{Y}_\varepsilon^i \times \overline{T}_{0,\varepsilon}^j$ with $i \in \tilde{I}_\varepsilon^k, j \in \tilde{J}_\varepsilon^k$, and $\Omega_\varepsilon \times (0,T)_\varepsilon = \bigcup \overline{Y}_\varepsilon^i \times \overline{T}_{0,\varepsilon}^j$ with $Y_\varepsilon^i \subset \Omega$ and $T_{0,\varepsilon}^j \subset (0,T)$ for any $\varepsilon > 0$.

Also we define $\tilde{I}_\varepsilon = \{i \in \mathbb{Z}^d : Y_\varepsilon^i \cap \Omega \neq \emptyset,\ Y_\varepsilon^i \setminus \Omega \neq \emptyset\}$ and $\tilde{J}_\varepsilon = \{j \in \mathbb{Z} : T_{0,\varepsilon}^j \cap (0,T) \neq \emptyset,\ T_{0,\varepsilon}^j \setminus (0,T) \neq \emptyset\}$.

Lemma II.13. *Let $\delta > 0$ be given, and ϕ and ψ be simple functions defined by*

$$\phi(x,t) = \sum_{k=1}^m \phi_k 1_{\Omega_k}(x) 1_{(0,T)_k}(t), \qquad \psi(x,t) = \sum_{k=1}^m \psi_k 1_{\Omega_k}(x) 1_{(0,T)_k}(t),$$

with $\phi_k \in \mathbb{R} \setminus \{0\}$, $\psi_k \in \mathbb{R}^d \setminus \{0\}$ such that $\|u-\phi\|_{\mathcal{U}} \le \delta$ and $\|D_x u - \psi\|_{\mathcal{U}} \le \delta$. Then we have

$$\limsup_{\varepsilon\to 0} \|P(\cdot,\cdot,M_\varepsilon u, M_\varepsilon D_x u) - P(\cdot,\cdot,\phi,\psi)\|_{\mathcal{U}}$$
$$\le C(|\Omega\times(0,T)| + \|M_\varepsilon u\|_{\mathcal{U}} + \|M_\varepsilon D_x u\|_{\mathcal{U}} + \|\phi\|_{\mathcal{U}} + \|\psi\|_{\mathcal{U}})^{\frac{p-1-s}{p-s}} \|D_x u - \psi\|_{\mathcal{U}}^{\frac{1}{p-s}} + o(1).$$

Proof. Let us set $\Omega_0 = \Omega \setminus \bigcup_{k=1}^m \Omega_k$, $(0,T)_0 = (0,T)\setminus\bigcup_{k=1}^m (0,T)_k$, and $\phi_0 = \psi_0 = 0$. Then ϕ and ψ can be rewritten as $\phi(x,t) = \sum_{k=0}^m \phi_k 1_{\Omega_k}(x) 1_{(0,T)_k}(t)$ and $\psi(x,t) = \sum_{k=0}^m \psi_k 1_{\Omega_k}(x) 1_{(0,T)_k}(t)$. If we take $\varepsilon > 0$ sufficiently small, then we have $\Omega_k \times (0,T)_k \subset \Omega_\varepsilon \times (0,T)_\varepsilon$ for all $k \neq 0$. Therefore, the definition (2.39) of the piecewise constant function M_ε and the simple functions ϕ and ψ imply

$$\begin{aligned}
&\|P(\cdot,\cdot,M_\varepsilon u, M_\varepsilon D_x u) - P(\cdot,\cdot,\phi,\psi)\|^p_{L^p(0,T;L^p(\Omega))} \\
&= \int_{(0,T)_\varepsilon}\int_{\Omega_\varepsilon} \left|P(\tfrac{x}{\varepsilon},\tfrac{t}{\varepsilon^2},M_\varepsilon u, M_\varepsilon D_x u) - P(\tfrac{x}{\varepsilon},\tfrac{t}{\varepsilon^2},\phi_k,\psi_k)\right|^p dx\,dt \\
&\le \sum_{k=0}^m \int_{E_\varepsilon^{ijk}} \left|P(\tfrac{x}{\varepsilon},\tfrac{t}{\varepsilon^2},M_\varepsilon u, M_\varepsilon D_x u) - P(\tfrac{x}{\varepsilon},\tfrac{t}{\varepsilon^2},\phi_k,\psi_k)\right|^p dx\,dt \\
&\quad + \sum_{k=0}^m \int_{\tilde{E}_\varepsilon^{ijk}} \left|P(\tfrac{x}{\varepsilon},\tfrac{t}{\varepsilon^2},M_\varepsilon u, M_\varepsilon D_x u) - P(\tfrac{x}{\varepsilon},\tfrac{t}{\varepsilon^2},\phi_k,\psi_k)\right|^p dx\,dt.
\end{aligned}$$

Now we put

$$\eta_{ij} = \frac{1}{|Y_\varepsilon^i \times T_{0,\varepsilon}^j|}\int_{T_{0,\varepsilon}^j}\int_{Y_\varepsilon^i} u(x,t)dx\,dt, \qquad \xi_{ij} = \frac{1}{|Y_\varepsilon^i \times T_{0,\varepsilon}^j|}\int_{T_{0,\varepsilon}^j}\int_{Y_\varepsilon^i} D_x u(x,t)dx\,dt.$$

Then by the lemma II.12, we obtain

$$
\begin{aligned}
&\|P(\cdot,\cdot,M_\varepsilon u, M_\varepsilon D_x u) - P(\cdot,\cdot,\phi,\psi)\|^p_{L^p(0,T;L^p(\Omega))} \\
&\leq \sum_{k=0}^{m}\sum_{I^i_\varepsilon, J^j_\varepsilon}\int_{T^j_{0,\varepsilon}}\int_{Y^i_\varepsilon}\left|P\left(\tfrac{x}{\varepsilon},\tfrac{t}{\varepsilon^2},\eta_{ij},\xi_{ij}\right) - P\left(\tfrac{x}{\varepsilon},\tfrac{t}{\varepsilon^2},\phi_k,\psi_k\right)\right|^p dx\,dt \\
&\quad + \sum_{k=0}^{m}\sum_{\tilde{I}^i_\varepsilon, \tilde{J}^j_\varepsilon}\int_{T^j_{0,\varepsilon}}\int_{Y^i_\varepsilon}\left|P\left(\tfrac{x}{\varepsilon},\tfrac{t}{\varepsilon^2},\eta_{ij},\xi_{ij}\right) - P\left(\tfrac{x}{\varepsilon},\tfrac{t}{\varepsilon^2},\phi_k,\psi_k\right)\right|^p dx\,dt \\
&\leq \sum_{k=0}^{m}\sum_{I^i_\varepsilon, J^j_\varepsilon}\Big\{C(1+|\eta_{ij}|^p+|\phi_k|^p+|\xi_{ij}|^p+|\psi_k|^p)^{\frac{p-1-s}{p-s}}|\xi_{ij}-\psi_k|^{\frac{p}{p-s}}|Y^i_\varepsilon\times T^j_{0,\varepsilon}| \\
&\qquad\qquad + C\int_{T^j_{0,\varepsilon}}\int_{Y^i_\varepsilon}(1+|\eta_{ij}|^p+|\phi_k|^p+|\xi_{ij}|^p+|\psi_k|^p)\ \nu(|\eta_{ij}-\phi_k|)^q dxdt\Big\} \\
&\quad + \sum_{k=0}^{m}\sum_{\tilde{I}^i_\varepsilon, \tilde{J}^j_\varepsilon}\Big\{C(1+|\eta_{ij}|^p+|\phi_k|^p+|\xi_{ij}|^p+|\psi_k|^p)^{\frac{p-1-s}{p-s}}|\xi_{ij}-\psi_k|^{\frac{p}{p-s}}|Y^i_\varepsilon\times T^j_{0,\varepsilon}| \\
&\qquad\qquad + C\int_{T^j_{0,\varepsilon}}\int_{Y^i_\varepsilon}(1+|\eta_{ij}|^p+|\phi_k|^p+|\xi_{ij}|^p+|\psi_k|^p)\ \nu(|\eta_{ij}-\phi_k|)^q dxdt\Big\}.
\end{aligned}
$$

By the Hölder's inequality with $r_1 = \frac{p-s}{p-1-s}$ and $r_2 = p-s$ and the Jensen's inequality, we obtain

$$
\begin{aligned}
&\|P(\cdot,\cdot,M_\varepsilon u, M_\varepsilon D_x u) - P(\cdot,\cdot,\phi,\psi)\|^p_{L^p(0,T;L^p(\Omega))} \\
&\leq C\left\{\sum_{k=0}^{m}\left(|E^{ijk}_\varepsilon| + \int_{E^{ijk}_\varepsilon}|M_\varepsilon u|^p dxdt + |\phi_k|^p|E^{ijk}_\varepsilon| + \int_{E^{ijk}_\varepsilon}|M_\varepsilon D_x u|^p dxdt + |\psi_k|^p|E^{ijk}_\varepsilon|\right)\right\}^{\frac{p-1-s}{p-s}} \\
&\qquad \times \|M_\varepsilon D_x u - \psi\|^{\frac{p}{p-s}} \\
&\quad + C\sum_{k=0}^{m}\int_{E^{ijk}_\varepsilon}(1+|M_\varepsilon u|^p + |\phi_k|^p + |M_\varepsilon D_x u|^p + |\psi_k|^p)\,\nu(|\eta_{ij}-\phi_k|)^q dxdt \\
&\quad + C\left\{\sum_{k=0}^{m}\left(|\tilde{E}^{ijk}_\varepsilon| + \int_{\tilde{E}^{ijk}_\varepsilon}|M_\varepsilon u|^p dxdt + |\phi_k|^p|\tilde{E}^{ijk}_\varepsilon| + \int_{\tilde{E}^{ijk}_\varepsilon}|M_\varepsilon D_x u|^p dxdt + |\psi_k|^p|\tilde{E}^{ijk}_\varepsilon|\right)\right\}^{\frac{p-1-s}{p-s}} \\
&\qquad \times \|M_\varepsilon D_x u - \psi\|^{\frac{p}{p-s}} \\
&\quad + C\sum_{k=0}^{m}\int_{\tilde{E}^{ijk}_\varepsilon}(1+|M_\varepsilon u|^p + |\phi_k|^p + |M_\varepsilon D_x u|^p + |\psi_k|^p)\ \nu(|\eta_{ij}-\phi_k|)^q dxdt.
\end{aligned}
$$

It follows that, for the last integral on this estimate, it goes to zero generically.

Therefore,

$$
\begin{aligned}
&\|P(\cdot,\cdot,M_\varepsilon u, M_\varepsilon D_x u) - P(\cdot,\cdot,\phi,\psi)\|_{\mathcal{U}}^p \\
\leq & C(|\Omega\times(0,T)| + \|M_\varepsilon u\|_{\mathcal{U}}^p + \|\phi\|_{\mathcal{U}}^p + \|M_\varepsilon D_x u\|_{\mathcal{U}}^p + \|\psi\|_{\mathcal{U}}^p)^{\frac{p-1-s}{p-s}} \|D_x u - \psi\|_{\mathcal{U}}^{\frac{p}{p-s}} \\
&+C\left\{\sum_{k=0}^{m}\left(|\tilde{E}_\varepsilon^{ijk}| + \int_{\tilde{E}_\varepsilon^{ijk}} |M_\varepsilon u|^p dxdt + |\phi_k|^p|\tilde{E}_\varepsilon^{ijk}| + \int_{\tilde{E}_\varepsilon^{ijk}} |M_\varepsilon D_x u|^p dxdt + |\psi_k|^p|\tilde{E}_\varepsilon^{ijk}|\right)\right\}^{\frac{p-1-s}{p-s}} \\
&\qquad \times \|M_\varepsilon D_x u - \psi\|_{\mathcal{U}}^{\frac{p}{p-s}} \\
&+o(1).
\end{aligned}
$$

Since $|\partial\Omega_k| = |\partial\delta_k| = 0$ for $k \neq 0$, $|\tilde{E}_\varepsilon^{ijk}| \to 0$ as $\varepsilon \to 0$ for all k. Thus we get the result we desired. □

The next lemma shows us the uniform boundedness of $P(\cdot,\cdot,M_\varepsilon u, M_\varepsilon D_x u)$.

Lemma II.14. *We have the following property for $P(\cdot,\cdot,M_\varepsilon u, M_\varepsilon D_x u)$:*

$$\|P(\cdot,\cdot,M_\varepsilon u, M_\varepsilon D_x u)\|_{L^p(0,T;L^p(\Omega))}^p \leq C,$$

with constant $C > 0$ independent of ε.

This lemma can be proved in the similar way in [31]. Now we prove main theorem in this section.

Proof of Theorem II.11. The monotonicity assumption **A2** of the operator and adding

and subtracting same quantities imply

$$
\begin{aligned}
&\int_0^T\!\!\int_\Omega \left|P(\tfrac{x}{\varepsilon},\tfrac{t}{\varepsilon^2},M_\varepsilon u,M_\varepsilon D_x u)-D_x u_\varepsilon\right|^p dx\,dt\\
&\le C\int_0^T\!\!\int_\Omega \big(a(\tfrac{x}{\varepsilon},\tfrac{t}{\varepsilon^2},u_\varepsilon,P(\tfrac{x}{\varepsilon},\tfrac{t}{\varepsilon^2},M_\varepsilon u,M_\varepsilon D_x u))-a(\tfrac{x}{\varepsilon},\tfrac{t}{\varepsilon^2},u_\varepsilon,D_x u_\varepsilon),\\
&\qquad\qquad P(\tfrac{x}{\varepsilon},\tfrac{t}{\varepsilon^2},M_\varepsilon u,M_\varepsilon D_x u)-D_x u_\varepsilon\big)\,dx\,dt\\
&= C\Big|\int_0^T\!\!\int_\Omega \big(a(\tfrac{x}{\varepsilon},\tfrac{t}{\varepsilon^2},u_\varepsilon,P(\tfrac{x}{\varepsilon},\tfrac{t}{\varepsilon^2},M_\varepsilon u,M_\varepsilon D_x u))-a(\tfrac{x}{\varepsilon},\tfrac{t}{\varepsilon^2},M_\varepsilon u,P(\tfrac{x}{\varepsilon},\tfrac{t}{\varepsilon^2},M_\varepsilon u,M_\varepsilon D_x u))\\
&\qquad\qquad +a(\tfrac{x}{\varepsilon},\tfrac{t}{\varepsilon^2},M_\varepsilon u,P(\tfrac{x}{\varepsilon},\tfrac{t}{\varepsilon^2},M_\varepsilon u,M_\varepsilon D_x u))-a(\tfrac{x}{\varepsilon},\tfrac{t}{\varepsilon^2},u_\varepsilon,D_x u_\varepsilon),\\
&\qquad\qquad P(\tfrac{x}{\varepsilon},\tfrac{t}{\varepsilon^2},M_\varepsilon u,M_\varepsilon D_x u)-D_x u_\varepsilon\big)\,dx\,dt\Big|
\end{aligned}
$$

$$
\begin{aligned}
&\le C\Big|\int_0^T\!\!\int_\Omega \big(a(\tfrac{x}{\varepsilon},\tfrac{t}{\varepsilon^2},u_\varepsilon,P(\tfrac{x}{\varepsilon},\tfrac{t}{\varepsilon^2},M_\varepsilon u,M_\varepsilon D_x u))-a(\tfrac{x}{\varepsilon},\tfrac{t}{\varepsilon^2},M_\varepsilon u,P(\tfrac{x}{\varepsilon},\tfrac{t}{\varepsilon^2},M_\varepsilon u,M_\varepsilon D_x u)),\\
&\qquad\qquad P(\tfrac{x}{\varepsilon},\tfrac{t}{\varepsilon^2},M_\varepsilon u,M_\varepsilon D_x u)-D_x u_\varepsilon\big)\,dx\,dt\Big| \qquad (2.41)\\
&\quad +C\left|\int_0^T\!\!\int_\Omega \big(a(\tfrac{x}{\varepsilon},\tfrac{t}{\varepsilon^2},M_\varepsilon u,P(\tfrac{x}{\varepsilon},\tfrac{t}{\varepsilon^2},M_\varepsilon u,M_\varepsilon D_x u))-a(\tfrac{x}{\varepsilon},\tfrac{t}{\varepsilon^2},u_\varepsilon,D_x u_\varepsilon),\right.\\
&\qquad\qquad \left. P(\tfrac{x}{\varepsilon},\tfrac{t}{\varepsilon^2},M_\varepsilon u,M_\varepsilon D_x u)-D_x u_\varepsilon\big)\,dx\,dt\right|. \qquad (2.42)
\end{aligned}
$$

The second term (2.42) is split into the following four terms

$$
\begin{aligned}
&C\int_0^T\!\!\int_\Omega \big(a(\tfrac{x}{\varepsilon},\tfrac{t}{\varepsilon^2},M_\varepsilon u,P(\tfrac{x}{\varepsilon},\tfrac{t}{\varepsilon^2},M_\varepsilon u,M_\varepsilon D_x u)),P(\tfrac{x}{\varepsilon},\tfrac{t}{\varepsilon^2},M_\varepsilon u,M_\varepsilon D_x u)\big)\,dxdt \qquad (2.43)\\
&-C\int_0^T\!\!\int_\Omega \big(a(\tfrac{x}{\varepsilon},\tfrac{t}{\varepsilon^2},M_\varepsilon u,P(\tfrac{x}{\varepsilon},\tfrac{t}{\varepsilon^2},M_\varepsilon u,M_\varepsilon D_x u)),D_x u_\varepsilon\big)\,dx\,dt \qquad (2.44)\\
&-C\int_0^T\!\!\int_\Omega \big(a(\tfrac{x}{\varepsilon},\tfrac{t}{\varepsilon^2},u_\varepsilon,D_x u_\varepsilon),P(\tfrac{x}{\varepsilon},\tfrac{t}{\varepsilon^2},M_\varepsilon u,M_\varepsilon D_x u)\big)\,dx\,dt \qquad (2.45)\\
&+C\int_0^T\!\!\int_\Omega \big(a(\tfrac{x}{\varepsilon},\tfrac{t}{\varepsilon^2},u_\varepsilon,D_x u_\varepsilon),D_x u_\varepsilon\big)\,dx\,dt. \qquad (2.46)
\end{aligned}
$$

We are going to get the limit in each term as $\varepsilon\to 0$.

Step 1. In (2.43), the domain of integration can be divided into inner cells and

boundary cells. Thus, (2.43) can be rewritten as

$$\begin{aligned}
&\int_0^T\int_\Omega \big(a(\tfrac{x}{\varepsilon},\tfrac{t}{\varepsilon^2},M_\varepsilon u,P(\tfrac{x}{\varepsilon},\tfrac{t}{\varepsilon^2},M_\varepsilon u,M_\varepsilon D_x u)),P(\tfrac{x}{\varepsilon},\tfrac{t}{\varepsilon^2},M_\varepsilon u,M_\varepsilon D_x u)\big)\,dx\,dt\\
=&\sum_{i\in I_\varepsilon}\sum_{j\in J_\varepsilon}\int_{T^j_{0,\varepsilon}}\int_{Y^i_\varepsilon}(a(\tfrac{x}{\varepsilon},\tfrac{t}{\varepsilon^2},M_\varepsilon u,P(\tfrac{x}{\varepsilon},\tfrac{t}{\varepsilon^2},M_\varepsilon u,M_\varepsilon D_x u)),P(\tfrac{x}{\varepsilon},\tfrac{t}{\varepsilon^2},M_\varepsilon u,M_\varepsilon D_x u))dx\,dt\\
&\quad+\int_{(0,T)\setminus(0,T)_\varepsilon}\int_{\Omega\setminus\Omega_\varepsilon}\big(a(\tfrac{x}{\varepsilon},\tfrac{t}{\varepsilon^2},0,P(\tfrac{x}{\varepsilon},\tfrac{t}{\varepsilon^2},0,0)),P(\tfrac{x}{\varepsilon},\tfrac{t}{\varepsilon^2},0,0)\big)\,dx\,dt. \qquad (2.47)
\end{aligned}$$

By the definition of the piecewise constant function $M_\varepsilon u$ the first term in (2.47) is going to be

$$\begin{aligned}
&\sum_{i\in I_\varepsilon}\sum_{j\in J_\varepsilon}\int_{T^j_{0,\varepsilon}}\int_{Y^i_\varepsilon}\big(a(\tfrac{x}{\varepsilon},\tfrac{t}{\varepsilon^2},\eta_{ij},\xi_{ij}+D_xN_{\eta_{ij},\xi_{ij}}(\tfrac{x}{\varepsilon},\tfrac{t}{\varepsilon^2})),\xi_{ij}+D_xN_{\eta_{ij}\xi_{ij}}(\tfrac{x}{\varepsilon},\tfrac{t}{\varepsilon^2})\big)\,dx\,dt\\
=&\sum_{i\in I_\varepsilon}\sum_{j\in J_\varepsilon}\int_{T^j_{0,\varepsilon}}\int_{Y^i_\varepsilon}1_{Y^i_\varepsilon}(x)\;1_{T^j_{0,\varepsilon}}(t)\left\langle\big(a(\cdot,\cdot,\eta_{ij},\xi_{ij}+D_xN_{\eta_{ij},\xi_{ij}}),\xi_{ij}+D_xN_{\eta_{ij},\xi_{ij}}\big)\right\rangle dxdt\\
=&\sum_{i\in I_\varepsilon}\sum_{j\in J_\varepsilon}\int_{T^j_{0,\varepsilon}}\int_{Y^i_\varepsilon}1_{Y^i_\varepsilon}(x)\;1_{T^j_{0,\varepsilon}}(t)\left\langle\big(a(\cdot,\cdot,\eta_{ij},\xi_{ij}+D_xN_{\eta_{ij},\xi_{ij}}),\xi_{ij}\big)\right\rangle dxdt \qquad (2.48)\\
&+\sum_{i\in I_\varepsilon}\sum_{j\in J_\varepsilon}\int_{T^j_{0,\varepsilon}}\int_{Y^i_\varepsilon}1_{Y^i_\varepsilon}(x)\;1_{T^j_{0,\varepsilon}}(t)\left\langle\big(a(\cdot,\cdot,\eta_{ij},\xi_{ij}+D_xN_{\eta_{ij},\xi_{ij}}),D_xN_{\eta_{ij}\xi_{ij}}\big)\right\rangle dxdt.
\end{aligned}$$

The average value in the second term of (2.48) is computed in the following way:

$$\begin{aligned}
&\left\langle\big(a(\cdot,\cdot,\eta_{ij},\xi_{ij}+D_xN_{\eta_{ij},\xi_{ij}}),D_xN_{\eta_{ij},\xi_{ij}}\big)\right\rangle\\
=&-\left\langle\big(\text{div }a(\cdot,\cdot,\eta_{ij},\xi_{ij}+D_xN_{\eta_{ij},\xi_{ij}}),N_{\eta_{ij},\xi_{ij}}\big)\right\rangle\\
=&-\left\langle\big(D_tN_{\eta_{ij},\xi_{ij}},N_{\eta_{ij},\xi_{ij}}\big)\right\rangle\\
=&-\left\langle\frac{1}{2}D_t\left|N_{\eta_{ij},\xi_{ij}}\right|^2\right\rangle=0,
\end{aligned}$$

which implies that the second term of (2.48) will be zero. Thus, (2.48) becomes the

followings

$$\begin{aligned}
&\sum_{i\in I_\varepsilon}\sum_{j\in J_\varepsilon}\int_{T^j_{0,\varepsilon}}\int_{Y^i_\varepsilon} 1_{y^i_\varepsilon}(x)\ 1_{T^j_{0,\varepsilon}}(t)\ (a^*(\eta_{ij},\xi_{ij}),\xi_{ij})\ dx\,dt \\
= &\int_0^T\int_\Omega (a^*(M_\varepsilon u, M_\varepsilon D_x u), M_\varepsilon D_x u)\ dx\,dt, \qquad (2.49)
\end{aligned}$$

which converges to

$$\int_0^T\int_\Omega (a^*(u, D_x u), D_x u)\ dx\,dt, \qquad (2.50)$$

as ε tends to zero. Indeed, we consider the difference between (2.49) and (2.50), and we add and subtract same quantity. Then we obtain the following estimates for the difference by using Hölder's inequality

$$\begin{aligned}
&\int_0^T\int_\Omega (a^*(M_\varepsilon u, M_\varepsilon D_x u), M_\varepsilon D_x u)dxdt - \int_0^T\int_\Omega (a^*(u, D_x u), D_x u)dxdt \\
=&\int_0^T\int_\Omega (a^*(M_\varepsilon u, M_\varepsilon D_x u) - a^*(u, D_x u), M_\varepsilon D_x u)\ dx\,dt \\
&+\int_0^T\int_\Omega (a^*(u, D_x u), M_\varepsilon D_x u - D_x u)\ dx\,dt \\
\le&\left(\int_0^T\int_\Omega |a^*(M_\varepsilon u, M_\varepsilon D_x u) - a^*(u, D_x u)|^q\,dx\,dt\right)^{1/q}\left(\int_0^T\int_\Omega |M_\varepsilon D_x u|^p dx\,dt\right)^{1/p} \\
&+\left(\int_0^T\int_\Omega |a^*(u, D_x u)|^q dx\,dt\right)^{1/q}\left(\int_0^T\int_\Omega |M_\varepsilon D_x u - D_x u|^p dx\,dt\right)^{1/p}.
\end{aligned}$$

By the continuity assumption **A4** we have the following estimate

$$\begin{aligned}
&\int_0^T\int_\Omega |a^*(M_\varepsilon u, M_\varepsilon D_x u) - a^*(u, D_x u)|^q\,dx\,dt \\
\le&\int_0^T\int_\Omega (1+|M_\varepsilon u|+|M_\varepsilon D_x u|+|u|+|D_x u|)^p \nu(|M_\varepsilon u - u|)^q dx\,dt \\
&+\int_0^T\int_\Omega (1+|M_\varepsilon u|+|M_\varepsilon D_x u|+|u|+|D_x u|)^{(p-1-s)q}|M_\varepsilon D_x u - D_x u|^{sq},
\end{aligned}$$

which converges to zero as $\varepsilon \to 0$. This implies that the difference between (2.49) and (2.50) tends to zero as ε approaches zero. Therefore, the first term of (2.47) converges

to

$$\int_0^T\int_\Omega (a^*(u, D_x u), D_x u)\, dx\, dt,$$

as $\varepsilon \to 0$. It remains to show that the second term of (2.47) goes to zero as ε tends to zero. The continuity assumption **A4** implies that

$$\begin{aligned}
&\int_{(0,T)\setminus(0,T)_\varepsilon}\int_{\Omega\setminus\Omega_\varepsilon} \big(a(\tfrac{x}{\varepsilon}, \tfrac{t}{\varepsilon^2}, 0, P(\tfrac{x}{\varepsilon}, \tfrac{t}{\varepsilon^2}, 0, 0)), P(\tfrac{x}{\varepsilon}, \tfrac{t}{\varepsilon^2}, 0, 0)\big)\, dx\, dt \\
&\le C\int_{(0,T)\setminus(0,T)_\varepsilon}\int_{\Omega\setminus\Omega_\varepsilon}(1+|P_{0,0}|)^p dxdt + \int_{(0,T)\setminus(0,T)_\varepsilon}\int_{\Omega\setminus\Omega_\varepsilon}(a(\tfrac{x}{\varepsilon}, \tfrac{t}{\varepsilon^2}, 0, 0), P_{0,0})dxdt \\
&\le C|(\Omega\setminus\Omega_\varepsilon)\times((0,T)\setminus(0,T)_\varepsilon)| + \int_{(0,T)\setminus(0,T)_\varepsilon}\int_{\Omega\setminus\Omega_\varepsilon}|P_{0,0}|^p dxdt \\
&\quad + C\left(\sum_{j\in\tilde{J}_\varepsilon}\sum_{i\in\tilde{I}_\varepsilon}|Y_\varepsilon^i\times T_{0,\varepsilon}^j|\right)^{1/q}\left(\int_{(0,T)\setminus(0,T)_\varepsilon}\int_{\Omega\setminus\Omega_\varepsilon}|P_{0,0}|^p\, dxdt\right)^{1/p}.
\end{aligned}$$

Since, as $\varepsilon\to 0$, $|(\Omega\setminus\Omega_\varepsilon)\times((0,T)\setminus(0,T)_\varepsilon)|$ tends to zero and $\sum_{j\in\tilde{J}_\varepsilon}\sum_{i\in\tilde{I}_\varepsilon}|Y_\varepsilon^i\times T_{0,\varepsilon}^j|$ goes to $|\partial\Omega\times\partial(0,T)|$, it is enough to show that $\int_{(0,T)\setminus(0,T)_\varepsilon}\int_{\Omega\setminus\Omega_\varepsilon}|P_{0,0}|^p dxdt$ approaches to zero. Indeed, by Hölder's inequality with $r_1=\frac{p+\gamma}{p}$ and $r_2=\frac{p+\gamma}{\gamma}$ for some $\gamma>0$ we have

$$\begin{aligned}
&\int_{(0,T)\setminus(0,T)_\varepsilon}\int_{\Omega\setminus\Omega_\varepsilon}|P_{0,0}|^p dxdt \\
\le\ & C\left(\sum_{j\in\tilde{J}_\varepsilon}\sum_{i\in\tilde{I}_\varepsilon}\|P_{0,0}\|^{p+\gamma}_{L^{p+\gamma}(T_{0,\varepsilon};L^{p+\gamma}(Y_\varepsilon^i))}\right)^{\frac{p}{p+\gamma}}|(\Omega\setminus\Omega_\varepsilon)\times((0,T)\setminus(0,T)_\varepsilon)|^{\frac{\gamma}{p+\gamma}} \\
\le\ & C\left(\sum_{\tilde{J}_\varepsilon}\sum_{\tilde{I}_\varepsilon}|Y_\varepsilon^i\times T_{0,\varepsilon}^j|\right)^{\frac{p}{p+\gamma}}|(\Omega\setminus\Omega_\varepsilon)\times((0,T)\setminus(0,T)_\varepsilon)|^{\frac{\gamma}{p+\gamma}},
\end{aligned}$$

which converges to zero as ε tends to zero.

Step 2. The second term (2.44) is

$$\begin{aligned}
&\int_0^T\int_\Omega \left(a(\tfrac{x}{\varepsilon},\tfrac{t}{\varepsilon^2},M_\varepsilon u,P(\tfrac{x}{\varepsilon},\tfrac{t}{\varepsilon^2},M_\varepsilon u,M_\varepsilon D_x u)),D_x u_\varepsilon\right)dx\,dt\\
&=\int_0^T\int_\Omega \left(a(\tfrac{x}{\varepsilon},\tfrac{t}{\varepsilon^2},M_\varepsilon u,P_{M_\varepsilon u,M_\varepsilon D_x u})-a(\tfrac{x}{\varepsilon},\tfrac{t}{\varepsilon^2},\phi,P_{\phi,\psi}),D_x u_\varepsilon\right)dx\,dt \qquad (2.51)\\
&\quad+\int_0^T\int_\Omega \left(a(\tfrac{x}{\varepsilon},\tfrac{t}{\varepsilon^2},\phi,P_{\phi,\psi}),D_x u_\varepsilon\right)dx\,dt, \qquad (2.52)
\end{aligned}$$

where ϕ and ψ are simple functions satisfying the conditions in Lemma II.13 for any $\delta>0$. The second term (2.52) is equal to

$$\sum_{k=0}^m\int_{(0,T)_k}\int_{\Omega_k}\left(a(\tfrac{x}{\varepsilon},\tfrac{t}{\varepsilon^2},\phi_k,P(\tfrac{x}{\varepsilon},\tfrac{t}{\varepsilon^2},\phi_k,\psi_k)),D_x u_\varepsilon\right)dx\,dt. \qquad (2.53)$$

Now we claim that $D_x u_\varepsilon$ is bounded in $L^p(0,T;L^p(\Omega))$ and $a(\frac{x}{\varepsilon},\frac{t}{\varepsilon^2},\phi_k,P(\frac{x}{\varepsilon},\frac{t}{\varepsilon^2},\phi_k,\psi_k))$ is bounded in $L^r((0,T)_k;L^r(\Omega_k))$ for $r>q$. Indeed, since $\|P(\cdot,\cdot,,\eta,\xi)\|_{\mathcal{U}}\le C(1+|\eta|^p+|\xi|^p)|\Omega\times(0,T)|$ and by using Meyers type estimates, $\|P(\cdot,\cdot,\phi_k,\psi_k)\|_{L^{p+\gamma}(0,T;L^{p+\gamma}(\Omega))}$ is uniformly bounded in $L^{p+\gamma}(0,T;L^{p+\gamma}(\Omega))$. This implies that $a(\frac{x}{\varepsilon},\frac{t}{\varepsilon^2},\phi_k,P(\frac{x}{\varepsilon},\frac{t}{\varepsilon^2},\phi_k,\psi_k))$ is uniformly bounded in $L^r(0,T;L^r(\Omega))$ for $r>q$. Therefore $(a(\frac{x}{\varepsilon},\frac{t}{\varepsilon^2},\phi_k,P(\frac{x}{\varepsilon},\frac{t}{\varepsilon^2},\phi_k,\psi_k)),D_x u_\varepsilon)$ is bounded in $L^\sigma(0,T;L^\sigma(\Omega))$ for $\sigma>1$. Thus there exists a subsequence such that $(a(\frac{x}{\varepsilon},\frac{t}{\varepsilon^2},\phi_k,P(\frac{x}{\varepsilon},\frac{t}{\varepsilon^2},\phi_k,\psi_k)),D_x u_\varepsilon)$ converges to g_k weakly. On the other hand, $a(\frac{x}{\varepsilon},\frac{t}{\varepsilon^2},\phi_k,\ P(\frac{x}{\varepsilon},\frac{t}{\varepsilon^2},\phi_k,\psi_k))$ converges to $a^*(\phi_k,\psi_k)$ weakly in $L^q(0,T;L^q(\Omega))$. By the compensated compactness, $g_k=(a^*(\phi_k,\psi_k),D_x u)$ as $\varepsilon\to 0$. From the boundedness of $D_x u_\varepsilon$, $D_x u_\varepsilon$ converges to $D_x u$ weakly. Consequently, (2.53) converges to

$$\sum_{k=0}^m\int_{(0,T)_k}\int_{\Omega_k}(a^*(\phi_k,\psi_k),D_x u)\,dx\,dt=\int_0^T\int_\Omega(a^*(\phi,\psi),D_x u)dx\,dt.$$

Now, we go back to (2.51). The fourth assumption **A4** implies that

$$\begin{aligned}
&\int_0^T\!\!\int_\Omega (a(\tfrac{x}{\varepsilon},\tfrac{t}{\varepsilon^2},M_\varepsilon u,P(\tfrac{x}{\varepsilon},\tfrac{t}{\varepsilon^2},M_\varepsilon u,M_\varepsilon D_x u))-a(\tfrac{x}{\varepsilon},\tfrac{t}{\varepsilon^2},\phi,P(\tfrac{x}{\varepsilon},\tfrac{t}{\varepsilon^2},\phi,\psi)),D_x u_\varepsilon)dx\,dt\\
&\le C\int_0^T\!\!\int_\Omega (1+|M_\varepsilon u|^{p-1}+|P(\cdot,\cdot,M_\varepsilon u,M_\varepsilon D_x u)|^{p-1}+|\phi|^{p-1}+|P(\cdot,\cdot,\phi,\psi)|^{p-1})\\
&\qquad\times\nu(|M_\varepsilon u-\phi|)|D_x u_\varepsilon|dx\,dt \qquad (2.54)\\
&+C\int_0^T\!\!\int_\Omega (1+|M_\varepsilon u|^{p-1-s}+|P(\cdot,\cdot,M_\varepsilon u,M_\varepsilon D_x u)|^{p-1-s}+|\phi|^{p-1-s}+|P(\cdot,\cdot,\phi,\psi)|^{p-1-s})\\
&\qquad\times|P(\cdot,\cdot,M_\varepsilon u,M_\varepsilon D_x u)-P(\cdot,\cdot,\phi,\psi)|^s\ |D_x u_\varepsilon|dx\,dt. \qquad (2.55)
\end{aligned}$$

By the Hölder's inequality with $r_1=q$ and $r_2=p$, the first term (2.54) is at most

$$\begin{aligned}
&C\bigg(\int_0^T\!\!\int_\Omega (1+|M_\varepsilon u|^p+|P_{M_\varepsilon u,M_\varepsilon D_x u}|^p+|\phi|^p+|P_{\phi,\psi}|^p)\,\nu(|M_\varepsilon u-\phi|)|^q dx\,dt\bigg)^{1/q}\\
&\qquad\times\bigg(\int_0^T\!\!\int_\Omega |D_x u_\varepsilon|^p\bigg)^{1/p},
\end{aligned}$$

which converges to zero as $\varepsilon\to 0$, since $|M_\varepsilon u-\phi|\to 0$ in $L^p(0,T;L^p(\Omega))$ and $\int_0^T\!\int_\Omega |D_x u_\varepsilon|^p dx\,dt$ is bounded. For the second term (2.55) we apply Hölder's inequality again with $r_1=\frac{p}{p-1-s}$, $r_2=\frac{p}{s}$, and $r_3=p$:

$$\begin{aligned}
&C\int_0^T\!\!\int_\Omega \big(1+|M_\varepsilon u|^{p-1-s}+|P(\cdot,\cdot,M_\varepsilon u,M_\varepsilon D_x u)|^{p-1-s}+|\phi|^{p-1-s}+|P(\cdot,\cdot,\phi,\psi)|^{p-1-s}\big)\\
&\qquad\times|M_\varepsilon D_x u-\psi|^s\ |D_x u_\varepsilon|dx\,dt\\
&\le C\bigg\{\int_0^T\!\!\int_\Omega (1+|M_\varepsilon u|^p+|P(\cdot,\cdot,M_\varepsilon u,M_\varepsilon D_x u)|^p+|\phi|^p+|P(\cdot,\cdot,\phi,\psi)|^p)\,dx\,dt\bigg\}^{\frac{p-1-s}{p}}\\
&\qquad\times\bigg\{\int_0^T\!\!\int_\Omega |P(\cdot,\cdot,M_\varepsilon u,M_\varepsilon D_x u)-P(\cdot,\cdot,\phi,\psi)|^p dx\,dt\bigg\}^{s/p}\bigg\{\int_0^T\!\!\int_\Omega |D_x u_\varepsilon|^p dx\,dt\bigg\}^{1/p}.
\end{aligned}$$

So by the Lemma II.13 and Lemma II.14, we get

$$\limsup_{\varepsilon\to 0}\left|\int_0^T\!\!\int_\Omega (a(\tfrac{x}{\varepsilon},\tfrac{t}{\varepsilon^2},M_\varepsilon u,P_{M_\varepsilon u,M_\varepsilon D_x u})-a(\tfrac{x}{\varepsilon},\tfrac{t}{\varepsilon^2},\phi,P_{\phi,\psi}),D_x u_\varepsilon)dx\,dt\right|=0.$$

Therefore, the second term (2.44) converges to

$$\int_0^T\int_\Omega (a^*(u, D_x u), D_x u)\ dx\, dt,$$

as $\varepsilon \to 0$.

Step 3. The third term (2.45) can be modified in the following way:

$$\begin{aligned}
&\int_0^T\int_\Omega \left(a(\tfrac{x}{\varepsilon}, \tfrac{t}{\varepsilon^2}, u_\varepsilon, D_x u_\varepsilon), P(\tfrac{x}{\varepsilon}, \tfrac{t}{\varepsilon^2}, M_\varepsilon u, M_\varepsilon D_x u)\right) dx\, dt \\
=&\int_0^T\int_\Omega \left(a(\tfrac{x}{\varepsilon}, \tfrac{t}{\varepsilon^2}, u_\varepsilon, D_x u_\varepsilon), P_{\phi,\psi}\right) dxdt + \int_0^T\int_\Omega \left(a(\tfrac{x}{\varepsilon}, \tfrac{t}{\varepsilon^2}, u_\varepsilon, D_x u_\varepsilon), P_{M_\varepsilon u, M_\varepsilon D_x u} - P_{\phi,\psi}\right) dxdt \\
=&\sum_{k=0}^m \int_{(0,T)_k}\int_{\Omega_k} \left(a(\tfrac{x}{\varepsilon}, \tfrac{t}{\varepsilon^2}, u_\varepsilon, D_x u_\varepsilon), P_{\phi,\psi}\right) dx\, dt \qquad (2.56) \\
&+\int_0^T\int_\Omega \left(a(\tfrac{x}{\varepsilon}, \tfrac{t}{\varepsilon^2}, u_\varepsilon, D_x u_\varepsilon), P_{M_\varepsilon u, M_\varepsilon D_x u} - P_{\phi,\psi}\right) dx\, dt. \qquad (2.57)
\end{aligned}$$

We note that, in (2.56), $a(\frac{x}{\varepsilon}, \frac{t}{\varepsilon^2}, u_\varepsilon, D_x u_\varepsilon)$ is bounded in $L^q(0,T; L^q(\Omega))$ and $P(\frac{x}{\varepsilon}, \frac{t}{\varepsilon^2}, \phi, \psi)$ is bounded in $L^{p+\gamma}(0,T; L^{p+\gamma}(\Omega))$. Similar to the Step 2, we claim that

$$\sum_{k=0}^m \int_{(0,T)_k}\int_{\Omega_k} \left(a\left(\tfrac{x}{\varepsilon}, \tfrac{t}{\varepsilon^2}, u_\varepsilon, D_x u_\varepsilon\right), P_{\phi,\psi}\right) dx\, dt \to \int_0^T\int_\Omega (a^*(u, D_x u), \psi) dx\, dt.$$

The Hölder's inequality and the analogous arguments in step 2 imply that the second term (2.57) converges to zero. Thus, we get the third term (2.45) converges to

$$\int_0^T\int_\Omega (a^*(u, D_x u), D_x u)\ dx\, dt,$$

as $\varepsilon \to 0$.

Step 4. The fourth term (2.46) is

$$\begin{aligned}
&\int_0^T\!\!\int_\Omega \left(a\left(\tfrac{x}{\varepsilon}, \tfrac{t}{\varepsilon^2}, u_\varepsilon, D_x u_\varepsilon\right), D_x u_\varepsilon\right) dx\, dt \\
= & -\int_0^T\!\!\int_\Omega \operatorname{div}\left(a\left(\tfrac{x}{\varepsilon}, \tfrac{t}{\varepsilon^2}, u_\varepsilon, D_x u_\varepsilon\right)\right) u_\varepsilon dx\, dt \\
= & -\int_0^T\!\!\int_\Omega \left(D_t u_\varepsilon + a_0\left(\tfrac{x}{\varepsilon}, \tfrac{t}{\varepsilon^2}, u_\varepsilon, D_x u_\varepsilon\right) - f\right) u_\varepsilon dx\, dt \\
= & -\left\langle D_t u_\varepsilon, u_\varepsilon\right\rangle + \left\langle -a_0\left(\tfrac{x}{\varepsilon}, \tfrac{t}{\varepsilon^2}, u_\varepsilon, D_x u_\varepsilon\right) + f,\ u_\varepsilon\right\rangle \\
= & -\frac{1}{2}\left(\|u_\varepsilon(T)\|^2_{L^2(\Omega)} - \|u_\varepsilon(0)\|^2_{L^2(\Omega)}\right) + \left\langle -a_0\left(\tfrac{x}{\varepsilon}, \tfrac{t}{\varepsilon^2}, u_\varepsilon, D_x u_\varepsilon\right) + f,\ u_\varepsilon\right\rangle.
\end{aligned}$$

When we pass to the limit in the right hand side, we have

$$\begin{aligned}
& -\frac{1}{2}\left(\|u(T)\|^2_{L^2} - \|u(0)\|^2_{L^2}\right) + \left\langle -a_0^*\left(u, D_x u\right) + f, u\right\rangle \\
= & -\left\langle D_t u, u\right\rangle + \left\langle -a_0^*\left(u, D_x u\right) + f, u\right\rangle \\
= & -\int_0^T\!\!\int_\Omega \left(D_t u + a_0^*\left(u, D_x u\right) - f\right) u dx\, dt \\
= & \int_0^T\!\!\int_\Omega (a^*(u, D_x u), D_x u) dx\, dt.
\end{aligned}$$

By assembling the four results from the four steps, we conclude that (2.42) converges to zero as $\varepsilon \to 0$.

The only remaining thing we have to show is (2.41) converges to zero. Since $D_x u_\varepsilon$ is bounded in $L^p(0,T;L^p(\Omega))$ and by Lemma II.14,$P_{M_\varepsilon u, M_\varepsilon D_x u}$–$D_x u_\varepsilon$ is bounded in $L^p(0,T;L^p(\Omega))$. By Hölder's inequality with $r_1 = q$ and $r_2 = p$ and Young's

inequality for some $\delta > 0$, we have

$$\left| \int_0^T \int_\Omega \left(a(\tfrac{x}{\varepsilon}, \tfrac{t}{\varepsilon^2}, u_\varepsilon, P_{M_\varepsilon u, M_\varepsilon D_x u}) - a(\tfrac{x}{\varepsilon}, \tfrac{t}{\varepsilon^2}, M_\varepsilon u, P_{M_\varepsilon u, M_\varepsilon D_x u}), P_{M_\varepsilon u, M_\varepsilon D_x u} - D_x u_\varepsilon \right) dx dt \right|$$

$$\leq \frac{C}{q\delta} \int_0^T \int_\Omega \left| \left(a(\tfrac{x}{\varepsilon}, \tfrac{t}{\varepsilon^2}, u_\varepsilon, P_{M_\varepsilon u, M_\varepsilon D_x u}) - a(\tfrac{x}{\varepsilon}, \tfrac{t}{\varepsilon^2}, M_\varepsilon u, P_{M_\varepsilon u, M_\varepsilon D_x u}) \right|^q dx dt \tag{2.58}$$

$$+ \frac{C\delta}{p} \int_0^T \int_\Omega |P_{M_\varepsilon u, M_\varepsilon D_x u} - D_x u_\varepsilon|^p \, dx \, dt. \tag{2.59}$$

The continuity assumption **A4** implies that

$$\int_0^T \int_\Omega \left| (a(\tfrac{x}{\varepsilon}, \tfrac{t}{\varepsilon^2}, u_\varepsilon, P_{M_\varepsilon u, M_\varepsilon D_x u}) - a(\tfrac{x}{\varepsilon}, \tfrac{t}{\varepsilon^2}, M_\varepsilon u, P_{M_\varepsilon u, M_\varepsilon D_x u}) \right|^q dx \, dt$$

$$\leq C \int_0^T \int_\Omega (1 + |u_\varepsilon|^p + |M_\varepsilon u|^p + |P_{M_\varepsilon u, M_\varepsilon D_x u}|^p) \, \nu(|u_\varepsilon - M_\varepsilon u|)^q dx \, dt.$$

By Lemma II.14, $P_{M_\varepsilon u, M_\varepsilon D_x u}$ is bounded in $L^p(0, T; L^p(\Omega))$, and hence (2.58) converges to zero as ε tends to zero. On the other hand, (2.59) can be moved to the left hand side by choosing $\delta > 0$ appropriately. Therefore we get our conclusion as desired. □

D. Numerical examples

In this section, we perform numerical homogenization of nonlinear parabolic equations. We consider the following nonlinear periodic parabolic equation in two dimensions:

$$D_t u_\varepsilon - \mathrm{div}_x(a(x/\varepsilon^\beta, t/\varepsilon^\alpha, u_\varepsilon) D_x u_\varepsilon) = f \quad \text{in } (0,1) \times (0,1), \tag{2.60}$$

with the zero initial condition and the following boundary conditions: $u_\varepsilon = 0$ on the left vertical edge, $u_\varepsilon = 1$ on the right vertical edge, and homogeneous Neumann

conditions on the both lateral edges. Here a is given by

$$a = \begin{pmatrix} d(1+F'(u_\varepsilon)) & -H(x/\varepsilon^\beta, t/\varepsilon^\alpha)F'(u_\varepsilon) \\ H(x/\varepsilon^\beta, t/\varepsilon^\alpha)F'(u_\varepsilon) & d(1+F'(u_\varepsilon)) \end{pmatrix},$$

the number d is the molecular diffusion of a periodic convection and periodic diffusion equation

$$D_t u_\varepsilon - \frac{1}{\varepsilon} v(x/\varepsilon^\beta, t/\varepsilon^\alpha) \cdot D_x F(u_\varepsilon) - d(1+F'(u_\varepsilon))\Delta_{xx} u_\varepsilon = f,$$

which is equivalent to (2.60), F is a flux function, f is a given source term which will be assumed to be zero in this section, and H is the stream function satisfying $v = (\frac{\partial H}{\partial x_2}, -\frac{\partial H}{\partial x_1})$, where v is the velocity field such that $\mathrm{div}_x v = 0$. In addition, the nonlinear operator $a(x/\varepsilon^\beta, t/\varepsilon^\alpha, u_\varepsilon)D_x u_\varepsilon$ satisfies the assumptions **A1**-**A4**.

Homogenization theory [11] gives us that u_ε converges to u, where u is the solution of the homogenized equation

$$D_t u - \mathrm{div}_x(a^*(u)D_x u) = 0.$$

Here $a^*(\eta)\xi = \langle a(y,\tau,\eta)(\xi + D_y N_{\eta,\xi})\rangle$, where $N_{\eta,\xi}$ is the solution of an auxiliary problem which depends on the ratio between α and β (see (2.16)). However, we consider only the case of $\alpha = 2\beta$ in this section. We note that, from the homogenization theory, $N_{\eta,\xi} = \chi^{(1)}(y)\xi_1 + \chi^{(2)}(y)\xi_2$, where $\xi = (\xi_1, \xi_2)^T$, and $\chi^{(1)}$ and $\chi^{(2)}$ are solutions of

$$D_\tau \chi^{(1)} - \mathrm{div}(a(y,\tau,\eta)(\nabla(\chi^{(1)} + y_1))) = 0,$$
$$D_\tau \chi^{(2)} - \mathrm{div}(a(y,\tau,\eta)(\nabla(\chi^{(2)} + y_2))) = 0,$$

respectively. This implies that $D_y N_{\eta,\xi}$ linear in ξ, that is,

$$D_y N_{\eta,\xi} = \begin{pmatrix} \frac{\partial \chi^{(1)}}{\partial y_1} & \frac{\partial \chi^{(2)}}{\partial y_1} \\ \frac{\partial \chi^{(1)}}{\partial y_2} & \frac{\partial \chi^{(2)}}{\partial y_2} \end{pmatrix} \begin{pmatrix} \xi_1 \\ \xi_2 \end{pmatrix}.$$

Thus, the homogenized coefficient a_{ij}^* can be computed by

$$a_{ij}^*(\eta) = d(1 + F'(\eta))\delta_{ij} + \langle H_{ik}F'(\eta)\frac{\partial \chi^j}{\partial y_k}\rangle, \tag{2.61}$$

where H_{ik} is the component of stream function matrix $\mathbf{H}$ satisfying $\mathrm{div}_x\mathbf{H} = \mathbf{v}$. Here the second term on the right-hand side of (2.61) is the enhanced diffusivity matrix because of the periodic flow.

Now we consider the numerical homogenization procedure. At each time step we calculate the average of u_ε over the domain. And then we use this average to solve the local problem and compute the enhanced diffusion. The numerical results will be presented to show the importance of the enhanced diffusivity, that is, we will compare them with the averaged solution without the enhanced diffusion.

We choose the period $\varepsilon = 0.1$ and the molecular diffusion $d = 0.1$. In addition, the periodic stream function H for convection terms is defined by

$$H(x/\varepsilon, t/\varepsilon^2) = \{\sin(2\pi x/\varepsilon)\sin(2\pi y/\varepsilon) + \delta\cos(2\pi x/\varepsilon)\cos(2\pi y/\varepsilon)\}\cos(t/\varepsilon^2),$$

and the flux function is taken to be Buckley-Leverett function

$$F(u) = u^2/(u^2 + 0.2(1 - u^2)).$$

Here, we vary δ, $\delta = 0.1, 0.2, 0.3, 0.4, 0.5$. In Figures 2-6 we compare the results with the enhanced diffusion on a coarse grid with the averages obtained from the solutions of original equations on a fine grid. In addition, the solutions of the equations without the effect of the enhanced diffusion are given. The averaged solution as a function of time is presented on the left figure of Figures 2-6. The solid line indicates the solution of fine scale equation, the dotted line stands for the solution of the equation obtained by the numerical homogenization procedure, and the dashed line designates the results without the enhanced diffusion in each figure. The solutions averaged in

the horizontal and vertical directions at the time $t = 0.5$ are plotted on the middle and right figure of Figures 2-6, respectively. The figures in all cases show the importance of the enhanced diffusion. The coarse models with the enhanced diffusion match well with the results of fine scale equations.

Next, we perform the same experiments except choosing $\varepsilon = 0.05$ instead of $\varepsilon = 0.1$. We demonstrate the results in Figures 7-8 for $\delta = 0.4, 0.5$. These results also show that the effect of the enhanced diffusion. We note that the coarse models with enhanced diffusion overapproximate the fine scale solutions, while they underapproximate in the case of $\varepsilon = 0.1$ (see Figures 5-6).

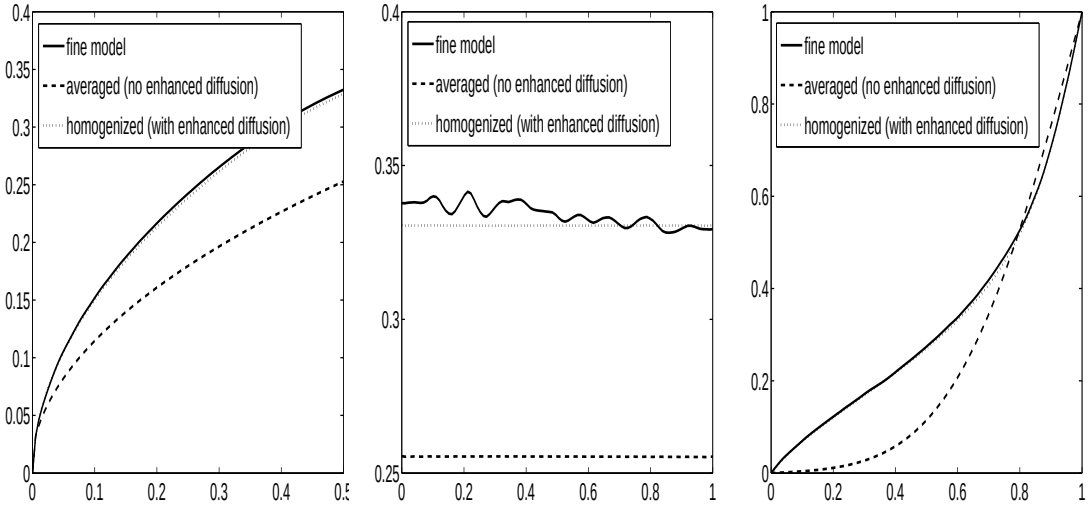

Fig. 2. Left figure: The solutions are averaged over the spatial domain. Middle figure: The solutions are averaged in horizontal direction. Right figure: The solutions are averaged in vertical direction. $\delta = 0.1, \varepsilon = 0.1$

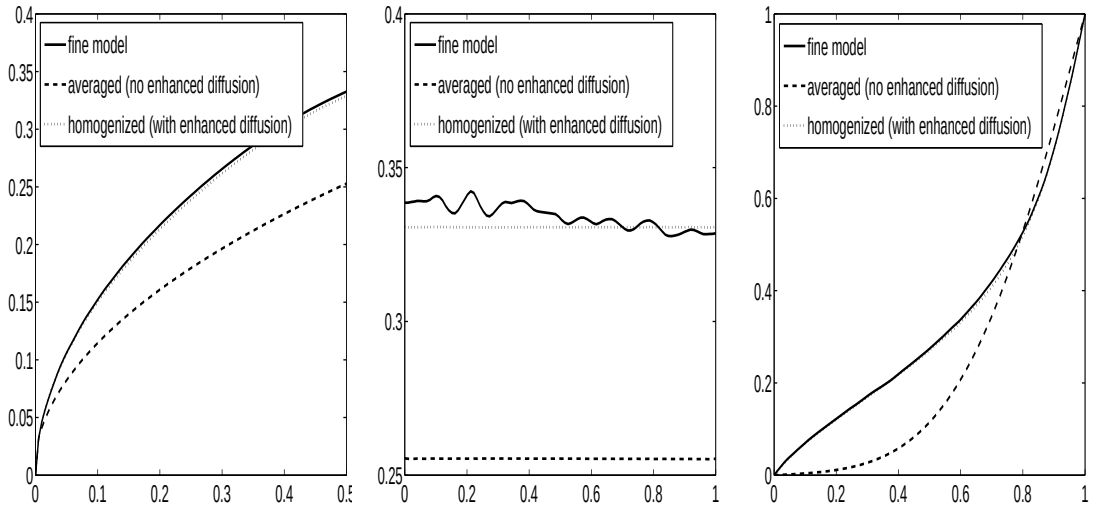

Fig. 3. Left figure: The solutions are averaged over the spatial domain. Middle figure: The solutions are averaged in horizontal direction. Right figure: The solutions are averaged in vertical direction. $\delta = 0.2, \varepsilon = 0.1$

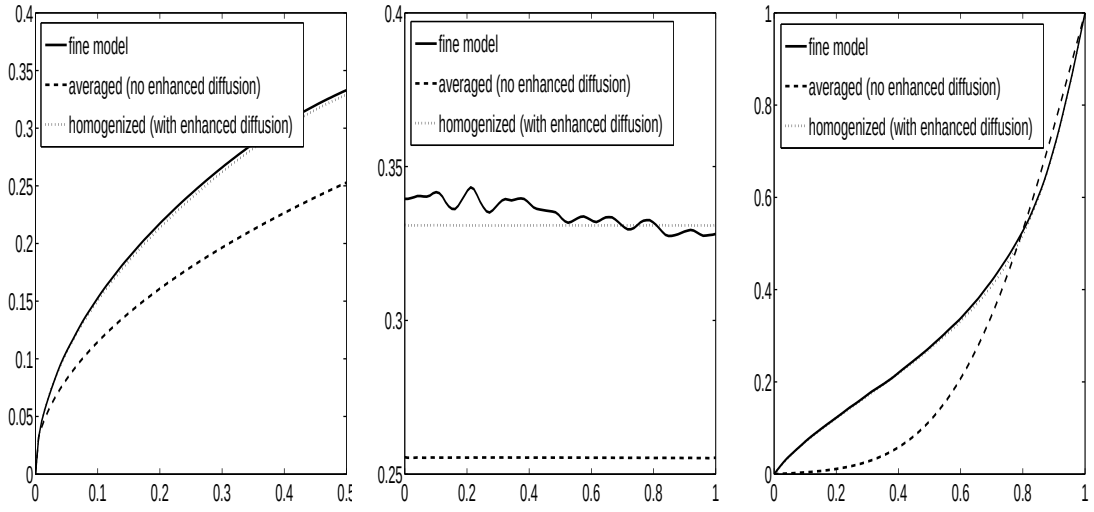

Fig. 4. Left figure: The solutions are averaged over the spatial domain. Middle figure: The solutions are averaged in horizontal direction. Right figure: The solutions are averaged in vertical direction. $\delta = 0.3, \varepsilon = 0.1$

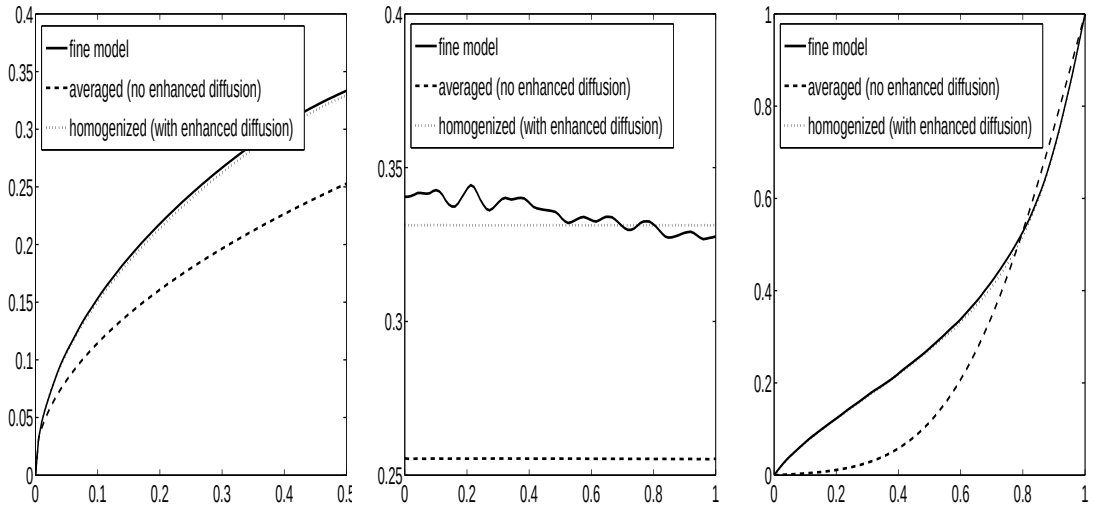

Fig. 5. Left figure: The solutions are averaged over the spatial domain. Middle figure: The solutions are averaged in horizontal direction. Right figure: The solutions are averaged in vertical direction. $\delta = 0.4, \varepsilon = 0.1$

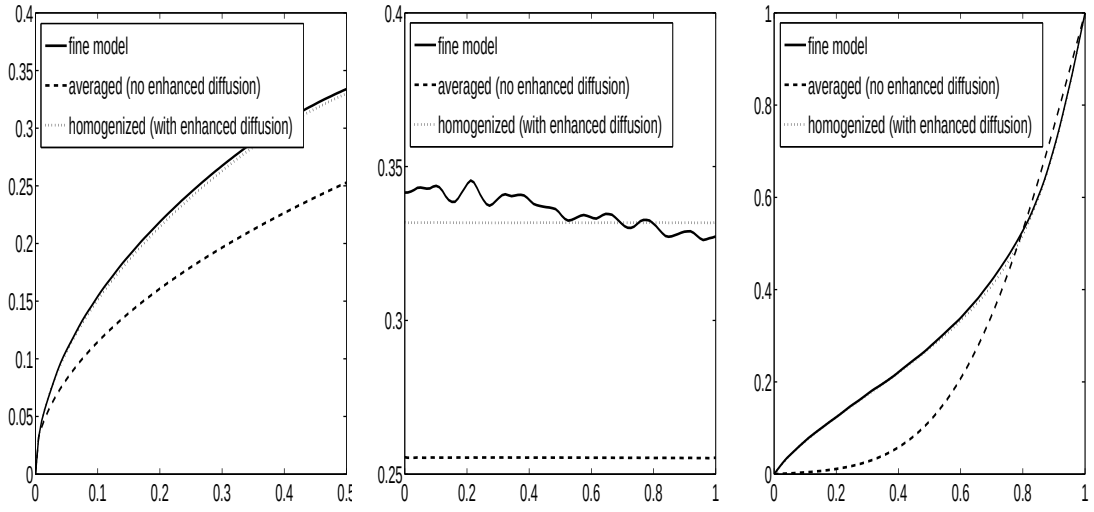

Fig. 6. Left figure: The solutions are averaged over the spatial domain. Middle figure: The solutions are averaged in horizontal direction. Right figure: The solutions are averaged in vertical direction. $\delta = 0.5, \varepsilon = 0.1$

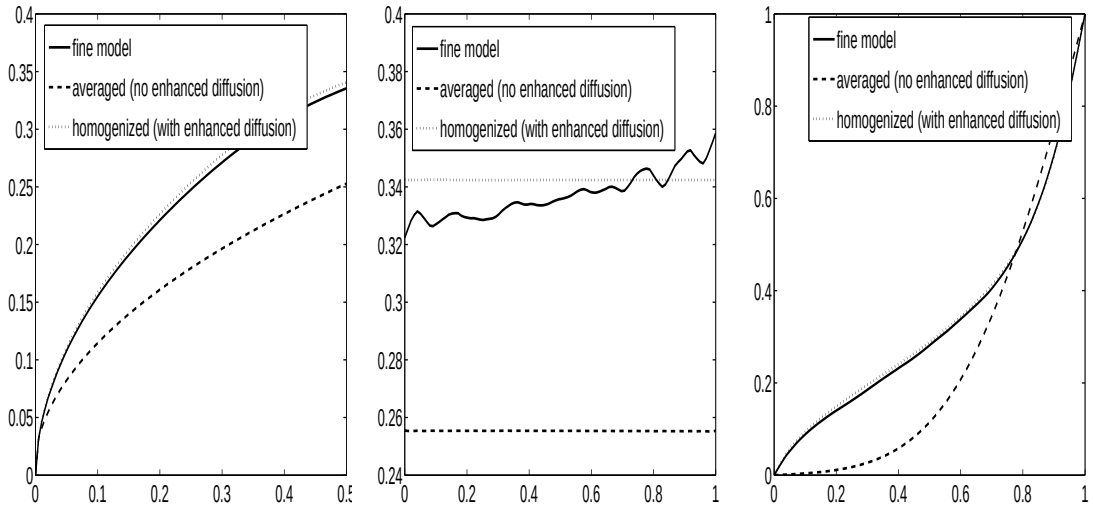

Fig. 7. Left figure: The solutions are averaged over the spatial domain. Middle figure: The solutions are averaged in horizontal direction. Right figure: The solutions are averaged in vertical direction. $\delta = 0.4, \varepsilon = 0.05$

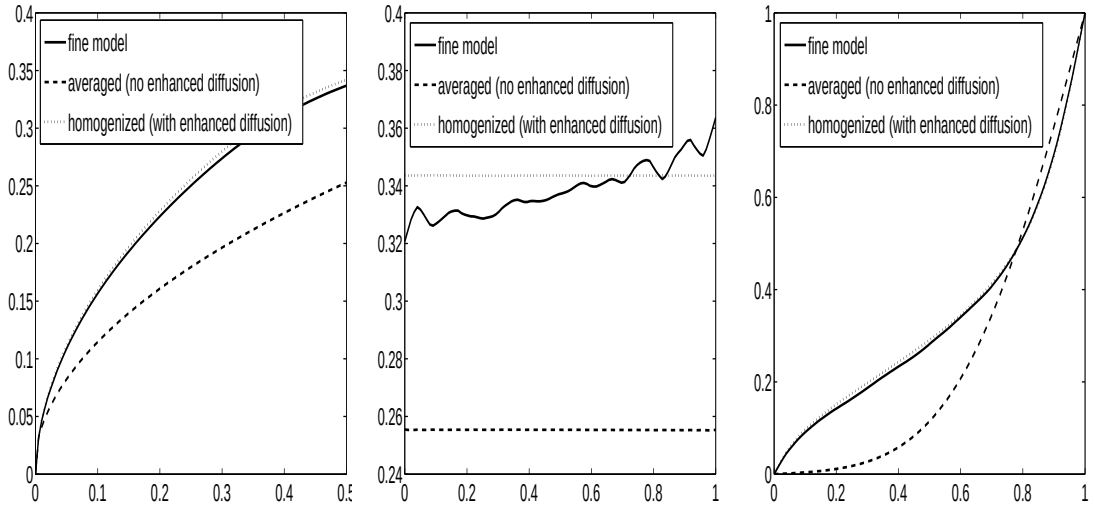

Fig. 8. Left figure: The solutions are averaged over the spatial domain. Middle figure: The solutions are averaged in horizontal direction. Right figure: The solutions are averaged in vertical direction. $\delta = 0.5, \varepsilon = 0.05$

For the next set of numerical tests we replace nothing but the diffusion term $d\,(1+F'(u_\varepsilon))$ by $d\,k(x/\varepsilon,t/\varepsilon^2)/(1+u_\varepsilon)^{k(x/\varepsilon,t/\varepsilon^2)+2}$ for some positive periodic function $k(x/\varepsilon,t/\varepsilon^2)$. Thus we have another types of periodic convection and periodic diffusion equations (2.60) such that

$$a=\begin{pmatrix} d\ k(x/\varepsilon,t/\varepsilon^2)/(1+u_\varepsilon)^{k(x/\varepsilon,t/\varepsilon^2)+2} & -H(x/\varepsilon,t/\varepsilon^2)F'(u_\varepsilon) \\ H(x/\varepsilon,t/\varepsilon^2)F'(u_\varepsilon) & d\ k(x/\varepsilon,t/\varepsilon^2)/(1+u_\varepsilon)^{k(x/\varepsilon,t/\varepsilon^2)+2} \end{pmatrix}.$$

Here we take $\varepsilon=0.1$ and $\delta=0.1$. We also investigate the importance of the enhanced diffusion in numerical homogenization procedure by taking various periodic functions k: $k(x/\varepsilon,t/\varepsilon^2)=\sin(2\pi x/\varepsilon)+\cos(2\pi y/\varepsilon)+3$, $k(x/\varepsilon,t/\varepsilon^2)=(\sin(2\pi x/\varepsilon)+\cos(2\pi y/\varepsilon)+3)(\cos(t/\varepsilon^2)+2)$, $k(x/\varepsilon,t/\varepsilon^2)=\frac{2+1.8\sin(2\pi x/\varepsilon)}{2+1.8\cos(2\pi y/\varepsilon)}+\frac{2+1.8\sin(2\pi y/\varepsilon)}{2+1.8\cos(2\pi x/\varepsilon)}+3$, and $k(x/\varepsilon,t/\varepsilon^2)=\left(\frac{2+1.8\sin(2\pi x/\varepsilon)}{2+1.8\cos(2\pi y/\varepsilon)}+\frac{2+1.8\sin(2\pi y/\varepsilon)}{2+1.8\cos(2\pi x/\varepsilon)}+3\right)(\cos(t/\varepsilon^2)+2)$.

Figures 9-12 show us the comparison of the homogenized solution with the enhanced diffusion with the fine scale solution and averaged solution without the enhanced diffusion as we did. Likewise, the left plots of each figure illustrate the behavior of solution averaged over the spatial domain, and the right plots of each figure indicate the solution averages in the vertical direction at $t=0.5$. The results on the left plots of the figures give us the averaged solutions without the enhanced diffusion. We observe that the solutions agree well with the solutions of fine model in the early stage, however, as time goes on, homogenized solutions with the enhanced diffusion are getting closer to the fine model. The right plot of each figure makes us confirm the importance of the enhanced diffusion. In fact, although the coarse solutions without enhanced diffusion effect look better than homogenized solutions in the comparison of averaged solutions over the spatial domain, homogenized solutions are better when comparing of averaged solution in vertical direction.

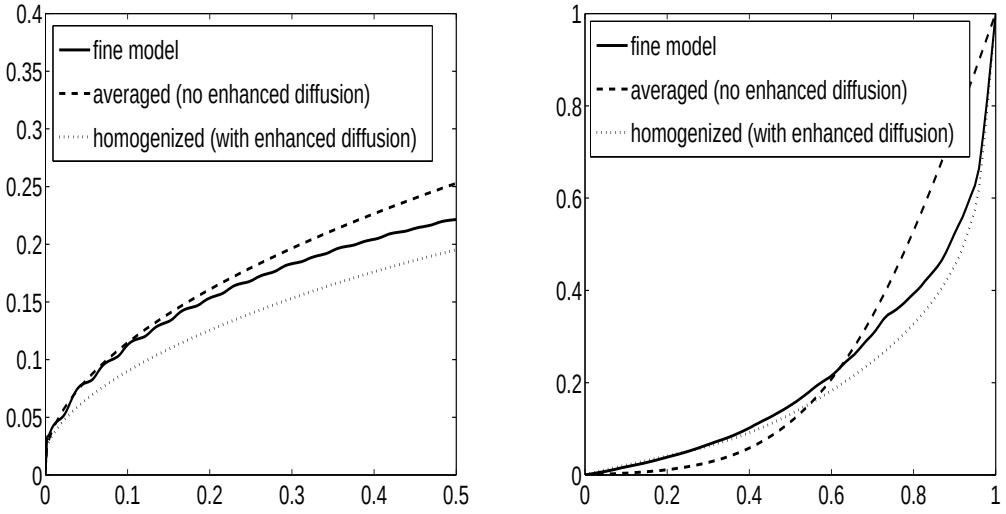

Fig. 9. Left figure: The solutions are averaged over the spatial domain. Right figure: The solutions are averaged in vertical direction. $k(x/\varepsilon, t/\varepsilon^2) = (\sin(2\pi x/\varepsilon) + \cos(2\pi y/\varepsilon) + 3)$.

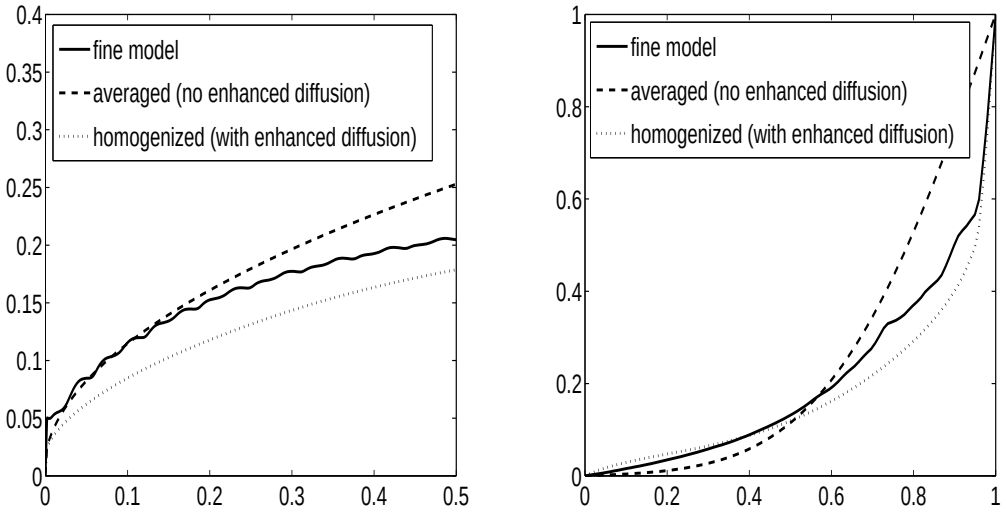

Fig. 10. Left figure: The solutions are averaged over the spatial domain. Right figure: The solutions are averaged in vertical direction. $k(x/\varepsilon, t/\varepsilon^2) = (\sin(2\pi x/\varepsilon) + \cos(2\pi y/\varepsilon) + 3)(\cos(t/\varepsilon^2) + 2)$.

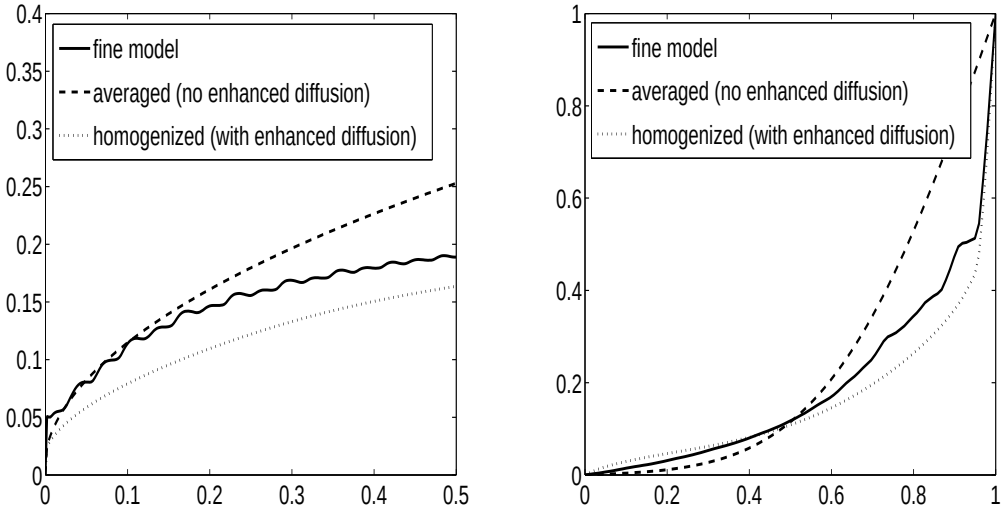

Fig. 11. Left figure: The solutions are averaged over the spatial domain. Right figure: The solutions are averaged in vertical direction. $k(x/\varepsilon, t/\varepsilon^2) = \frac{2+1.8\sin(2\pi x/\varepsilon)}{2+1.8\cos(2\pi y/\varepsilon)} + \frac{2+1.8\sin(2\pi y/\varepsilon)}{2+1.8\cos(2\pi x/\varepsilon)} + 3$.

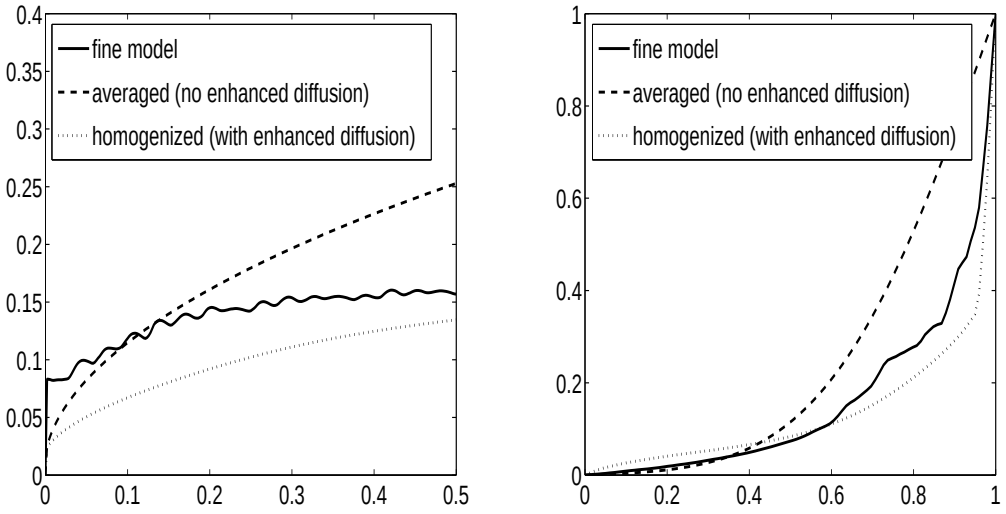

Fig. 12. Left figure: The solutions are averaged over the spatial domain. Right figure: The solutions are averaged in vertical direction. $k(x/\varepsilon, t/\varepsilon^2) = \left(\frac{2+1.8\sin(2\pi x/\varepsilon)}{2+1.8\cos(2\pi y/\varepsilon)} + \frac{2+1.8\sin(2\pi y/\varepsilon)}{2+1.8\cos(2\pi x/\varepsilon)} + 3\right)(\cos(t/\varepsilon^2) + 2)$.

For the third set of numerical tests we use the stream function H which is from random velocity field (see p265-266 in [10]). By taking it into account, we have random convection and periodic diffusion equations (2.60) satisfying

$$a = \begin{pmatrix} d\ k(x/\varepsilon, t/\varepsilon^2)/(1+u_\varepsilon)^{k(x/\varepsilon,t/\varepsilon^2)+2} & -H\ F'(u_\varepsilon) \\ H\ F'(u_\varepsilon) & d\ k(x/\varepsilon, t/\varepsilon^2)/(1+u_\varepsilon)^{k(x/\varepsilon,t/\varepsilon^2)+2} \end{pmatrix},$$

with $\varepsilon = 0.1$ and $\delta = 0.1$. Further, we use the same periodic functions k as we did in the second set of numerical tests. We present the results of these experiments in Figures 13-16, and we have similar results to the second set of tests. These comparisons show that the effect of the enhanced diffusion is significant in numerical homogenization procedure. Similar to the second set of numerical tests, coarse solutions with enhanced diffusion close to fine scale solution on the left plots of each figure, and right plots of the figures enable us to notice that homogenized solutions with enhanced diffusion in the coarse models match well with reference solution.

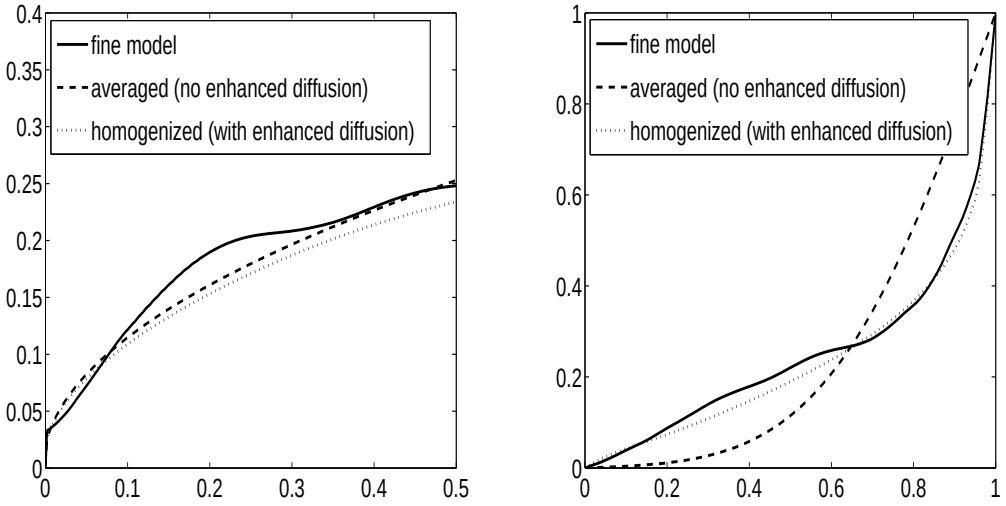

Fig. 13. Left figure: The solutions are averaged over the spatial domain. Right figure: The solutions are averaged in vertical direction. $k(x/\varepsilon, t/\varepsilon^2) = (\sin(2\pi x/\varepsilon) + \cos(2\pi y/\varepsilon) + 3)$.

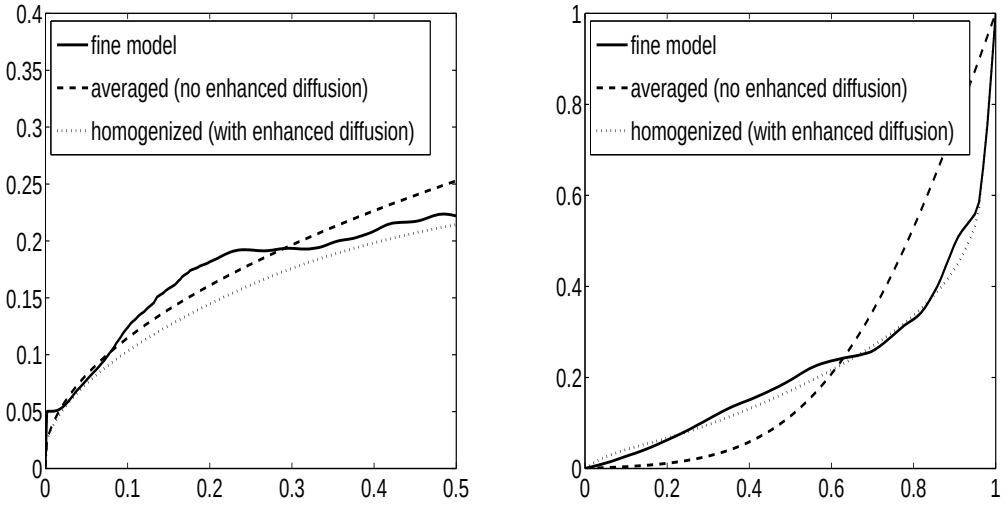

Fig. 14. Left figure: The solutions are averaged over the spatial domain. Right figure: The solutions are averaged in vertical direction. $k(x/\varepsilon, t/\varepsilon^2) = (\sin(2\pi x/\varepsilon) + \cos(2\pi y/\varepsilon) + 3)(\cos(t/\varepsilon^2) + 2)$.

For the last set of numerical tests, we again use the same stream function H from random velocity field and the same periodic function k as in the previous examples. However, we change the diffusion term by $d\,k(x/\varepsilon, t/\varepsilon^2)(|\nabla u_\varepsilon| + i)$ with integer i. Then we have another nonlinear parabolic equation (2.60) such that

$$a = \begin{pmatrix} d\ k(x/\varepsilon, t/\varepsilon^2)(|\nabla u_\varepsilon| + i) & -H\ F'(u_\varepsilon) \\ H\ F'(u_\varepsilon) & d\ k(x/\varepsilon, t/\varepsilon^2)(|\nabla u_\varepsilon| + i) \end{pmatrix}.$$

Here we choose $i = 1$, $\varepsilon = 0.1$, and $\delta = 0.1$. In Figures 17-20 we compare the solutions of fine scale equations with the solutions of homogenized equations as we did before. These results also support the significance of the enhanced diffusion in numerical homogenization scheme.

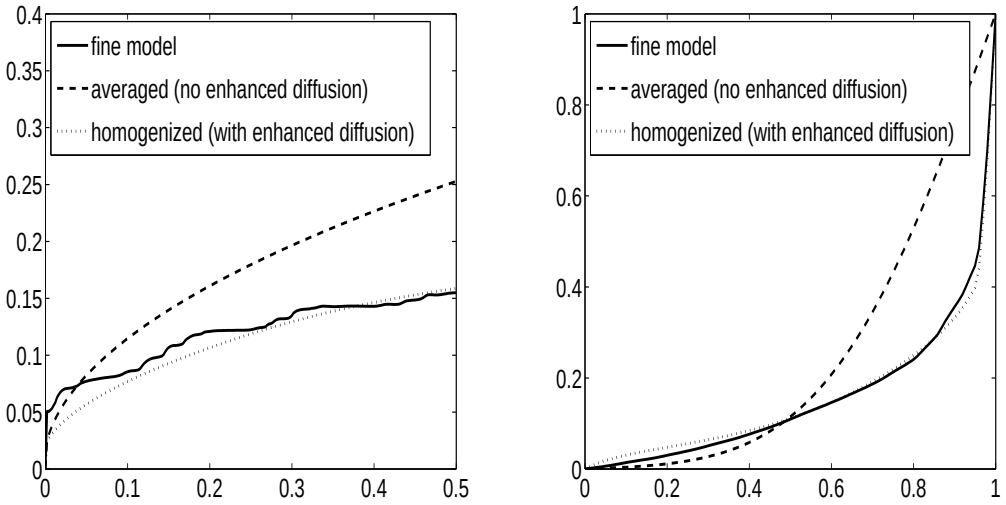

Fig. 15. Left figure: The solutions are averaged over the spatial domain. Right figure: The solutions are averaged in vertical direction. $k(x/\varepsilon, t/\varepsilon^2) = \frac{2+1.8\sin(2\pi x/\varepsilon)}{2+1.8\cos(2\pi y/\varepsilon)} + \frac{2+1.8\sin(2\pi y/\varepsilon)}{2+1.8\cos(2\pi x/\varepsilon)} + 3$.

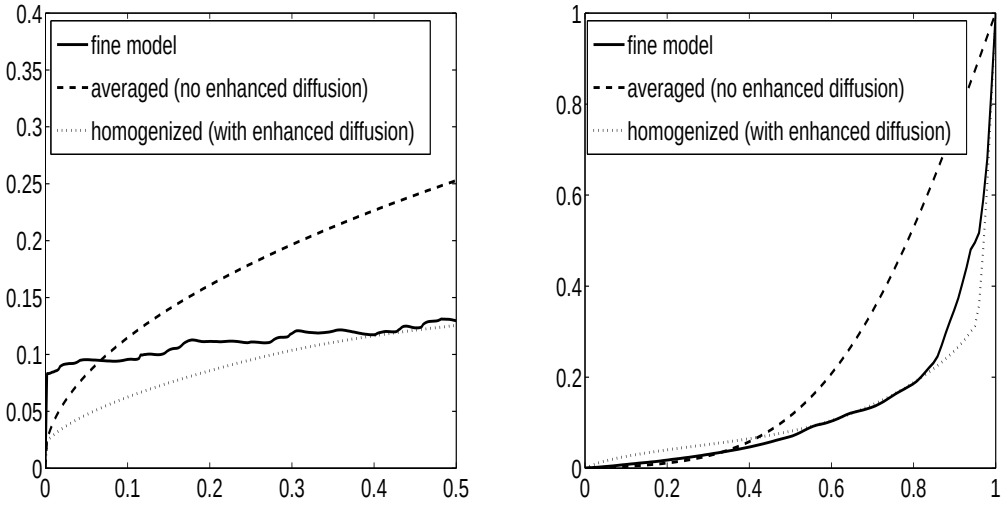

Fig. 16. Left figure: The solutions are averaged over the spatial domain. Right figure: The solutions are averaged in vertical direction. $k(x/\varepsilon, t/\varepsilon^2) = \left(\frac{2+1.8\sin(2\pi x/\varepsilon)}{2+1.8\cos(2\pi y/\varepsilon)} + \frac{2+1.8\sin(2\pi y/\varepsilon)}{2+1.8\cos(2\pi x/\varepsilon)} + 3\right)(\cos(t/\varepsilon^2) + 2)$.

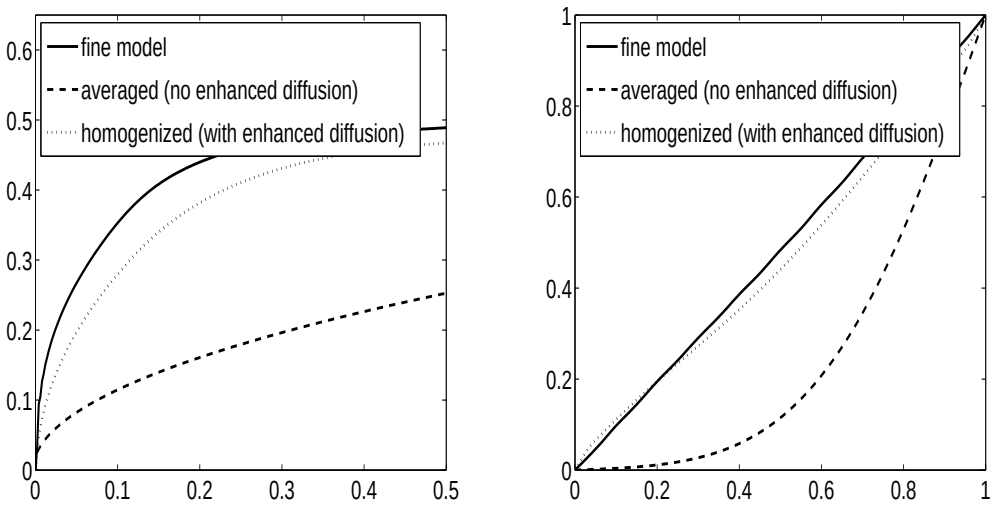

Fig. 17. Left figure: The solutions are averaged over the whole spatial domain. Right figure: The solutions are averaged in vertical direction. $i = 1$ and $k(x/\varepsilon, t/\varepsilon^2) = (\sin(2\pi x/\varepsilon) + \cos(2\pi y/\varepsilon) + 3)$.

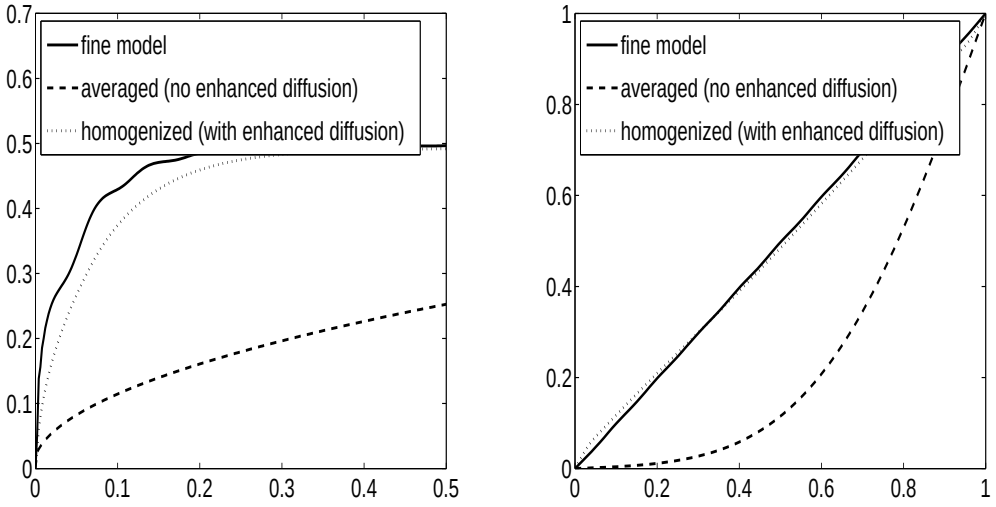

Fig. 18. Left figure: The solutions are averaged over the whole spatial domain. Right figure: The solutions are averaged in vertical direction. $i = 1$ and $k(x/\varepsilon, t/\varepsilon^2) = (\sin(2\pi x/\varepsilon) + \cos(2\pi y/\varepsilon) + 3)(\cos(t/\varepsilon^2) + 2)$.

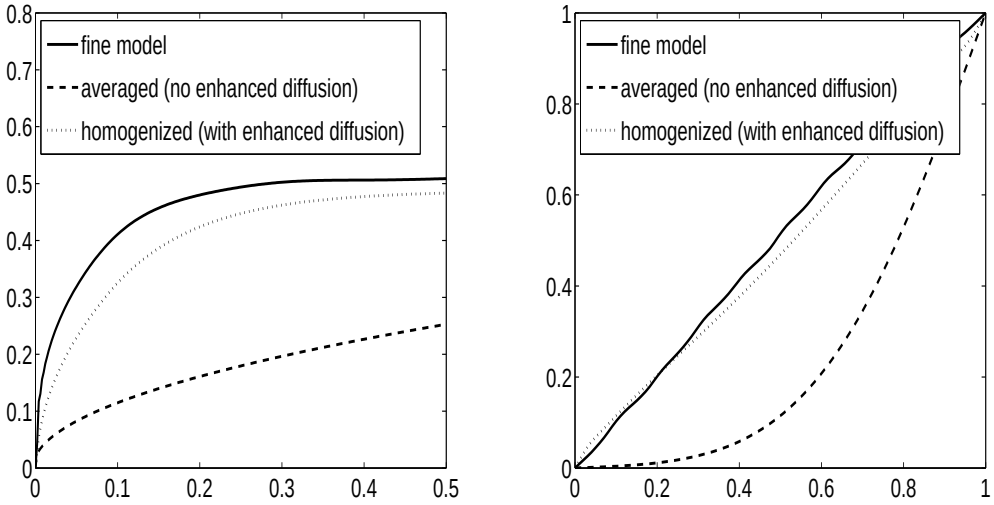

Fig. 19. Left figure: The solutions are averaged over the whole spatial domain. Right figure: The solutions are averaged in vertical direction. $i = 1$ and $k(x/\varepsilon, t/\varepsilon^2) = \left(\frac{2+1.8\sin(2\pi x/\varepsilon)}{2+1.8\cos(2\pi y/\varepsilon)} + \frac{2+1.8\sin(2\pi y/\varepsilon)}{2+1.8\cos(2\pi x/\varepsilon)} + 3\right)$.

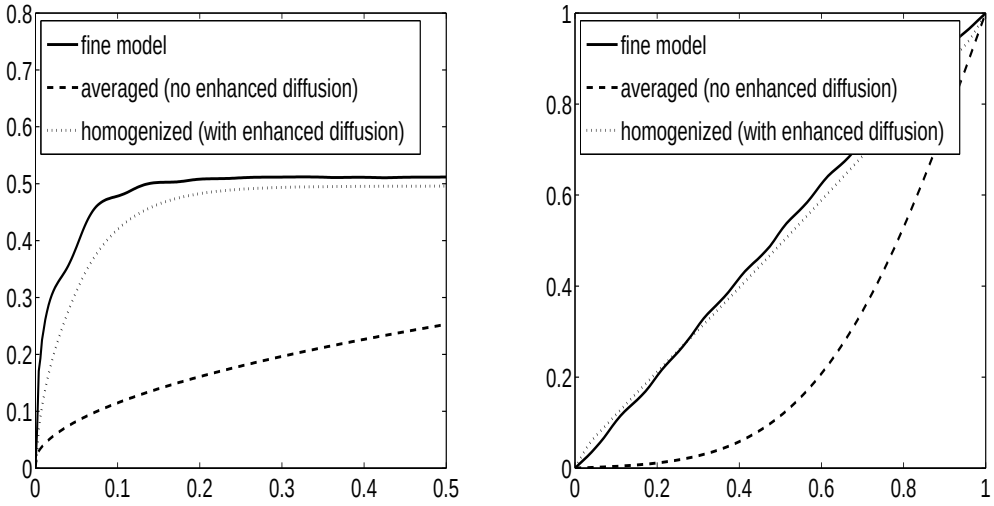

Fig. 20. Left figure: The solutions are averaged over the whole spatial domain. Right figure: The solutions are averaged in vertical direction. $i = 1$ and $k\left(\frac{x}{\varepsilon}, \frac{t}{\varepsilon^2}\right) = \left(\frac{2+1.8\sin(2\pi x/\varepsilon)}{2+1.8\cos(2\pi y/\varepsilon)} + \frac{2+1.8\sin(2\pi y/\varepsilon)}{2+1.8\cos(2\pi x/\varepsilon)} + 3\right)\left(\cos\left(\frac{t}{\varepsilon^2}\right) + 2\right)$.

CHAPTER III

MULTISCALE NUMERICAL METHODS FOR TURBULENT DIFFUSION EQUATIONS*

In this chapter we present an approach to solve turbulent diffusion equations governed by cellular periodic flows. First, we briefly describe the asymptotic way, proposed in [24], to solve the problem.

A. Background

Let Ω be a simply connected, bounded domain in $\mathbb{R}^2$. We consider the time-dependent advection-diffusion equations for periodic flows

$$\begin{aligned} &\frac{\partial T}{\partial t} = \varepsilon \Delta T - v \cdot \nabla T \\ &T(0, x_1, x_2) = T_0(x_1, x_2). \end{aligned} \tag{3.1}$$

Here, $v(x_1, x_2, t)$ is the fluid velocity which is heterogeneous (with fast temporal and spatial variations) time-dependent (in general) and incompressible:

$$\operatorname{div} v = 0,$$

and $\varepsilon > 0$ is the molecular diffusivity which is small. Since the flow v is assumed to be incompressible, there is a stream function $\Psi(x_1, x_2)$ such that $v = \nabla^{\perp}\Psi = (\frac{\partial \Psi}{\partial x_2}, -\frac{\partial \Psi}{\partial x_1})$.

We assume v is a time-independent and incompressible flow with mean zero.

*Portions of this chapter are reprinted with permission from "Boundary layers for cellular flows at high Péclet numbers" by A. Novikov, G. Papanicolaou, and L. Ryzhik, 2005. Comm. Pure Appl. Math., 58, 867-922, Copyright [2001] by John Wiley & Sons, Inc.

Then there is a skew-symmetric matrix $\mathbf{H} = (H_{ij}(x))$ such that

$$\text{div}\mathbf{H} = v.$$

Thus (3.1) becomes

$$\frac{\partial T}{\partial t} = \text{div}(\varepsilon I + \mathbf{H})\nabla T,$$

which can be rewritten to

$$\frac{\partial T}{\partial t} = \sum_{i,j=1}^{2} \frac{\partial}{\partial x_i}\left(a_{ij}(x)\frac{\partial T}{\partial x_j}\right), \tag{3.2}$$

where

$$a_{ij}(x) = \varepsilon\,\delta_{ij} + H_{ij}(x).$$

Note that (a_{ij}) is not symmetric, but the right hand side of (3.2) is uniformly elliptic.

Assume that the flow is cellular with the cell size δ. Then we have

$$\frac{\partial T}{\partial t} = \sum_{i,j=1}^{2} \frac{\partial}{\partial x_i}\left(a_{ij}(\frac{x}{\delta})\frac{\partial T}{\partial x_j}\right) \tag{3.3}$$

under the assumption $T(0,x) = T_0(x)$. Due to the uniform ellipticity of the periodic diffusivity coefficients in (3.3), the solution $T(t,x) = T^{\delta}(t,x)$ of (3.3) converges in L^2 to the solution $\overline{T}(t,x)$ of

$$\frac{\partial \overline{T}}{\partial t} = \sum_{i,j=1}^{2} \overline{a}_{ij}\frac{\partial^2 \overline{T}}{\partial x_i \partial x_j}, \qquad \overline{T}(0,x) = T_0(x)$$

To obtain the symmetric effective diffusivity matrix $(\overline{a}_{ij})$, we solve the following cell problem:

For each unit vector e, let $\chi = \chi(x,e)$ be the unique (up to a constant) periodic solution of

$$-\sum_{i,j=1}^{2} \frac{\partial}{\partial x_i} a_{ij}(x)\frac{\partial \chi(x)}{\partial x_j} = \sum_{i,j=1}^{2} \frac{\partial}{\partial x_i} a_{ij}(x)e_j$$

Then $\overline{a}$ is determined by

$$\overline{a}\, e \cdot e = \langle a\,(\nabla\chi + e) \cdot (\nabla\chi + e)\rangle\,,$$

where $\langle\ \rangle$ denotes the average over the cell.

The cell problem for (3.2):

$$\operatorname{div}\left[(\varepsilon I + \mathbf{H})(\nabla\chi + e)\right] = 0. \tag{3.4}$$

The effective diffusivity matrix ($\overline{a}$) is defined by

$$\overline{a}\, e \cdot e = \varepsilon\,\langle(\nabla\chi + e) \cdot (\nabla\chi + e)\rangle\,.$$

Since $\operatorname{div}\mathbf{H} = v$, (3.4) is equivalent to

$$\varepsilon\Delta\chi - v \cdot \nabla\chi + v \cdot e = 0. \tag{3.5}$$

Consider the above cell problem (3.5) with the stream function given by $\Psi(x_1, x_2) = \sin x_1 \sin x_2$. Then the periodic function $\chi(x_1, x_2)$ $(0 < x_1 < \pi, 0 < x_2 < \pi)$ can be determined up to a constant. When $e = (1, 0)$, if $\rho = \chi + x_1$, then we can get

$$\begin{aligned} &\varepsilon\Delta\rho - v \cdot \nabla\rho = 0, \\ &\rho(0, x_2) = 0, \qquad \rho(\pi, x_2) = \pi, \\ &\frac{\partial\rho}{\partial x_2}(x_1, 0) = \frac{\partial\rho}{\partial x_2}(x_1, \pi) = 0, \end{aligned} \tag{3.6}$$

Motivated by the above cell problem (3.5), we consider the following steady advection-diffusion problem

$$\varepsilon\Delta\phi^{\varepsilon} - v \cdot \nabla\phi^{\varepsilon} = f, \tag{3.7}$$

where the flow v is incompressible, $\operatorname{div} v = 0$, and nonpenetrating through the bound-

ary of Ω, i.e., $v \cdot n = 0$ at $\partial\Omega$, and ϕ^ε is a temperature in turbulent flows and f is a given source term. The small parameter $\varepsilon = \mathrm{Pe}^{-1} \ll 1$ is the inverse of the Péclet number, where $\mathrm{Pe} = \frac{vl}{D}$, where v is the velocity, l is a length scale, and D is the molecular diffusivity. Equation (3.7) is supplemented by the Dirichlet boundary data:

$$\phi^\varepsilon(x) = T_0(x), \quad x \in \partial\Omega, \tag{3.8}$$

where T_0 is a given temperature.

1. Asymptotic computational approach

At high Péclet numbers the numerical solution of (3.7) becomes expensive if a discretization method does not take into account diffusive boundary layers which arise where the stream function $\Psi(x_1, x_2)$ for the incompressible flow v vanishes: $\Psi(x_1, x_2) = 0$. We propose here to use a detailed analysis of (3.7) developed in [24]. Let us summarize some results obtained in [24].

As ε tends to zero, the solution to (3.7) converges to a solution of a coupled one-dimensional heat equations on a graph. This *diffusion on a graph model* is independent of Péclet number, and the relative H^1 error between the solution to (3.7) and the solution to the diffusion on a graph model was estimated a priori as $O(\varepsilon^{1/2})$ (Theorem 6.1 in [24]).

The edges of the graph are associated with the separatrices of the fluid flow, and the vertices of this graph are associated with saddle-points of the stream function $\Psi(x_1, x_2)$. Let us first describe the simplest case when we have just two vertices.

a. The two-cell case

We describe the asymptotic problem first on the simplest example of a domain Ω that consists of two cells $\mathcal{C}_1$ and $\mathcal{C}_2$ depicted in the left plot of Figure 21. We denote by

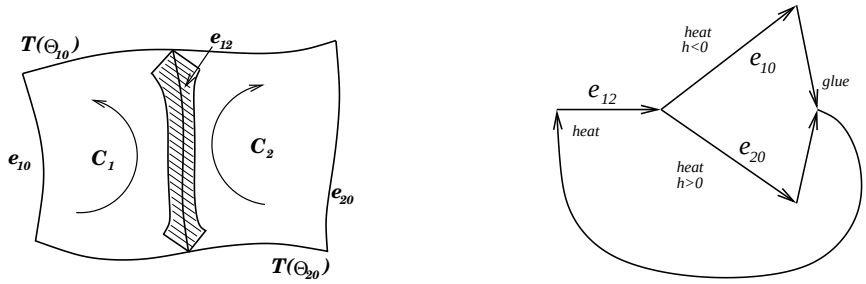

Fig. 21. The two-cell problem (left) and the gluing procedure (right).

$e_{j0} = \partial\Omega \cap \partial\mathcal{C}_j$, $j = 1, 2$, the part of the boundary of Ω along the cell $\mathcal{C}_j$ and by e_{12} the common edge of the two cells. We also introduce the boundary layer coordinates h and θ_{12}, θ_{j0}, $j = 1, 2$. The coordinate θ_{12} represents parameterization along the edge $e_{12} = \{h = 0\} \cap \{0 \le \theta_{12} \le l_{12}\}$, while the coordinates θ_{j0} parameterize along the boundaries $e_{j0} = \{h = 0\} \cap \{l_{12} \le \theta_{j0} \le l_{j0}\}$. We first solve the heat equation "along e_{12}":

$$\frac{\partial f_{12}}{\partial \theta_{12}} = \frac{\partial^2 f_{12}}{\partial h^2}, \quad h \in (-\infty, \infty), \quad 0 \le \theta_{12} \le l_{12} \tag{3.9}$$

with prescribed initial data f_{12}^0 and the decaying at $h = \pm\infty$:

$$\lim_{h \to \pm\infty} \frac{\partial f_{12}(\theta_{12}, h)}{\partial h} = 0. \tag{3.10}$$

Then we solve two half-space problems "along the outer boundaries e_{j0}" with the prescribed Dirichlet data that comes from (3.8):

$$\frac{\partial f_{10}}{\partial \theta_{10}} = \frac{\partial^2 f_{10}}{\partial h^2}, \quad -\infty < h \le 0, \quad l_{12} \le \theta_{10} \le l_{10} \tag{3.11}$$

and

$$\frac{\partial f_{20}}{\partial \theta_{20}} = \frac{\partial^2 f_{20}}{\partial h^2}, \quad 0 \le h < \infty, \quad l_{12} \le \theta_{20} \le l_{20} \tag{3.12}$$

with (3.10) $h = \pm\infty$, and with the Dirichlet data $f_{j0}(\theta_{j0}, 0) = T_0(\theta_{j0})$ at $h = 0$. The initial data for (3.11) and (3.12) comes from (3.9):

$$f_{10}(l_{12}, h) = f_{12}(l_{12}, h), \quad -\infty < h \leq 0, \tag{3.13}$$
$$f_{20}(l_{12}, h) = f_{12}(l_{12}, h), \quad 0 \leq h < \infty.$$

Finally we glue together the functions $f_{10}(l_{10}, h)$, $h \leq 0$ and $f_{20}(l_{20}, h)$, $h \geq 0$:

$$f_{12}^g(h) = \begin{cases} f_{10}(l_{10}, h), & -\infty < h \leq 0 \\ f_{20}(l_{20}, h), & 0 \leq h < \infty. \end{cases} \tag{3.14}$$

The asymptotic problem is to construct a periodic solution of the above, that is, to find a function $f_{12}^0(h)$ so that $f_{12}^0(h) = f_{12}^g(h)$, $h \in (-\infty, \infty)$. This problem is described schematically in the right plot of Figure 21. There exists a unique function $f_{12}^0 \in L^2(-\infty, \infty)$ such that $f_{12}^0 = f_{12}^g$ (Proposition 5.1 in [24]).

An alternative approach to the proof of the existence of a periodic solution of (3.9)-(3.14), that is somewhat less transparent in the two-cell case but is easier to generalize to the case of multiple cells is as follows. We introduce an operator $\mathcal{L} = L_{12} \otimes L_{10} \otimes L_{20}$ defined on $L^2(\mathbb{R}) \times L^2(\mathbb{R}_-) \times L^2(\mathbb{R}_+)$ as

$$\mathcal{L} \begin{pmatrix} f_{12} \\ f_{10} \\ f_{20} \end{pmatrix} = \begin{pmatrix} L_{12} f_{12} \\ L_{10} f_{10} \\ L_{20} f_{20} \end{pmatrix}.$$

We also define a re-distribution operator $\mathcal{R}$ on the same space $L^2(\mathbb{R}) \times L^2(\mathbb{R}_-) \times L^2(\mathbb{R}_+)$ as

$$\mathcal{R} \begin{pmatrix} f_{12} \\ f_{10} \\ f_{20} \end{pmatrix} = \begin{pmatrix} \mathcal{G}[f_{10}, f_{20}] \\ \mathcal{R}_- f_{12} \\ \mathcal{R}_+ f_{12} \end{pmatrix}.$$

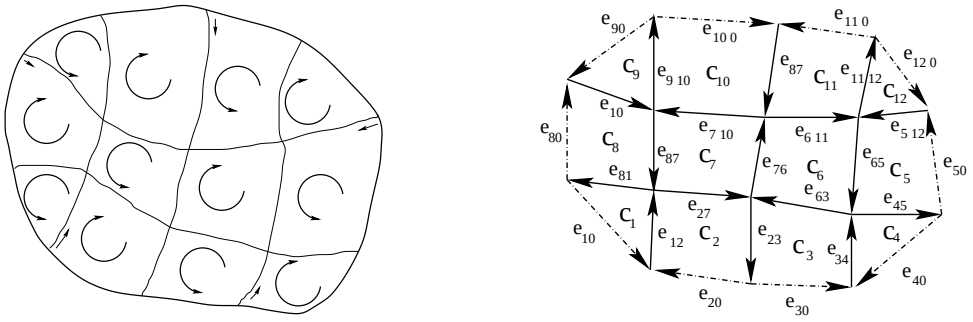

Fig. 22. The velocity profile (left) and the graph (right).

Then the existence of a unique function $f_{12}^0 \in L^2(-\infty, \infty)$ such that $f_{12}^0 = f_{12}^g$ means

$$\mathcal{RL} \begin{pmatrix} f_{12}^0(h) \\ f_{10}(l_{12}, h) \\ f_{20}(l_{12}, h) \end{pmatrix} + \begin{pmatrix} g(h) \\ 0 \\ 0 \end{pmatrix} = \begin{pmatrix} f_{12}^0(h) \\ f_{10}(l_{12}, h) \\ f_{20}(l_{12}, h) \end{pmatrix}, \tag{3.15}$$

where the function $g(h)$ is obtained by solving (3.9)-(3.14) with $f_{12}^0 = 0$ and inhomogeneous boundary conditions. Equation (3.15) has a straightforward generalization to the case of more than two cells.

b. The general multiple-cell case

We now consider the general case when the domain Ω consists of a finite number of cells. The asymptotic model is described in terms of an oriented graph constructed using the stream function Ψ as shown on Figure 22. The vertices of this graph are associated with the saddle points of Ψ. The edges e_{ij} of the graph are associated with the separatrices of the stream function. The direction of an edge is determined by the direction of the velocity field on the corresponding separatrix. The length of an edge is determined by the length of the separatrix in the boundary layer coordinate θ associated with Ψ. The boundary edges are those that are associated with the separatrices at the boundary of the domain. The cells $\mathcal{C}_i$ are quadrangles (or triangles)

bounded by minimal cycles of the graph. The interior edges (drawn as solid arrows on the right figure of Figure 22) are indexed so that a common edge of two cells $\mathcal{C}_i$ and $\mathcal{C}_j$ is denoted by e_{ij}. The boundary edges (drawn as dotted arrows on the right figure of Figure 22) are indexed so that the outer part of a boundary cell $\mathcal{C}_i$ is denoted by e_{i0}. The boundary value problem is:

- [i] Given the values of the temperature T_0 on the boundary edges e_{i0}, determine the values of the temperature f_{ij} on all the edges. Note that the value of f_{ij} may vary along each edge.

- [ii] Given the values of f_e on all the edges, find the solutions f_i of the Childress' problem for each cell $\mathcal{C}_i$:

$$\begin{cases} \frac{\partial^2 f_i}{\partial h^2} - \frac{\partial f_i}{\partial \theta} = 0, \\ h \in [0, \infty), \;\; \theta \in]-\infty, +\infty[, \\ f_i(h = 0, \theta) = f_{ik}(\theta), \\ \lim_{h \to \infty} \frac{\partial f_i}{\partial h}(h, \theta) = 0, \\ f_i(h, \theta) = f(h, \theta + l_i), \end{cases} \tag{3.16}$$

  where the index k takes four values of the adjacent cells, $l_i = l_{ik_1} + \cdots + l_{ik_4}$ is the length in θ of the four edges $e_{ik_1}, \ldots \; e_{ik_4}$, bounding $\mathcal{C}_i$ and $f_{ik}(\theta) = f_{ik_1}(\theta)$, $\ldots$, $f_{ik}(\theta) = f_{ik_4}(\theta)$ are the values of the temperature on respective edges.

- [iii] When any two cells $\mathcal{C}_i$ and $\mathcal{C}_j$ share a common edge, the normal derivatives from the left and from the right match point-wise on this edge:

$$\frac{\partial f_i}{\partial h}\Big|_{h=0} + \frac{\partial f_j}{\partial h}\Big|_{h=0} = 0 \text{ on } e_{ij}.$$

There exists a unique solution of the boundary value problem [i], [ii], [iii] (Theorem 5.2 in [24]).

B. Numerical discretization techniques

In this section, we assume that the domain Ω of the problem (3.7) is the square $(0,\pi)\times(0,\pi)$ in $\mathbb{R}^2$, which can be either one cell or two or four cells. In the case of two cells, we assume that the separatrix is the line $x_1 = \frac{\pi}{2}$. For the spectral methods, we impose the homogeneous Dirichlet boundary condition on the left vertical edge, identically constant π on the right vertical edge, and the homogeneous Neumann boundary condition on the lateral sides.

1. Spectral methods

In order to solve the heat equation (3.16) over the unbounded domains, the Laguerre functions will be used as basis elements in Galerkin methods for one-cell case problems. On the other hand, we use the Hermite functions for two-cell case problems.

a. Preliminaries

For a natural number n the nth Laguerre polynomial on positive real numbers $\mathbb{R}_+$ is defined by

$$L_n(x) = \frac{1}{n!}e^x\frac{d^n}{dx^n}(x^n e^{-x}), \quad n = 0,1,2,....$$

These polynomials have the following recursive property:

$$\begin{aligned} &L_0(x) = 1, \quad L_1(x) = 1 - x, \\ &L_n(x) = \frac{2n-1-x}{n}L_{n-1}(x) - \frac{n-1}{n}L_{n-2}(x) \quad \text{for } n \geq 2, \end{aligned}$$

and the orthonormal relations

$$\int_0^\infty L_n(x)L_m(x)e^{-x}dx = \delta_{mn} \quad \text{for } n, m \geq 0.$$

The Hermite polynomials are defined on $\mathbb{R}$ by

$$H_n(x) = (-1)^n e^{x^2} \frac{d^n}{dx^n} e^{-x^2}.$$

These polynomials are orthogonal with respect to the weight function e^{-x^2}, i.e., we have

$$\int_{-\infty}^\infty H_n(x)H_m(x)e^{-x^2}dx = n!2^n\sqrt{\pi}\delta_{nm}.$$

Similar to the Laguerre polynomials, the Hermite polynomials satisfy the recurrence relation

$$\begin{aligned} &H_0(x) = 1, \quad H_1(x) = 2x, \\ &H_{n+1}(x) = 2xH_n(x) - 2nH_{n-1}(x) \quad \text{for } n \geq 1, \end{aligned}$$

and

$$H_n'(x) = 2nH_{n-1}(x).$$

The Laguerre function $\hat{L}_n(x)$ and the Hermite function $\hat{H}_n(x)$ of degree n is defined by

$$\begin{aligned} \hat{L}_n(x) &= L_n(x)e^{-x/2} \quad \text{on } \mathbb{R}_+, \\ \hat{H}_n(x) &= H_n(x)e^{-x^2/2} \quad \text{on } \mathbb{R}, \end{aligned} \tag{3.17}$$

respectively [18, 28]. Due to the orthonormal relations of the Laguerre polynomials, the Laguerre functions form a orthonormal basis for $L^2(\mathbb{R}_+)$. On the other hand, we use the normalized Hermite functions

$$\hat{H}_n(x) = \frac{1}{\sqrt{n!2^n\sqrt{\pi}}} H_n(x)e^{-x^2/2},$$

as the basis elements for $L^2(\mathbb{R})$.

In computing the integration from Galerkin formulation we use the Gaussian quadratures for Laguerre functions and Hermite functions. The Gaussian quadrature for Laguerre functions over $\mathbb{R}_+$ is

$$\int_0^\infty f(x)e^{-x}dx = \sum_{i=0}^{N} f(x_i)w_i \quad \text{for any polynomial } f \text{ of degree } \leq 2N+1,$$

where the Laguerre-Gauss-Radau points $\{x_i\}_{i=0}^N$ are the roots of $xL'_{N+1}(x)$ and $w_i = \frac{1}{(N+1)L_N^2(x_i)}$, for $i = 0, 1, \cdots, N$ [28]. Similarly, the Gaussian quadrature for Hermite functions over the $\mathbb{R}$ is

$$\int_{-\infty}^\infty g(y)e^{-y^2}dy = \sum_{i=0}^{N} g(y_i)\omega_i \quad \text{for any polynomial } g \text{ of degree } \leq 2N+1,$$

where $\{y_i\}_{i=0}^N$ are the roots of $H_{N+1}(y)$ and $\omega_i = \frac{(N+1)!}{2^{N+1}}\frac{\sqrt{\pi}}{(H_{N+2}(y_i))^2}$, for $i = 0, 1, \cdots, N$ [18].

b. Galerkin approach

We approximate the solution of the Childress' problem (3.16) via the following Galerkin methods:

Find $f \in \hat{X}_N$ such that

$$(\frac{\partial f_N}{\partial \theta}, v) + (\frac{\partial f_N}{\partial h}, \frac{\partial v}{\partial h}) = 0, \quad \text{for all } v \in \hat{X}_N,$$

where $(\cdot, \cdot)$ is the standard inner product of $L^2(\mathbb{R})$ or $L^2(\mathbb{R}_+)$. Here $\hat{X}_N$ is a finite dimensional space generated by either Laguerre or Hermite functions. We use the backward Euler method for time-discretization with step $\Delta\theta$ of the above formulation:

$$(f_N^{(n+1)}, v) + \Delta\theta(\frac{\partial f_N^{(n+1)}}{\partial h}, \frac{\partial v}{\partial h}) = (f_N^{(n)}, v), \quad \text{for all } v \in \hat{X}_N, \tag{3.18}$$

where $f_N^{(n)}$ is the approximating solution at the nth time step.

(a) One-cell case. We assume the domain Ω consists of one cell only. In the boundary layer coordinate system, as $\varepsilon \to 0$, the problem (3.7) becomes

$$\begin{aligned}
&(1) \quad \tfrac{\partial^2 f}{\partial h^2} - \tfrac{\partial f}{\partial \theta} = 0, \qquad h > 0, \quad 0 < \theta < 4\pi, \\
&(2) \quad f(0,\theta) = \pi, \qquad 0 < \theta < \pi, \\
&(3) \quad \tfrac{\partial f}{\partial h}(0,\theta) = 0, \qquad \pi < \theta < 2\pi, \\
&(4) \quad f(0,\theta) = 0, \qquad 2\pi < \theta < 3\pi, \\
&(5) \quad \tfrac{\partial f}{\partial h}(0,\theta) = 0, \qquad 3\pi < \theta < 4\pi, \\
&(6) \quad \tfrac{\partial f}{\partial h}(\infty,\theta) = 0, \qquad 0 < \theta < 4\pi.
\end{aligned} \tag{3.19}$$

Note that the approximate solution we seek is periodic in the variable θ, which implies that the function $f(h,0)$ at initial time is unknown. We let $f(h,0)$ be expressed in the form of the linear combination of the Laguerre functions $\hat{L}_i, i = 0, \cdots, N$. Since the operator corresponding to the heat equation (3.19) is linear, it can be represented by the matrix, denoted by A, corresponding to the linear transformation. Each column of the matrix A can be obtained by solving the equations (3.19) sequentially with homogeneous Dirichlet data and each initial function $\hat{L}_i (i = 0, \cdots, N)$. On the other hand, we denote by g the solution vector by solving the heat equation (3.19) with zero initial condition and non-homogeneous Dirichlet conditions. Then that u is the coefficient vector of the periodic solution $f(h,0)$ at $\theta = 0$ is equivalent to:

$$Au + g = u.$$

Finally we have the system of linear equations

$$(I - A)u = g \tag{3.20}$$

to obtain the periodic solution.

In order to formulate the matrix A and the solution vector g, we find numerical solutions of the heat equations with a given initial function and corresponding boundary conditions at $h = 0$: homogeneous Dirichlet, non-homogeneous Dirichlet, and homogeneous Neumann conditions. We present the numerical scheme for each case.

First we consider the heat equation with homogeneous Dirichlet boundary condition at $h = 0$ and the initial condition $f^{(0)}$. Let $\hat{\varphi}_i(h) = \hat{L}_i(h) - \hat{L}_{i+1}(h)$ so that $\hat{X}_N = \text{span}\{\hat{\varphi}_0, \hat{\varphi}_1, \ldots, \hat{\varphi}_{N-1}\}$. Let $\hat{I}_N : C(\mathbb{R}_+) \to \hat{P}_N$ be the interpolation operator based on the Laguerre Gauss-Radau points $\{h_j\}_{j=0}^N$ [28], where $\hat{P}_N = \{u : u = ve^{-h/2}$ for all polynomials v of degree at most $N, h \in \mathbb{R}_+\}$, and set

$$f_N^{(0)} = \hat{I}_N f^{(0)} = \sum_{i=0}^{N} c_i \hat{L}_i(h),$$
$$f_N^{(n)} = \sum_{i=0}^{N-1} \tilde{f}_i^{(n)} \hat{\varphi}_i(h) \quad \text{for } n = 1, 2, \cdots$$

and for $n = 0, 1, 2, \cdots$

$$\bar{u} = (\tilde{f}_0^{(n+1)}, \tilde{f}_1^{(n+1)}, \ldots, \tilde{f}_{N-1}^{(n+1)})^T$$
$$\bar{b} = ((f_N^{(n)}, \hat{\varphi}_0), (f_N^{(n)}, \hat{\varphi}_1), \ldots, (u_N^{(n)}, \hat{\varphi}_{N-1}))^T$$
$$s_{ij} = (\hat{\varphi}_j', \hat{\varphi}_i'), \quad S = (s_{ij})_{i,j=0,1,\cdots,N-1},$$
$$m_{ij} = (\hat{\varphi}_j, \hat{\varphi}_i), \quad M = (m_{ij})_{i,j=0,1,\cdots,N-1}.$$

Using the formulation (3.18) we arrive to the following system of linear equations:

$$(M + \Delta\theta S)\bar{u} = \bar{b}.$$

Now, for non-homogeneous boundary condition $f(0, \theta) = a$, where constant a

equals to π or 0 in (3.19.2) or (3.19.4), respectively, we write the solution f as $f = \tilde{f} + a\, e^{-h/2}$, where $\tilde{f}$ is the solution of the problem with homogeneous boundary condition:

Find $\tilde{f} \in L^2(0, \Theta; H_0^1(\mathbb{R}_+))$ so that:

$$\frac{\partial \tilde{f}}{\partial \theta} - \frac{\partial^2 \tilde{f}}{\partial h^2} = \frac{a}{2} e^{-h/2}$$
$$\tilde{f}(h, \theta = 0) = f(h, \theta = 0) - a\, e^{-h/2},$$

where Θ is a fixed constant which is the length of the edge corresponding to the boundary condition. Here $\Theta = \pi$ for each case of the one-cell problem. The above Galerkin procedure can be applied in order to approximate $\tilde{f}$.

Finally, for the homogeneous Neumann boundary condition at $h = 0$, the variational formulation is:

Find $f \in L^2(0, \Theta; H^1(\mathbb{R}_+))$ such that

$$(\frac{\partial f}{\partial \theta}, v) + (\frac{\partial f}{\partial h}, \frac{\partial v}{\partial h}) = 0 \quad \text{for all } v \in H^1(\mathbb{R}_+).$$

Let

$$\tilde{\varphi}_i(h) = \hat{L}_i(h) - a_i \hat{L}_{i+1}(h) \quad \text{with } a_i = \frac{i + \frac{1}{2}}{(i+1) + \frac{1}{2}}, \quad i = 0, \cdots, N-1,$$

and $\tilde{X}_N = \text{span}\{\tilde{\varphi}_0, \tilde{\varphi}_1, \ldots, \tilde{\varphi}_{N-1}\}$. It is easy to check that each $\tilde{\varphi}_i$ satisfies the homogeneous Neumann boundary condition at $h = 0$. Then the Galerkin method for this problem is the following.

Find $f_N \in \tilde{X}_N$ such that

$$(\frac{\partial f_N}{\partial \theta}, v) + (\frac{\partial f_N}{\partial h}, \frac{\partial v}{\partial h}) = 0 \quad \text{for all } v \in \tilde{X}_N.$$

After using the backward Euler method for time-discretization we have

$$(f_N^{(n+1)}, v) + \Delta\theta(\frac{\partial f_N^{(n+1)}}{\partial h}, \frac{\partial v}{\partial h}) = (f_N^{(n)}, v) \quad \text{for all } v \in \tilde{X}_N. \tag{3.21}$$

In computing the right hand side at the initial step ($n = 0$) we obtain

$$(f_N^{(0)}, \tilde{\varphi}_i) = \left(\sum_{n=1}^{N} c_n \hat{L}_n, \tilde{\varphi}_i \right) = c_i - a_i \, c_{i+1},$$

due to the orthonormality of $\hat{L}_i$'s.

(b) Two-cell case. Next we consider a two-cell case. Similar to the one-cell problem, the problem (3.7) becomes the following system of heat equations in the boundary layer coordinate system. First, for $0 < \theta < \pi$

$$\frac{\partial^2 f}{\partial h^2} - \frac{\partial f}{\partial \theta} = 0, \quad -\infty < h < \infty, \tag{3.22}$$

with the homogeneous Neumann boundary conditions at $\pm\infty$ and unknown initial data $f^0(h)$ which will be determined below in (3.25). Next, for $\pi < \theta < 3\pi$ we consider two problems for positive and negative half real lines on the variable h, respectively:

$$\begin{aligned}
\frac{\partial f^+}{\partial \theta} - \frac{\partial^2 f^+}{\partial h^2} &= 0, \quad h > 0, \quad \pi < \theta < 3\pi, \\
\frac{\partial f^+}{\partial h}(0, \theta) &= 0, \quad \pi < \theta < \tfrac{3\pi}{2}, \\
f^+(0, \theta) &= \pi, \quad \tfrac{3\pi}{2} < \theta < \tfrac{5\pi}{2}, \\
\frac{\partial f^+}{\partial h}(0, \theta) &= 0, \quad \tfrac{5\pi}{2} < \theta < 3\pi,
\end{aligned} \tag{3.23}$$

and

$$\begin{aligned}
\frac{\partial f^-}{\partial \theta} - \frac{\partial^2 f^-}{\partial h^2} &= 0, \quad h < 0, \quad \pi < \theta < 3\pi, \\
\frac{\partial f^-}{\partial h}(0, \theta) &= 0, \quad \pi < \theta < \tfrac{3\pi}{2}, \\
f^-(0, \theta) &= 0, \quad \tfrac{3\pi}{2} < \theta < \tfrac{5\pi}{2}, \\
\frac{\partial f^-}{\partial h}(0, \theta) &= 0, \quad \tfrac{5\pi}{2} < \theta < 3\pi,
\end{aligned} \tag{3.24}$$

with the initial data

$$f^+(h,\pi) = f(h,\pi), \quad h > 0,$$

$$f^-(h,\pi) = f(h,\pi), \quad h < 0,$$

where f solves (3.22), and the homogeneous Neumann boundary conditions at $\pm\infty$. Hence due to the periodicity we have

$$f^0(h) = \begin{cases} f^+(h,3\pi), & h > 0, \\ f^-(h,3\pi), & h < 0. \end{cases} \tag{3.25}$$

Instead of using Laguerre functions as in the one-cell case, we use the Hermite functions to solve the two-cell problem, because the heat equation has to be solved in $(-\infty,\infty)$. In addition, we write the solution in the following form:

$$f(h,\theta) = \alpha_0(\theta)\mathrm{erf}(\frac{h}{\sqrt{2}}) + \sum_{i=1}^{N} \alpha_i(\theta)\hat{H}_{i-1}(h) + \hat{C} = f_1(h,\theta) + f_2(h,\theta) + \hat{C}, \tag{3.26}$$

where $\alpha_0(\theta)$ and $\alpha_i(\theta)$ are the θ-dependent coefficients in the expansion of $f(h,\theta)$. Here $\mathrm{erf}(h)$ is the Gauss error function given by

$$\mathrm{erf}(h) = \frac{2}{\sqrt{\pi}} \int_0^h e^{-t^2} dt,$$

and $f_1(h,\theta)$ denotes the odd part of the solution $f(h,\theta)$[1], $f_2(h,\theta)$ the even part which vanishes at $h = \pm\infty$, and $\hat{C}$ the constant part defined by

$$\hat{C} = \frac{1}{2}\left(\lim_{h\to\infty} f(h,\theta) + \lim_{h\to-\infty} f(h,\theta)\right).$$

Note that developing Galerkin approximation we use an even integer N in order to include 0 in the quadrature points. Due to the property that the Hermite functions with Hermite polynomials of odd degree are odd and the Hermite functions with Hermite polynomials of even degree are even, the linear combination of the Hermite

[1] "odd" part of solution f is $f_{odd} = \frac{f(h)-f(-h)}{2}$ and "even" is $f_{even} = \frac{f(h)+f(-h)}{2}$.

functions can be split into the linear combinations of the odd part and even part. Hence, we solve the equation for the even part and the odd part separately, splitting the initial function into the even and odd parts, respectively.

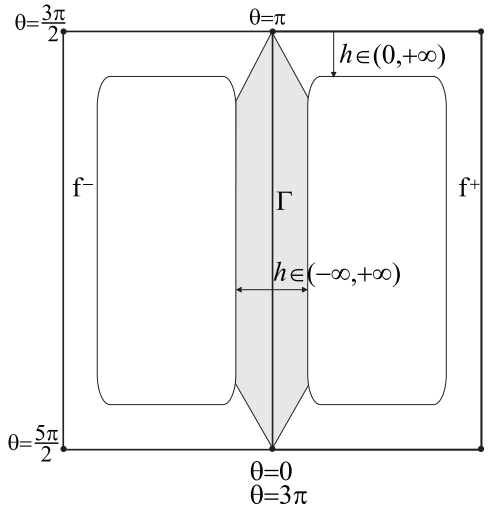

Fig. 23. Two cell problem

Next we are going to describe the method to obtain the periodic solution for the two-cell problem. In the same way as for the one-cell case, we formulate the overall matrix equation (3.20) to find the periodic solution. The matrix A and the vector g can be obtained by solving numerically the system of heat equations (3.22)-(3.24) with homogeneous Dirichlet conditions and each Hermite function as an initial data, and non-homogeneous Dirichlet conditions and zero initial condition, respectively. Thus, we present the procedure in steps 1-3 to solve a set of heat equations (3.22)-(3.24) sequentially with an initial function. In step 1, we show the way to set up the equation and the initial data to solve the problem (3.22) denoted by Γ shown on Figure 23 corresponding to the intermediate layer in boundary layer coordinates $h \in (-\infty, \infty)$. In step 2, we rewrite the solution function $f(h, \pi)$ obtained from step 1 in order to

use $f(h,\pi)$ as an initial data for the rest of the problem. In step 3, different types of basis functions are used in our Galerkin formulation, since the equations (3.23) and (3.24) have the various types of boundary conditions.

Step 1. We begin with solving the problem in Γ numerically. Here the initial function can be rewritten into sum of even and the odd parts

$$f(h,\theta=0)=f_0(h)=\frac{f_0(h)+f_0(-h)}{2}+\frac{f_0(h)-f_0(-h)}{2}.$$

We consider the problem for the even part

$$\begin{aligned}\frac{\partial^2 f_2}{\partial h^2}-\frac{\partial f_2}{\partial \theta} &= 0,\\ f_2(\pm\infty) &= 0,\\ f_2(\theta=0) &= \frac{f_0(h)+f_0(-h)}{2}.\end{aligned} \tag{3.27}$$

On the other hand, since the odd part $f_1(h,\theta)$ in (3.26) does not necessarily vanish at $h=\pm\infty$, we do not apply our Galerkin approach for $f_1(h,\theta)$. Instead, we consider the problem for its derivative which is an even function $p_1(h,\theta)=\frac{\partial f_1}{\partial h}(h,\theta)$:

$$\begin{aligned}\frac{\partial^2 p_1}{\partial h^2}-\frac{\partial p_1}{\partial \theta} &= 0,\\ p_1(\pm\infty) &= 0,\\ p_1(\theta=0) &= \frac{p_0(h)+p_0(-h)}{2},\end{aligned} \tag{3.28}$$

where $p_0(h)=\frac{\partial f_0}{\partial h}(h)$. Since the derivative of $\mathrm{erf}(\frac{h}{\sqrt{2}})$ and odd Hermite functions are expressed in terms of even Hermite functions, and this problem is exactly same as the problem for f_2 (3.27) except the initial function. Later we would be able to reconstruct

the function $f_1(h,\theta)$ from its derivative $p_1(h,\theta)$ using condition $f_1(0,\theta)=0$

$$f_1(h,\theta)=\int p_1(h,\theta)dh=\int\sum_{i=0}^{\frac{N}{2}-1}\bar{\alpha}_{2i}(\theta)\hat{H}_{2i}(h)dh=\sum_{i=0}^{\frac{N}{2}-1}\bar{\alpha}_{2i}(\theta)\int\hat{H}_{2i}(h)dh,\ ^{2}$$

where $\bar{\alpha}_{2i}(\theta)$ are the coefficients of the linear combination representing $p_1(h,\theta)$. After solving both equations (3.27) and (3.28) for $0<\theta<\pi$, we obtain the function

$$f(h,\pi)=f_1(h,\pi)+f_2(h,\pi)+\hat{C}, \tag{3.29}$$

which will be used as initial functions for the next problems. The value of "constant part" of f stays the same in time since any constant satisfies the equation (3.22).

Step 2. After solving the problem in Γ, we split the solution into two defined for $h>0$ and $h<0$, respectively. We use the functions as initial functions of the equation (3.23) and (3.24), respectively. Furthermore, we consider the projection of the Gaussian error function onto the subspace spanned by the Hermite functions. The Gaussian error function tends to ±1 at $\pm\infty$ but our Galerkin formulation needs that any function should vanish at $\pm\infty$. Thus, different modifications are considered over the positive and negative half spaces in performing the projection of the Gaussian error function:

$$\operatorname{erf}(\frac{h}{\sqrt{2}})=\begin{cases}[\operatorname{erf}(\frac{h}{\sqrt{2}})+1]-1, & \text{for } h<0\\ [\operatorname{erf}(\frac{h}{\sqrt{2}})-1]+1, & \text{for } h>0.\end{cases}$$

[2]Note that the antiderivative of even Hermite function contains $\operatorname{erf}(h/\sqrt{2})$, which implies that $f_1(h,\theta)$ is expressed by the linear combination of the Gaussian error function and the odd Hermite functions. In finding the coefficient of $\operatorname{erf}(h/\sqrt{2})$ in the expansion of $f_1(h,\theta)$, we use the following formula:

$$\int\hat{H}_{2n}(h)dh=\sqrt{2\pi}\,\frac{1\cdot3\cdot5\cdots(2n-1)}{2}\operatorname{erf}(h/\sqrt{2})+\cdots.$$

Then the solution at $\theta = \pi$ can be rewritten by

$$f(h,\pi) = \begin{cases} f^- = \beta_0[\mathrm{erf}(\frac{h}{\sqrt{2}}) + 1] + \sum_{i=1}^{N} \beta_i \hat{H}_{i-1}(h) + \hat{C} - \beta_0, & \text{for } h < 0, \\ f^+ = \beta_0[\mathrm{erf}(\frac{h}{\sqrt{2}}) - 1] + \sum_{i=1}^{N} \beta_i \hat{H}_{i-1}(h) + \hat{C} + \beta_0, & \text{for } h > 0, \end{cases}$$

where β_i are the coefficients in the expansion of $f_1(h,\pi) + f_2(h,\pi)$ in (3.29). Hence, we can decompose $f(h,\pi)$ into even and odd Hermite functions and constant over regions $h < 0$, $h > 0$.

Step 3. Next, we consider the problems (3.23) and (3.24) for positive and negative half spaces. Furthermore, for each half space problem we separate it into the problems for the even and odd parts. Note that the odd Hermite functions satisfy the zero Dirichlet boundary condition at $h = 0$ and the even Hermite functions satisfy the zero Neumann boundary condition at $h = 0$. These properties imply that the odd Hermite functions can be used as basis elements to solve the half space problems for the odd part with zero Dirichlet boundary condition. Similarly, the even Hermite functions can be used to solve the half space problems for the even part with zero Neumann boundary condition.

On the other hand, the different types of basis functions are used in solving the half space problems for the odd part with zero Neumann boundary condition and the half space problems for the even part with zero Dirichlet condition at $h = 0$, respectively. Namely, we use

$$\hat{\psi}_i(h) = \frac{1}{\hat{H}_{2(i-1)}(0)} \hat{H}_{2(i-1)}(h) - \frac{1}{\hat{H}_{2i}(0)} \hat{H}_{2i}(h) \tag{3.30}$$

as basis elements in formulating stiffness and mass matrices in the Galerkin approach solving the half space problems, for the even parts with zero Dirichlet condition at

$h = 0$, and we use the functions

$$\tilde{\psi}_i(h) = \sqrt{\frac{2i+1}{2i}}\hat{H}_{2i-1}(h) + \hat{H}_{2i+1}(h)$$

as basis elements in solving the half space problems for the odd part with zero Neumann condition at $h = 0$, with $i = 1, 2, \cdots, \frac{N}{2} - 1$.

Here, the half space problems with Dirichlet conditions should be considered carefully. Since the odd Hermite functions vanish at $h = 0$, the odd parts f_1 spanned by the odd Hermite functions satisfy zero Dirichlet condition. Thus, the sum of the even f_2 and constant parts should have same Dirichlet boundary conditions as f has. Since any constant is one of the solutions of the equation in solving the problem in Γ, we decompose the even part of the solution into the constant and even Hermite functions. However the even and constant parts are considered simultaneously as for the half space problems with Dirichlet data, that is,

$$\begin{aligned}
&\frac{\partial f_2}{\partial \theta} = \frac{\partial^2 f_2}{\partial h^2}, \qquad \frac{3\pi}{2} < \theta < \frac{5\pi}{2}, \quad h < 0 \text{ or } h > 0, \\
&f_2(h = 0, \theta) = a - \hat{C}, \\
&\frac{\partial f_2}{\partial h}(h = \infty, \theta) = 0,
\end{aligned}$$

where $f_2(h, \frac{3\pi}{2})$ found earlier is used as the initial data and a is the number corresponding to the boundary condition (3.8) of the original problem, that is, $a = 0$ for the left cell ($h < 0$) and $a = \pi$ for the right cell ($h > 0$). Note that the boundary conditions $a - \hat{C}$ at $h = 0$ are generally not zero. In the case of non-homogeneous problem, we assume the solution has the form $f_2 = \tilde{f}_2 + (a - \hat{C})e^{-h^2/2}$, where $\tilde{f}_2$ is

the solution of the following homogeneous problem

$$\frac{\partial \tilde{f}_2}{\partial \theta} - \frac{\partial^2 \tilde{f}_2}{\partial h^2} = (a - \hat{C})(h^2 - 1)e^{-h^2/2}, \qquad \frac{3\pi}{2} < \theta < \frac{5\pi}{2}, \quad h < 0 \text{ or } h > 0,$$
$$\tilde{f}_2(h, \theta = \tfrac{3\pi}{2}) = f_2(h, \tfrac{3\pi}{2}) - (a - \hat{C})e^{-h^2/2},$$
$$\tilde{f}_2(h = 0, \theta) = 0,$$
$$\frac{\partial \tilde{f}_2}{\partial h}(h = \infty, \theta) = 0.$$

Finally, the Galerkin method with basis elements $\{\hat{\psi}_i\}$ defined in (3.30) can be applied to obtain $\tilde{f}_2$ from which one obtains $f_2 = \tilde{f}_2 + (a - \hat{C})e^{-h^2/2}$.

c. Collocation approach

In this section we consider a collocation method. Its main idea is to write differential equations at certain collocation points, which are chosen later. We assume that the approximate solution of the heat equations is

$$f(h, \theta) = \sum_i F_i(\theta) T_i(h),$$

where $T_0(h) = 1$, $T_1(h) = \text{erf}(\frac{h}{\sqrt{2}})$, $T_2(h) = \hat{H}_0(h)$, $T_3(h) = \hat{H}_1(h)$, $\cdots$. Furthermore, we assume we have some grid points $\{h_j\}$ in the domain $(-\infty, \infty)$. Then for each grid point h_j the equation becomes

$$\sum_i \frac{F_i^{n+1} - F_i^n}{\Delta\theta} T_i(h_j) = \sum_i F_i^{n+1} T_i''(h_j),$$

where F_i^{n+1} is the approximating solution at the nth time step. Then it can be rewritten by

$$\sum_i \{T_i(h_j) - \Delta\theta T_i''(h_j)\} U_i^{n+1} = \sum_i T_i(h_j) U_i^n. \tag{3.31}$$

Hence, we obtain the system of the linear equations $Ax = b$, where

$$a_{ji} = T_i(h_j) - \Delta\theta T_i''(h_j), \quad b_j = \sum_i T_i(h_j) F_i^n, \quad x_i = F_i^{n+1}.$$

In computing a_{ji}, it is easy to find the second derivatives $T_0''(h)$ and $T_1''(h)$, but it is not obvious to find $T_i''(h)$ for $i \geq 2$. Since the Hermite polynomials satisfy the differential equation

$$H_n''(h) - 2hH_n'(h) + 2nH_n(h) = 0,$$

and the relation

$$H_n'(h) = 2nH_{n-1}(h),$$

we have the second derivative of the Hermite polynomial

$$H_n''(h) = 2hH_n'(h) - 2nH_n(h) = 2n(2hH_{n-1}(h) - H_n(h)).$$

Thus the second derivative of Hermite functions can be obtained by

$$\hat{H}_n''(h) = \{4n(n-1)H_{n-2}(h) - 4nhH_{n-1}(h) + (h^2-1)H_n(h)\}e^{-h^2/2},$$

and for $i \geq 2$, we have

$$\begin{aligned} a_{ji} &= T_i(h_j) - \Delta\theta T_i''(h_j) \\ &= \frac{1}{\sqrt{2^{i-2}(i-2)!\sqrt{\pi}}} \left[H_{i-2}(h_j) - \Delta t\{4(i-2)(i-3)H_{i-4}(h_j) \right. \\ &\qquad \left. -4(i-2)h_jH_{i-3}(h_j) + (h_j^2-1)H_{i-2}(h_j)\}\right] e^{-h_j^2/2}. \end{aligned}$$

Since all $T_i(h)$ satisfy the homogeneous Neumann boundary condition at $\pm\infty$, the above formulation (3.31) solves the problem Γ. In solving the half space problems with Dirichlet boundary conditions after splitting into positive and negative parts, we formulate the system of the linear equations $By = z$ by modifying the matrix A slightly, that is, the matrix B is the same as the matrix A except the row correspond-

ing the grid point $x_j = 0$ satisfying

$$f(0,\theta) = F_0(\theta) + F_1(\theta)\mathrm{erf}(0) + \sum_{i=2} F_i(\theta)\hat{H}_{i-2}(0) = D(\theta),$$

where $D(\theta)$ is the Dirichlet boundary conditions at $h = 0$, which are described in (3.38) and (3.39). Here $y_i = F_i^{n+1}$, and $z_i = b_i$ for $i \neq j$ and $z_j = D(\theta)$.

2. Finite difference methods on exponential grids

Finding approximate solutions of the Childress' problem (3.16) for each cell, we use the finite difference scheme instead of spectral methods described in the previous section. For the infinite and semi-infinite domain $(-\infty, \infty)$, $(0, \infty)$ we do not use a finite difference scheme over the uniform grid. Instead, we use an exponential grid. Note that the Hermite and Laguerre functions decay exponentially. Here we define an exponential grid. Let $\{0 = y_0, y_1, \cdots, y_N = 1\}$ be the uniformly distributed points in the interval $[0, 1]$. Then for an appropriate positive constant C which is a stretching parameter, the positive part of the exponential grid points are defined by

$$t_j = -C \ln y_j, \qquad \text{for each} \quad j = 1, \cdots, N. \tag{3.32}$$

We define the negative part of the exponential grid points by reflecting the points $\{t_j\}_{i=1}^{N}$ about the origin. Thus the all grid points $\{x_i\}_{i=1}^{2N-1}$ can be obtained by merging those two parts

$$x_1 = -t_1, x_2 = -t_2, \cdots, x_N = -t_N = 0, x_{N+1} = t_{N-1}, \cdots, x_{2N-1} = t_1.$$

We considered the general multiple-cell case for the asymptotic problem explained in Section 3. However, we start looking at simplest case of the problems. For one-cell case it is obvious how to use this approach and hence we begin with investigating the two-cell case.

a. Two-cell problem

Now we consider the two-cell problem (3.22)-(3.24) again. Similar to the spectral approaches, we develop the overall matrix equation (3.20) to find the periodic solution. The matrix A and the vector g for two-cell problem with finite difference methods are determined as follows. Each "hat" function is used as an initial function to solve the problem (3.22), where "hat" is a function taking the value 1 on a subinterval (x_i, x_{i+1}), and zero elsewhere. In addition, the restriction of $f(h, \pi)$ in (3.22) over the $(0, x_{2N-1})$ is used as an initial condition for (3.23) and the restriction of $f(h, \pi)$ in (3.22) over the $(x_1, 0)$ is used as a initial condition for (3.23) with zero Dirichlet boundary condition at $h = 0$. Each column of the matrix A is the solution of the above procedure for each hat function of the grid. On the other hand, we obtain the solution vector g by solving (3.22)-(3.24) sequentially with zero initial condition and non-homogeneous Dirichlet boundary conditions. Then we have the system of the linear equations (3.20). Thus, we present the procedure to find an approximate solution of a sequence of heat equations (3.22)-(3.24) with an initial function by using finite difference scheme on the exponential grid points. We approximate the solution of the problem (3.22)-(3.24) by the solution of the same equations in the interval (x_1, x_{2N-1}). Here we impose the Neumann boundary condition at end points of the interval

$$\frac{\partial f}{\partial h}(h = x_1, \theta) = \frac{\partial f}{\partial h}(h = x_{2N-1}, \theta) = 0.$$

First, we consider the problem (3.22) in (x_1, x_{2N-1}). Integrating the equation over each subinterval $[x_i, x_{i+1}]$, $i = 1, \cdots, 2N-2$, gives us

$$\int_{x_i}^{x_{i+1}} \frac{\partial f}{\partial \theta} dh = \int_{x_i}^{x_{i+1}} \frac{\partial^2 f}{\partial h^2} dh,$$

$$\frac{\partial f}{\partial \theta} \Delta x = \frac{\partial f}{\partial h}(x_{i+1}) - \frac{\partial f}{\partial h}(x_i), \tag{3.33}$$

where $\Delta x = x_{i+1} - x_i$. Following the standard practice of finite volume methods [14], for each subinterval (x_i, x_{i+1}), the solution has only one value, denoted by $f_{i+1/2}$, due to piecewise constant approximation. Then (3.33) can be rewritten by

$$\frac{\partial f_{i+1/2}}{\partial \theta}\Delta x = \frac{\partial f}{\partial h}(x_{i+1}) - \frac{\partial f}{\partial h}(x_i).$$

By applying the finite difference scheme for $\frac{\partial f}{\partial h}$ and using the backward Euler method in time-discretization with step size $\Delta\theta$, we obtain the difference equation at $(n+1)$th time step

$$\frac{f_{i+1/2}^{n+1} - f_{i+1/2}^{n}}{\Delta\theta}\Delta x = \frac{f_{i+3/2}^{n+1} - f_{i+1/2}^{n+1}}{x_{i+3/2} - x_{i+1/2}} - \frac{f_{i+1/2}^{n+1} - f_{i-1/2}^{n+1}}{x_{i+1/2} - x_{i-1/2}} \tag{3.34}$$

for $i = 1, \cdots, 2N-2$. For $i = 0, 2N-2$ we use Neumann boundary conditions:

$$\left(1 + \frac{\Delta\theta}{\Delta x}\frac{1}{x_{3/2} - x_{1/2}}\right) f_{1/2}^{n+1} - \frac{\Delta\theta}{\Delta x}\frac{1}{x_{3/2} - x_{1/2}} f_{3/2}^{n+1} = f_{1/2}^{n} \tag{3.35}$$

$$\left(1 + \frac{\Delta\theta}{\Delta x}\frac{1}{x_{2N-3/2} - x_{2N-5/2}}\right) f_{2N-3/2}^{n+1} - \frac{\Delta\theta}{\Delta x}\frac{1}{x_{2N-3/2} - x_{2N-5/2}} f_{2N-5/2}^{n+1} = f_{2N-3/2}^{n} \tag{3.36}$$

and then the numerical solution $f(h, \pi)$ of (3.22) can be obtained by solving the matrix equation (3.34)-(3.36) from the backward Euler method.

Next we consider splitting the problem into (3.23) and (3.24). Since the basis functions are defined in the whole domain $(-\infty, \infty)$ in spectral approach, it is hard to split and merge a function into positive and negative parts. However, the fact that the functions in finite difference method are defined pointwise enables to make splitting and merging procedures easily. The half of grid points associated to positive part $\{x_i\}_{i=N}^{2N-1}$ is used to solve the problem (3.23) and half of grid points associated to negative part $\{x_i\}_{i=1}^{N}$ is used to solve the problem (3.24). We use the formulation (3.34)-(3.36) to solve those half space problems with the corresponding boundary conditions at $h = 0$.

Our numerical results for two-cell problem will be presented in the next section.

b. Four-cell problem

Another example is four-cell problem with the exponential grid technique. We consider the same equation as the two-cell case except that the domain Ω is divided into four cells whose separatrices are the line $x_1 = \frac{\pi}{2}$ and $x_2 = \frac{\pi}{2}$ (see the Figure 24).

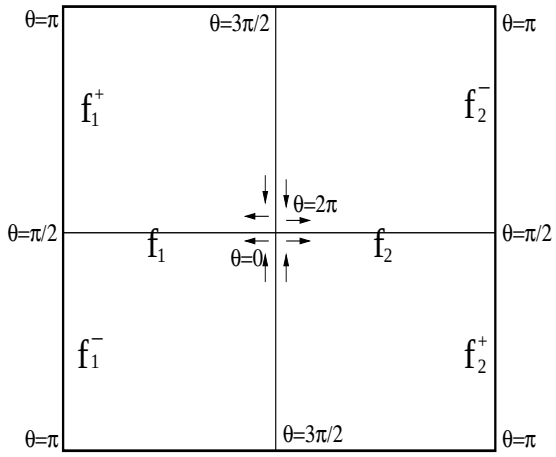

Fig. 24. Four cell problem

We start solving the Childress' problem (3.16) at the center point in four-cell problem. Since the flows at the center point have opposite directions, the solution at the center points have two different forms, and f_1 and f_2 denote the solution at the center point going to left and right directions, respectively.

First for $0 < \theta < \frac{\pi}{2}$, we solve the problems in Γ, where Γ is the region $(-\infty, \infty)$ for boundary layer variable h along separatrices, for f_1 and f_2 independently,

$$\begin{aligned} \frac{\partial f_1}{\partial \theta} - \frac{\partial^2 f_1}{\partial h^2} = 0, \quad -\infty < h < \infty, \\ \frac{\partial f_2}{\partial \theta} - \frac{\partial^2 f_2}{\partial h^2} = 0, \quad -\infty < h < \infty, \end{aligned} \tag{3.37}$$

with the homogeneous Neumann boundary conditions at $\pm\infty$ and a prescribed initial functions $f_1^0(h)$ and $f_2^0(h)$ determined below by periodicity. At $\theta = \frac{\pi}{2}$ we split the solution into two corresponding to $h > 0$ and $h < 0$:

$$f_1(h,\pi) = \begin{cases} f_1^+(h,\pi), & h > 0, \\ f_1^-(h,\pi), & h < 0, \end{cases} \qquad f_2(h,\pi) = \begin{cases} f_2^+(h,\pi), & h > 0, \\ f_2^-(h,\pi), & h < 0, \end{cases}$$

and use those functions as initial conditions of the half space problems

$$\begin{cases} \dfrac{\partial f_1^+}{\partial\theta} - \dfrac{\partial^2 f_1^+}{\partial h^2} = 0, & h > 0 \\ f_1^+(0,\theta) = 0, & \pi/2 < \theta < \pi, \\ \dfrac{\partial f_1^+}{\partial h}(0,\theta) = 0, & \pi < \theta < 3\pi/2 \end{cases} \qquad \begin{cases} \dfrac{\partial f_1^-}{\partial\theta} - \dfrac{\partial^2 f_1^-}{\partial h^2} = 0, & h < 0 \\ f_1^-(0,\theta) = \pi, & \pi/2 < \theta < \pi, \\ \dfrac{\partial f_1^-}{\partial h}(0,\theta) = 0, & \pi < \theta < 3\pi/2. \end{cases}$$

and

$$\begin{cases} \dfrac{\partial f_2^+}{\partial\theta} - \dfrac{\partial^2 f_2^+}{\partial h^2} = 0, & h > 0 \\ f_2^+(0,\theta) = 0, & \pi/2 < \theta < \pi, \\ \dfrac{\partial f_2^+}{\partial h}(0,\theta) = 0, & \pi < \theta < 3\pi/2 \end{cases} \qquad \begin{cases} \dfrac{\partial f_2^-}{\partial\theta} - \dfrac{\partial^2 f_2^-}{\partial h^2} = 0, & h < 0 \\ f_2^-(0,\theta) = \pi, & \pi/2 < \theta < \pi, \\ \dfrac{\partial f_2^-}{\partial h}(0,\theta) = 0, & \pi < \theta < 3\pi/2 \end{cases}$$

At $\theta = \frac{3\pi}{2}$ we glue those functions together in order to solve the problems in Γ. We define $\tilde{f}_1$ and $\tilde{f}_2$ by

$$\tilde{f}_1(h,\tfrac{3\pi}{2}) = \begin{cases} f_1^+(h,\frac{3\pi}{2}), & h > 0, \\ f_2^-(h,\frac{3\pi}{2}), & h < 0, \end{cases} \qquad \tilde{f}_2(h,\tfrac{3\pi}{2}) = \begin{cases} f_2^+(h,\frac{3\pi}{2}), & h > 0, \\ f_1^-(h,\frac{3\pi}{2}), & h < 0, \end{cases}$$

and use them as initial data of the equation (3.37) for $\frac{3\pi}{2} < \theta < 2\pi$. After getting $\tilde{f}_1(h,2\pi)$ and $\tilde{f}_2(h,2\pi)$, we split $\tilde{f}_1(h,2\pi)$ and $\tilde{f}_2(h,2\pi)$ two corresponding to $h > 0$ and $h < 0$ and glue them together by

$$f_1(h,2\pi) = \begin{cases} \tilde{f}_1^+(h,2\pi), & h > 0, \\ \tilde{f}_2^-(h,2\pi), & h < 0, \end{cases} \qquad f_2(h,2\pi) = \begin{cases} \tilde{f}_2^+(h,2\pi), & h > 0, \\ \tilde{f}_1^-(h,2\pi), & h < 0, \end{cases}$$

in order to match the solutions with initial data

$$f_1^0(h) = f_1(h, 2\pi), \quad -\infty < h < \infty,$$
$$f_2^0(h) = f_2(h, 2\pi), \quad -\infty < h < \infty,$$

which implies the periodicity of the solution. The numerical results for the four-cell case problem will be given in the next section.

C. Numerical results

In this section, we present some numerical results which are obtained from the cases discussed above. First results we show are for the one-cell problem solved by the spectral Galerkin method. Figure 25 illustrates the periodic initial condition for reduced Childress' problem (3.19) for one-cell case. Furthermore, the L_2-norms of the difference between initial function and solution function on $[4M\pi, 4(M+1)\pi]$ are computed for $M = 0, 1, 2, 3$ in Table I, which shows the periodicity of the solution.

Table I. L_2-norms of the difference between initial and solution functions on $[4M\pi, 4(M+1)\pi](M = 0, 1, 2, 3)$

M	L_2-norm
0	7.2721e-15
1	2.8771e-15
2	1.1075e-14
3	3.6108e-15

In Figure 26 we plot the periodic solution. The left plot represents a periodic solution of reduced equations related to Childress' problem (3.16) in the region $h > 0,\ 0 < \theta < 4\pi$, and the right plot shows the reconstructed solution in the original

domain Ω from the periodic solution of the left plot.

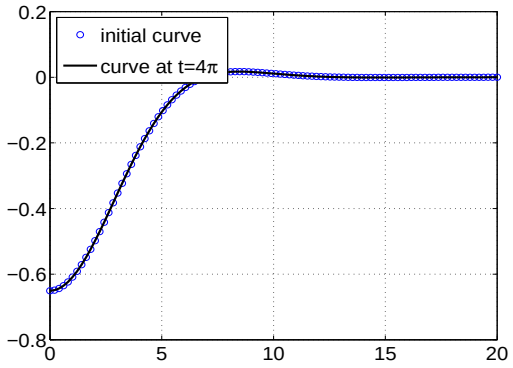

Fig. 25. Initial and final curve of periodic solution

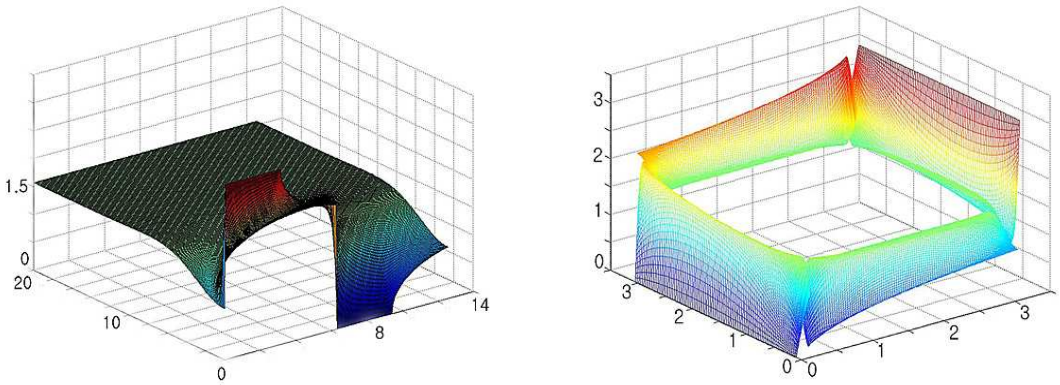

Fig. 26. Periodic solution (left) and reconstructed solution of Childress problem (right).

Next we present the solution of the two-cell problem using the finite difference scheme on exponential grids. The stretching parameter C in (3.32) was chosen to be 5. In Figure 27 we present the periodic solution for the two-cell problem (3.22)-(3.24). The left figure there indicates the periodicity of the solution we obtained. In

the right figure we make a comparison with a curve from the 2-D solution we obtained by MATLAB PDE toolbox for $\varepsilon = 10^{-3}$.

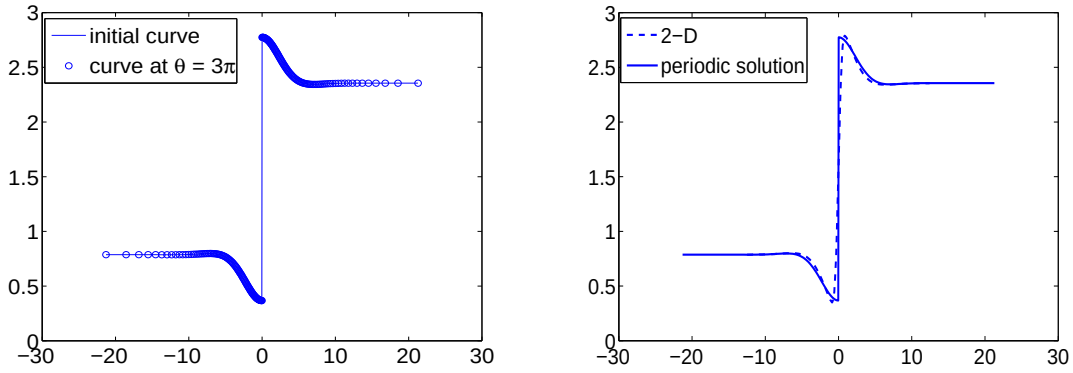

Fig. 27. Periodic solution at $t = 0$ and $t = 3\pi$ (left), and comparison of initial curve from periodic solution with curve from 2-D solution (right).

Next results we show are for the four-cell problem solved by the finite difference methods on exponential grids. Figure 28 demonstrate the periodic initial curve at the center point of four-cell. Note that there are two curves at the center point due to the separation of the flow at that point and the behavior of the solution along the opposite edge are different. We present the solution of the four-cell problem for some small number $\varepsilon = 10^{-3}$ by using MATLAB PDE toolbox in the left of Figure 29 and the comparison our periodic initial curve with some curve from the solution in the left of Figure 29.

Finally, we consider another two-cell problem with Dirichlet boundary condition

$$f(x, y) = x \quad \text{on } \partial\Omega.$$

For this boundary conditions, the system of the heat equation (3.22)-(3.24) is changed slightly. We begin with the equation (3.22) for $0 < \theta < \pi$. Next we consider splitting

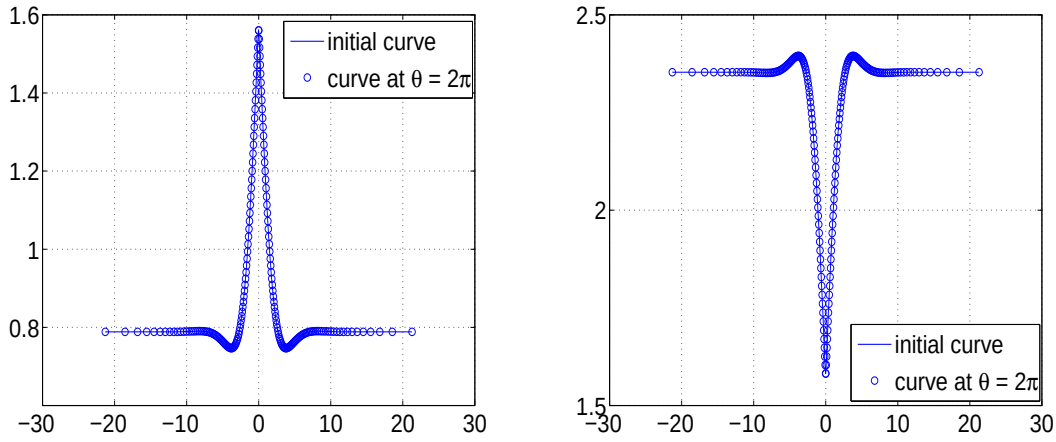

Fig. 28. Periodic solution u_1 (left) and u_2 (right) at $\theta = 0$

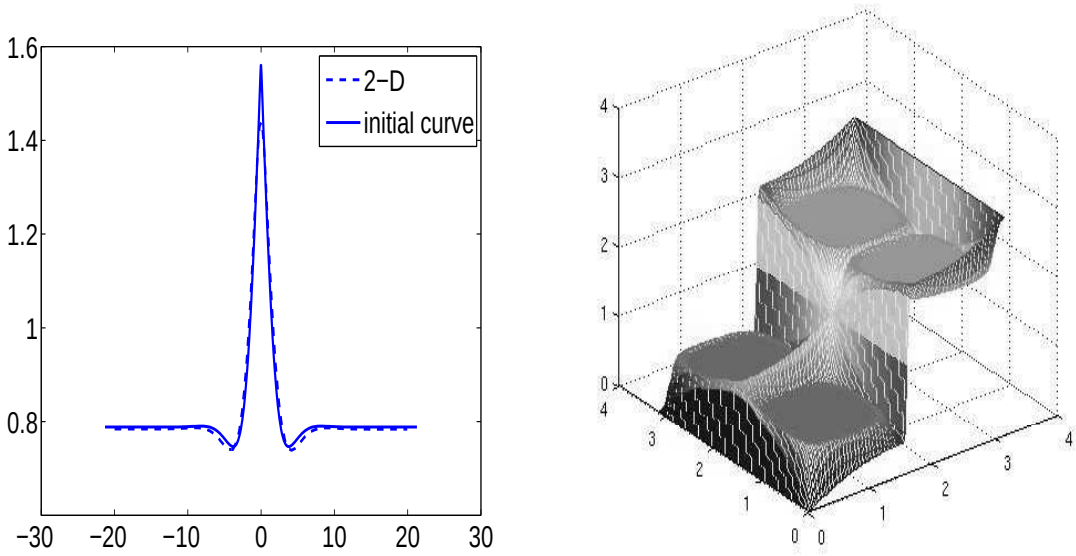

Fig. 29. Comparison of periodic solution with curve from 2-D solution

for positive and negative half spaces for the variable h, respectively:

$$\begin{aligned}
&\frac{\partial f^+}{\partial \theta} - \frac{\partial^2 f^+}{\partial h^2} = 0, && h > 0, \quad \pi < \theta < 3\pi, \\
&f^+(0,\theta) = (\theta - \pi) + \pi/2, && \pi < \theta < 3\pi/2, \\
&f^+(0,\theta) = \pi, && 3\pi/2 < \theta < 5\pi/2, \\
&f^+(0,\theta) = -(\theta - 5\pi/2) + \pi, && 5\pi < \theta < 3\pi,
\end{aligned} \tag{3.38}$$

and

$$\begin{aligned}
&\frac{\partial f^-}{\partial \theta} - \frac{\partial^2 f^-}{\partial h^2} = 0, && h < 0, \quad \pi < \theta < 3\pi, \\
&f^-(0,\theta) = -(\theta - \pi) + \pi/2, && \pi < \theta < 3\pi/2, \\
&f^-(0,\theta) = 0, && 3\pi/2 < \theta < 5\pi/2, \\
&f^-(0,\theta) = (\theta - 5\pi/2), && 5\pi < \theta < 3\pi.
\end{aligned} \tag{3.39}$$

with homogeneous Neumann boundary conditions at $h = \pm\infty$. Figures 30 - 33 show the solution of the system of heat equations (3.22), (3.38), (3.39) at some particular time. Especially, the curve in the left plot of the Figure 30 is the periodic initial condition which is obtained by solving the system of the linear equations (3.20) for two-cell case. In addition, we compare the initial curve in Figure 30 with the curve from the solution which is obtained by MATLAB PDE toolbox and Figure 34 shows us that there is a curve matching with the periodic initial condition.

1. Truncated region approach

We mentioned "water-pipe network" modeling to approximate the solution of the steady advection-diffusion problem (3.7) by restricting the domain to the region of width $K\sqrt{\varepsilon}$ near the separatrices for some positive fixed number K. Here we present a so-called the "truncated region" approach is described as follows. The domain is restricted to the region $\Omega_K^\varepsilon = \Omega \cap \{|\Psi(x)| \leq K\sqrt{\varepsilon}\}$ and hence the boundary of Ω_K^ε

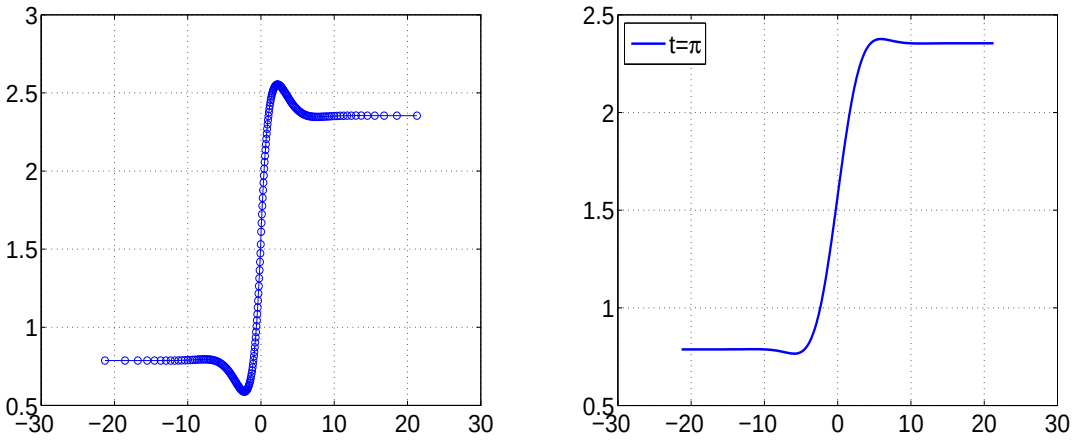

Fig. 30. Periodic solution at $t = 0$ and $t = 3\pi$ (left) and at $t = \pi$ (right)

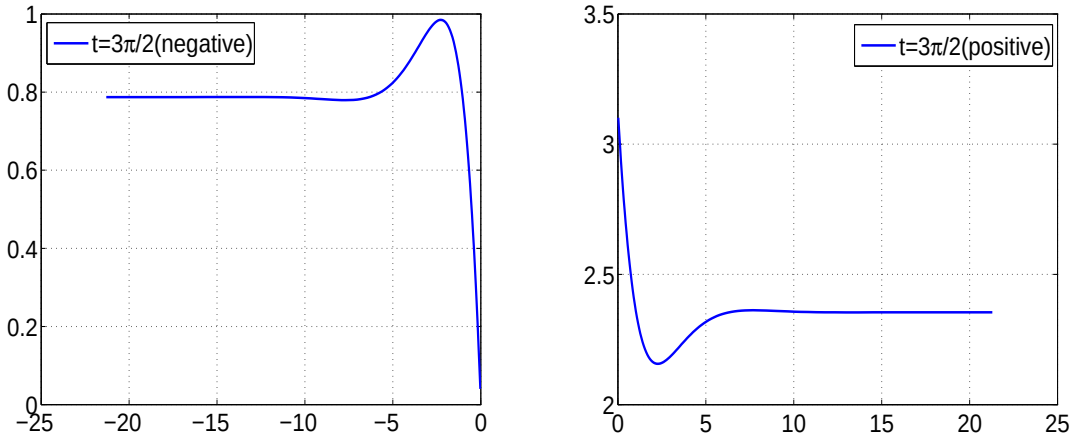

Fig. 31. Periodic solution (negative and positive parts) at $t = \frac{3\pi}{2}$

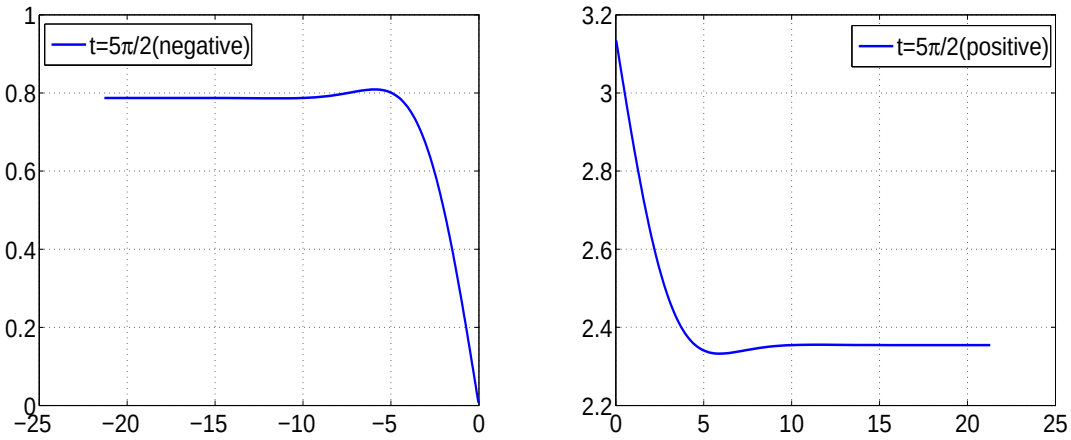

Fig. 32. Periodic solution (negative and positive parts) at $t = \frac{5\pi}{2}$

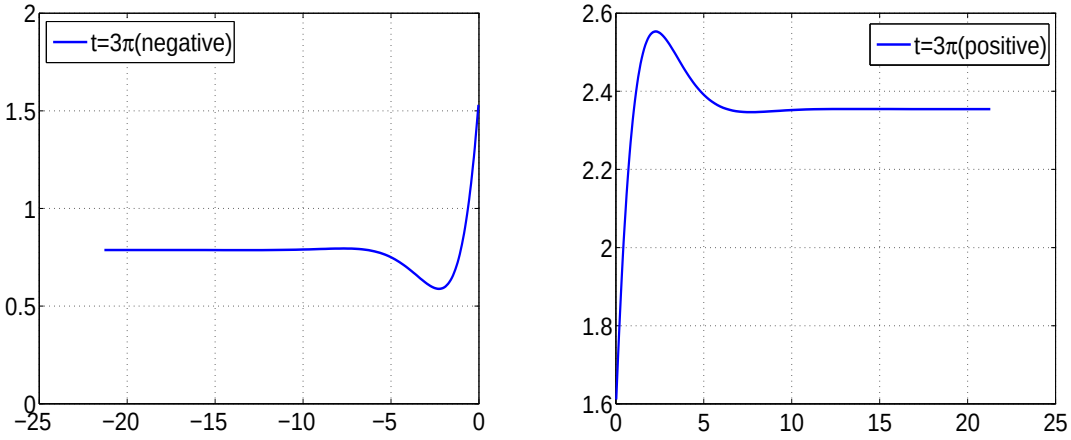

Fig. 33. Periodic solution (negative and positive parts) at $t = 3\pi$

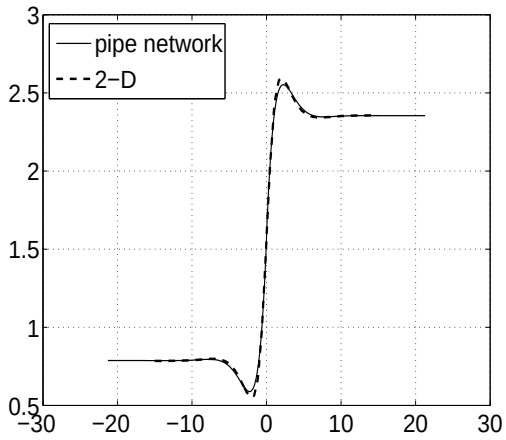

Fig. 34. Comparison of periodic solution with curve from exact solution

consists of $\partial\Omega$ and the level curves $l_K = \{x \in \Omega : \Psi(x) = K\sqrt{\varepsilon}\}$. Then we approximate the solution of (3.7) by the solution of the following equation

$$\varepsilon\Delta\phi_K^\varepsilon - u \cdot \nabla\phi_K^\varepsilon = 0, \quad x \in \Omega_K^\varepsilon$$

with the boundary conditions

$$\phi_K^\varepsilon|_{\partial\Omega} = T_0, \quad \left.\frac{\partial\phi_K^\varepsilon}{\partial n}\right|_{l_K} = 0.$$

We perform numerical tests for this approach with MATLAB PDE toolbox and focus on the one-cell and four-cell cases in these test. The square $(0,1)\times(0,1)$ and $(-1,1)\times(-1,1)$ in $\mathbb{R}^2$ are considered as the domains for one-cell and four-cell cases, respectively. We set the stream function $\Psi(x)$ by $\Psi(x_1,x_2) = \sin(\pi x_1)\sin(\pi x_2)$, and the small molecular diffusivity by $\varepsilon = 10^{-2}$ and $\varepsilon = 10^{-3}$ for one-cell and four-cell case, respectively. The positive number K was chosen by 5 in both cases.

According to the right plot of Figure 35 the solutions of the truncated region approach approximate the solutions of the (3.7) presented in Figure 29 in the case

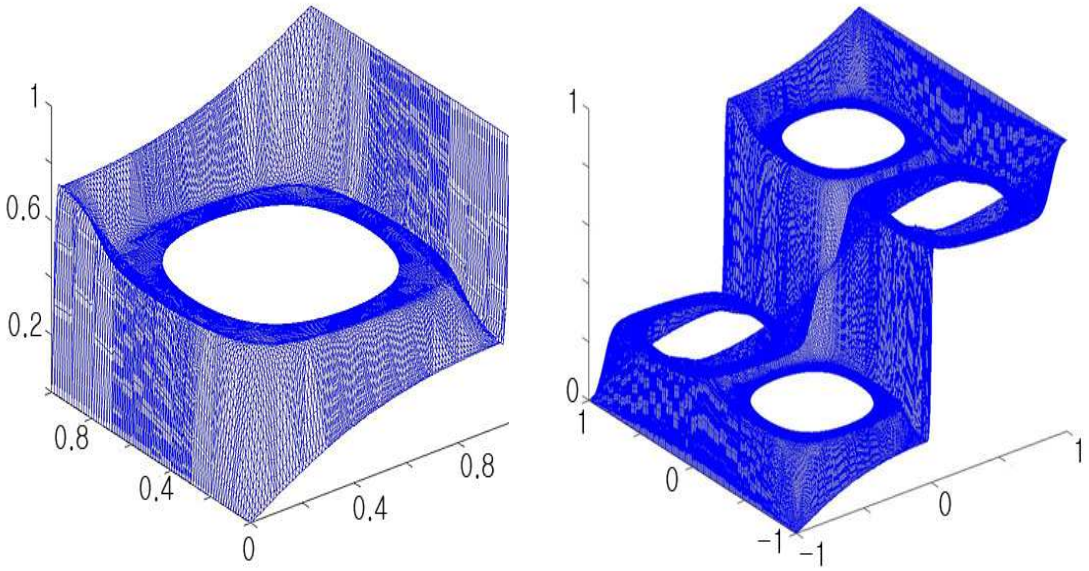

Fig. 35. Approximating solutions by truncated region approach

of 10^{-3}. However, it turns out that the method with MATLAB PDE toolbox is not good for much smaller parameter ε due to difficulty in mesh generation in the narrow pipes.

CHAPTER IV

EFFICIENT MULTISCALE METHODS FOR PARABOLIC EQUATIONS IN HIGH CONTRAST MEDIA

In this chapter we discuss an efficient multiscale methods for parabolic equations in highly contrast media. A modified multiscale finite element method for the computations of two-phase flows was proposed in [8]. The main idea of this approach is to use a global information in constructing finite element basis functions. This approach is intended for the problems without apparent scale separation. We analyze the asymptotic results needed for the analysis of global MsFEM. In particular, we show that under some assumptions the solution is a smooth function of the steady state solution. We note that these results are used in [21] for analysis of MsFEM.

We begin with describing the domain Ω which is a unit square in $\mathbb{R}^2$. We assume that there is a high permeable channel in Ω, that is, the permeability in the channel is larger than outside the channel (see, e.g., Figure 36).

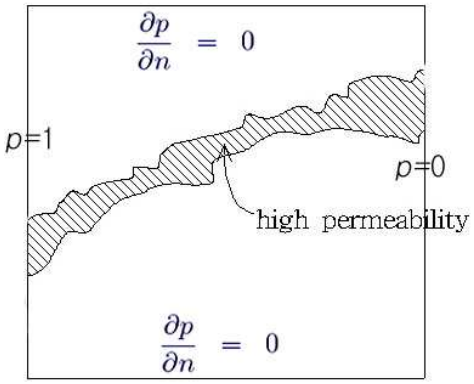

Fig. 36. High flow channel

Consider the following parabolic equations

$$D_t p - \mathrm{div}(a(x)\nabla p) = 0 \quad \text{in} \quad \Omega, \tag{4.1}$$

where we impose the boundary conditions in the following way: $p = 1$ on the left vertical edge, $p = 0$ on the right vertical edge, and no flow condition on the lateral edges. Initial condition is given by the function defined by $p = 1$ on the left vertical edge, and $p = 0$ elsewhere. Here the velocity field v is assumed $v = a(x)\nabla p = a(x)I\nabla p$. Furthermore, The stream function Ψ is defined as $v = (-\frac{\partial \Psi}{\partial x_2}, \frac{\partial \Psi}{\partial x_1})$.

Let us denote by p_0 the steady solution of the parabolic equation satisfying

$$\mathrm{div}(a(x)\nabla p_0) = 0,$$

with the same boundary condition as in (4.1). Denote by $\Psi_0 = \Psi(t = \infty)$ the stream function at steady state defined by zero at the bottom edge. For the analysis, we use streamline-pressure coordinates $\eta = \Psi_0$, $\zeta = p_0$. We note that (Ψ_0, p_0) define an orthogonal curvilinear coordinate system. Indeed, since $v = (a(x)\frac{\partial p_o}{\partial x_1}, a(x)\frac{\partial p_o}{\partial x_2}) = (-\frac{\partial \Psi_0}{\partial x_2}, \frac{\partial \Psi_0}{\partial x_1})$,

$$\nabla \Psi_0 \cdot \nabla p_0 = \frac{\partial p_o}{\partial x_1}\frac{\partial \Psi_o}{\partial x_1} + \frac{\partial p_o}{\partial x_2}\frac{\partial \Psi_o}{\partial x_2} = 0.$$

In the streamline-pressure coordinate system, the second term $\mathrm{div}(a(x)\nabla p)$ in (4.1) is changed to

$$\mathrm{div}(a(x)\nabla p) = \sqrt{det(g)}\left(\frac{\partial}{\partial \Psi}\left(\frac{|\nabla \Psi|^2}{|\nabla p|^2}\frac{\partial \nabla p}{\partial \Psi}\right) + \frac{\partial^2 \nabla p}{\partial p^2}\right), \tag{4.2}$$

where g is the associated Euclidean metric tensor [8]. It is also mentioned in [8] that

$$a(x) = \frac{|\nabla \Psi|}{|\nabla p|}.$$

Then the equation (4.1) becomes (taking (4.2) into account)

$$D_t\, p = \frac{|v|^2}{a(x)} \left(\frac{\partial}{\partial \eta} (a(x))^2 \frac{\partial p}{\partial \eta} + \frac{\partial^2 p}{\partial \zeta^2} \right).$$

Under some assumptions, we justify rigorously the formal asymptotic expansion

$$p(\eta, \zeta, t) = p_0(\zeta, t) + \delta p_1(\eta, \zeta, t) + \cdots,$$

which implies that the pressure mainly depends on ζ. Now let us consider the following equation

$$D_t\, p = g(\eta, \zeta) \left(\frac{\partial}{\partial \eta} h(\eta, \zeta) \frac{\partial p}{\partial \eta} + \frac{\partial^2 p}{\partial \zeta^2} \right), \tag{4.3}$$

where g is positive in the domain Ω. Since the channel has high permeability, the flow will change in the channel rapidly. And hence we use the time scaling $\tau = \frac{t}{\delta}$ and define the function q by $g = \frac{1}{\delta} q$. Then the equation (4.3) is changed to

$$D_\tau\, p = q(\eta, \zeta) \left(\frac{\partial}{\partial \eta} h(\eta, \zeta) \frac{\partial p}{\partial \eta} + \frac{\partial^2 p}{\partial \zeta^2} \right), \tag{4.4}$$

And we perform formal expansion for pressure p and the function q:

$$\begin{aligned} q(\eta, \zeta) &= q_0(\zeta) + q_1(\eta, \zeta) \\ p(\eta, \zeta, t) &= p_0(\zeta, t) + p_1(\eta, \zeta, t), \end{aligned} \tag{4.5}$$

where p_0 is the solution of the equation

$$D_t\, p_0 = q_0 \frac{\partial^2 p_0}{\partial \zeta^2}, \tag{4.6}$$

imposing the same boundary conditions and initial condition with p, and $q_0(\zeta)$ is computed by the average of $q(\eta, \zeta)$ over each vertical line in the domain Ω. In addition,

we assume that $\frac{\partial^2 p_0}{\partial \zeta^2}$ is bounded in $L^\infty(\Omega)$. Plugging those into (4.4), we have

$$D_\tau(p_0+p_1) = (q_0+q_1)\left(\frac{\partial}{\partial\eta}h(\eta,\zeta)\frac{\partial(p_0+p_1)}{\partial\eta} + \frac{\partial^2(p_0+p_1)}{\partial\zeta^2}\right).$$

After simple computations we get

$$D_\tau\, p_0 + D_\tau\, p_1 = q(\eta,\zeta)\frac{\partial}{\partial\eta}h(\eta,\zeta)\frac{\partial p_1}{\partial\eta} + q_0(\zeta)\frac{\partial^2 p_0}{\partial\zeta^2} + q_1(\eta,\zeta)\frac{\partial^2 p_0}{\partial\zeta^2} + q(\eta,\zeta)\frac{\partial^2 p_1}{\partial\zeta^2}.$$

Taking into account (4.6) in the above equation produces the equation for p_1:

$$D_\tau\, p_1 - q(\eta,\zeta)\frac{\partial}{\partial\eta}h(\eta,\zeta)\frac{\partial p_1}{\partial\eta} - q(\eta,\zeta)\frac{\partial^2 p_1}{\partial\zeta^2} = q_1(\eta,\zeta)\frac{\partial^2 p_0}{\partial\zeta^2}. \tag{4.7}$$

Now we consider the simplest layered case such that the boundary of the channel is parallel to the boundary of the domain Ω and the permeability of each region is constant. Then the functions q and h depend on η only, and the equation (4.7) becomes

$$D_\tau\, p_1 - q(\eta)\frac{\partial}{\partial\eta}h(\eta)\frac{\partial p_1}{\partial\eta} - q(\eta)\frac{\partial^2 p_1}{\partial\zeta^2} = q_1(\eta)\frac{\partial^2 p_0}{\partial\zeta^2}. \tag{4.8}$$

Integrating (4.8) after multiplying by p_1 makes

$$\frac{1}{2}D_\tau\int_\Omega p_1^2 - \int_\Omega q(\eta)\frac{\partial}{\partial\eta}h(\eta)\frac{\partial p_1}{\partial\eta}p_1 - \int_\Omega q(\eta)\frac{\partial^2 p_1}{\partial\zeta^2}p_1 = \int_\Omega q_1(\eta)\frac{\partial^2 p_0}{\partial\zeta^2}p_1,$$

$$\frac{1}{2}D_\tau\,\|p_1\|^2_{L^2(\Omega)} - \int_\Omega q(\eta)\frac{\partial}{\partial\eta}h(\eta)\frac{\partial p_1}{\partial\eta}p_1 - \int_\Omega q(\eta)\frac{\partial^2 p_1}{\partial\zeta^2}p_1 = \int_\Omega q_1(\eta)\frac{\partial^2 p_0}{\partial\zeta^2}p_1. \tag{4.9}$$

Integration by parts on the third term in the left hand side gives us

$$\begin{aligned}
-\int_\eta\int_\zeta q(\eta)\,p_1\frac{\partial^2 p_1}{\partial\zeta^2}d\zeta d\eta &= -\int_\eta q(\eta)\int_\zeta p_1\frac{\partial^2 p_1}{\partial\zeta^2}d\zeta d\eta \\
&= -\int_\eta q(\eta)\int_{\partial\zeta} p_1\frac{\partial p_1}{\partial\zeta}ds d\eta + \int_\eta q(\eta)\int_\zeta \frac{\partial p_1}{\partial\zeta}\frac{\partial p_1}{\partial\zeta}d\zeta d\eta \\
&= \int_\eta q(\eta)\int_\zeta \frac{\partial p_1}{\partial\zeta}\frac{\partial p_1}{\partial\zeta}d\zeta d\eta,
\end{aligned}$$

which is positive. In order to compute the second term in (4.9), let us divide the

domain Ω into three parts in the streamline-pressure coordinate system: let Ω_1 denote the subdomain which is corresponding to the inside of the channel, and let Ω_2 and Ω_3 denote the subdomains corresponding to each of the outside of the channel. Since q and h are constant on each subdomain, we have

$$\begin{aligned} & -\int_\Omega q(\eta)\, p_1 \frac{\partial}{\partial \eta} h(\eta) \frac{\partial p_1}{\partial \eta} d\eta d\zeta \\ = & -\int_{\Omega_1} p_1 \frac{\partial}{\partial \eta} \frac{\partial p_1}{\partial \eta} d\eta d\zeta - \int_{\Omega_2 \cup \Omega_3} \delta\, p_1 \frac{\partial}{\partial \eta} \delta^2 \frac{\partial p_1}{\partial \eta} d\eta d\zeta \\ = & -\int_{\Omega_1} \frac{\partial^2 p_1}{\partial \eta^2} p_1 d\eta d\zeta - \delta^3 \int_{\Omega_2} \frac{\partial^2 p_1}{\partial \eta^2} p_1 d\eta d\zeta - \delta^3 \int_{\Omega_3} \frac{\partial^2 p_1}{\partial \eta^2} p_1 d\eta d\zeta. \end{aligned} \tag{4.10}$$

After integrating each of those by parts (4.10) becomes

$$\begin{aligned} & -\int_{e_2} \frac{\partial p_1}{\partial \eta} p_1 d\eta + \int_{e_3} \frac{\partial p_1}{\partial \eta} p_1 d\eta + \int_{\Omega_1} \frac{\partial p_1}{\partial \eta} \frac{\partial p_1}{\partial \eta} d\eta d\zeta \\ & +\delta^3 \left(-\int_{e_1} \frac{\partial p_1}{\partial \eta} p_1 d\eta + \int_{e_2} \frac{\partial p_1}{\partial \eta} p_1 d\eta + \int_{\Omega_1} \frac{\partial p_1}{\partial \eta} \frac{\partial p_1}{\partial \eta} d\eta d\zeta \right) \\ & +\delta^3 \left(-\int_{e_3} \frac{\partial p_1}{\partial \eta} p_1 d\eta + \int_{e_4} \frac{\partial p_1}{\partial \eta} p_1 d\eta + \int_{\Omega_1} \frac{\partial p_1}{\partial \eta} \frac{\partial p_1}{\partial \eta} d\eta d\zeta \right) \\ = & \int_{\Omega_1} \frac{\partial p_1}{\partial \eta} \frac{\partial p_1}{\partial \eta} d\eta d\zeta + \delta^3 \int_{\Omega_2} \frac{\partial p_1}{\partial \eta} \frac{\partial p_1}{\partial \eta} d\eta d\zeta + \delta^3 \int_{\Omega_3} \frac{\partial p_1}{\partial \eta} \frac{\partial p_1}{\partial \eta} d\eta d\zeta, \end{aligned}$$

due to the boundary conditions for p_1 and the symmetricity of p_1 over the domain Ω. And hence the second term in (4.9) is also positive. Thus we have the following inequality:

$$\frac{1}{2} D_\tau \left\| p_1 \right\|^2_{L^2(\Omega)} \leq \int_\Omega |q_1(\eta)|\, |p_1| \left| \frac{\partial^2 p_0}{\partial \zeta^2} \right| d\eta d\zeta.$$

By the assumption for the $\frac{\partial^2 p_0}{\partial \zeta^2}$ and the Cauchy inequality we get

$$\begin{aligned} D_\tau \left\| p_1 \right\|^2_{L^2(\Omega)} & \leq C \int_\Omega |q_1(\eta)|\, |p_1| d\eta d\zeta \\ & \leq C\gamma \int_\Omega |p_1|^2 d\eta d\zeta + \frac{C}{4\gamma} \int_\Omega |q_1(\eta)|^2 d\eta d\zeta \\ & = C\gamma \left\| p_1 \right\|^2_{L^2(\Omega)} + \frac{C}{4\gamma} \int_\Omega |q_1(\eta)|^2 d\eta d\zeta. \end{aligned} \tag{4.11}$$

Now let $\alpha(\tau) := \|p_1\|^2_{L^2(\Omega)}$ and $\beta(\tau) := \|q_1\|^2_{L^2(\Omega)} = \int_\Omega |q_1(\eta)|^2 d\eta d\zeta$. Then (4.11) implies

$$\alpha(\tau) \le C\gamma\, \alpha(\tau) + \frac{C}{4\gamma}\beta(\tau),$$

for a.e. $0 \le \tau \le T$. Therefore the differential form of Gronwall's inequality (see, e.g., [13]) gives us the estimate

$$\alpha(\tau) \le e^{C\gamma\,\tau}\left(\alpha(0) + \frac{C}{4\gamma}\int_0^\tau \beta(s)ds\right) \qquad (0 \le \tau \le T).$$

Since $\alpha(0) = \|p_1(0)\|^2_{L^2(\Omega)} = 0$, we obtain the estimate

$$\max_{0\le\tau\le T} \|p_1\|^2_{L^2(\Omega)} \le C\int_0^T\!\!\int_\Omega |q_1|^2 d\eta d\zeta d\tau = O(\delta).$$

Thus we can say that p_1 is of order δ in $L^\infty(0,T;L^2(\Omega))$.

On the other hands, integrating (4.8) after multiplying by p_1 produces

$$\int_0^T\!\!\int_\Omega \frac{1}{2}D_\tau p_1^2 - \int_0^T\!\!\int_\Omega q(\eta)\frac{\partial}{\partial\eta}h(\eta)\frac{\partial p_1}{\partial\eta}p_1 - \int_0^T\!\!\int_\Omega q(\eta)\frac{\partial^2 p_1}{\partial\zeta^2}p_1 = \int_0^T\!\!\int_\Omega q_1(\eta)\frac{\partial^2 p_0}{\partial\zeta^2}p_1.$$

From the initial condition for p_0 we have

$$\int_\Omega \frac{1}{2}|p_1(\eta,\zeta,T)|^2 - \int_0^T\!\!\int_\Omega q(\eta)\frac{\partial}{\partial\eta}h(\eta)\frac{\partial p_1}{\partial\eta}p_1 - \int_0^T\!\!\int_\Omega q(\eta)\frac{\partial^2 p_1}{\partial\zeta^2}p_1 = \int_0^T\!\!\int_\Omega q_1(\eta)\frac{\partial^2 p_0}{\partial\zeta^2}p_1. \tag{4.12}$$

Integration by parts on the second and third terms in the left hand side gives us

$$\begin{aligned}
& -\int_0^T\int_\Omega q(\eta)\frac{\partial}{\partial\eta}h(\eta)\frac{\partial p_1}{\partial\eta}p_1 + q(\eta)\frac{\partial^2 p_1}{\partial\zeta^2}p_1 \\
= & -\int_0^T\int_{\Omega_1}\left(\frac{\partial}{\partial\eta}h(\eta)\frac{\partial p_1}{\partial\eta}p_1 + \frac{\partial^2 p_1}{\partial\zeta^2}p_1\right) - \delta\int_0^T\int_{\Omega_2\cup\Omega_3}\left(\frac{\partial}{\partial\eta}h(\eta)\frac{\partial p_1}{\partial\eta}p_1 + \frac{\partial^2 p_1}{\partial\zeta^2}p_1\right) \\
= & -\int_0^T\int_{e_2} h(\eta)\frac{\partial p_1}{\partial\eta}p_1 d\eta + \int_0^T\int_{e_3} h(\eta)\frac{\partial p_1}{\partial\eta}p_1 d\eta + \int_0^T\int_{\Omega_1} h(\eta)\left|\frac{\partial p_1}{\partial\eta}\right|^2 + \left|\frac{\partial p_1}{\partial\eta}\right|^2 \\
& +\delta\left(-\int_0^T\int_{e_1} h(\eta)\frac{\partial p_1}{\partial\eta}p_1 d\eta + \int_0^T\int_{e_2} h(\eta)\frac{\partial p_1}{\partial\eta}p_1 d\eta + \int_0^T\int_{\Omega_2} h(\eta)\left|\frac{\partial p_1}{\partial\eta}\right|^2 + \left|\frac{\partial p_1}{\partial\eta}\right|^2\right) \\
& +\delta\left(-\int_0^T\int_{e_3} h(\eta)\frac{\partial p_1}{\partial\eta}p_1 d\eta + \int_0^T\int_{e_4} h(\eta)\frac{\partial p_1}{\partial\eta}p_1 d\eta + \int_0^T\int_{\Omega_3} h(\eta)\left|\frac{\partial p_1}{\partial\eta}\right|^2 + \left|\frac{\partial p_1}{\partial\eta}\right|^2\right).
\end{aligned}$$

Because of the boundary conditions for p_1 and the symmetricity of p_1 over the domain Ω, we get

$$\begin{aligned}
& -\int_0^T\int_\Omega q(\eta)\frac{\partial}{\partial\eta}h(\eta)\frac{\partial p_1}{\partial\eta}p_1 + q(\eta)\frac{\partial^2 p_1}{\partial\zeta^2}p_1 \\
= & \int_0^T\int_{\Omega_1} h(\eta)\left|\frac{\partial p_1}{\partial\eta}\right|^2 + \left|\frac{\partial p_1}{\partial\eta}\right|^2 + \delta\int_0^T\int_{\Omega_2} h(\eta)\left|\frac{\partial p_1}{\partial\eta}\right|^2 + \left|\frac{\partial p_1}{\partial\eta}\right|^2 + \delta\int_0^T\int_{\Omega_3} h(\eta)\left|\frac{\partial p_1}{\partial\eta}\right|^2 + \left|\frac{\partial p_1}{\partial\eta}\right|^2,
\end{aligned}$$

which is exactly the same as the energy norm $\|p_1\|_E^2$ for this problem. Since the first term in (4.12) is non-negative, we obtain the following inequality:

$$\|p_1\|_E^2 \le \int_0^T\int_\Omega |q_1(\eta)||p_1|\left|\frac{\partial^2 p_0}{\partial\zeta^2}\right| d\eta d\zeta d\tau.$$

By the assumption for the $\frac{\partial^2 p_0}{\partial\zeta^2}$ and the Cauchy inequality we get

$$\begin{aligned}
\|p_1\|_E^2 &\le C\int_0^T\int_\Omega |q_1(\eta)|\,|p_1| d\eta d\zeta d\tau \\
&\le C\int_0^T\int_\Omega |p_1|^2 d\eta d\zeta d\tau + C\int_0^T\int_\Omega |q_1(\eta)|^2 d\eta d\zeta d\tau \le C\delta.
\end{aligned}$$

CHAPTER V

CONCLUSIONS AND FUTURE WORK

In the dissertation, we consider multiscale numerical methods for 3 parabolic equations. In all cases, the parabolic equations have some small scale involved and our goal is to design and study numerical methods which can capture the effects of the small scales locally.

In the first case, we consider multiscale numerical methods for nonlinear parabolic equations where the coefficients have both spatial and temporal heterogeneities. Our numerical methods are based on previously developed numerical homogenization techniques. The main goal of this approach is to find the coarse-scale solution via the solutions of the local problems. In this dissertation, we study nonlinear periodic problems with periodic heterogeneities. The novelty of my work is in providing quantitive estimates for the convergence of the correctors for monotone operators as well as the quantitative estimates for some parts of the truncation error presented in (2.26). These error estimates show that numerical homogenization methods suffer from the resonance errors. Our analysis reveals the sources for these resonance errors. In particular, we show that the first resonance error is due to linear boundary conditions which are imposed on local problems. Because the actual solution does not vary linearly on a coarse grid level, the linear boundary conditions result in a mismatch between the solution and the local problems. The second resonance error is due to the fact that the period does not contain integer number of periods. In future work, we would like to extend these results to almost periodic and stochastic cases. In these cases, the resonance errors are known only for linear problems.

In the second case, we consider singularly perturbed parabolic equations and are interested in the computation of effective diffusion coefficients. The effective diffusion

coefficients are computed via the solution of the local elliptic problem. This elliptic problem is a convection-diffusion equation with very small diffusion. Our goal is to approximate the solution of the convection-diffusion equation as the diffusion coefficient approaches to zero. We are interested when the fluid velocity has cellular nature which often occurs in turbulent flows. In this case, the solution can be approximated by the solution of one dimensional coupled parabolic equations on the graph and the solution away from separatrices of the flow is constant. In the dissertation, we study several methods for finding an approximate solution of the nearly degenerate convection-diffusion equation. One of the difficulties is in designing numerical approaches which can approximate the constant states of the solution, which occur away from separatrices. We study spectral and finite difference methods on exponential grids. We find that finite difference methods are easy to implement and provides accurate solutions while spectral methods have difficulties finding the constant states without major reformulation. In future, we would like to provide an error analysis and present numerical results for more general flows with a large number of cells.

In the third case, we study a special problem where linear parabolic equations with high contrast coefficients are studied. In this problem, our goal is to show that the solution smoothly depends on the steady state solution under some assumptions. Our methods use special coordinate system and employ asymptotic analysis with respect to high contrast. Our results show that the solution is smooth function of the steady state. These results are used in numerical convergence results [21]. In future, we would like extend these results to compressible two-phase flow which consists of both elliptic and hyperbolic equations.

REFERENCES

[1] P. B. Bochev, M. D. Gunzburger, and J. N. Shadid, *Stability of the supg finite element method for transient advection-diffusion problems*, Comput. Methods Appl. Mech. Engrg., 193 (2004), pp. 2301–2323.

[2] D. Braess, *Finite elements*, Cambridge University Press, Cambridge, 2001.

[3] A. Cangiani and E. Süli, *Enhanced residual-free bubble method for convection-diffusion problems*, Int. J. Numer. Meth. Fluids, 47 (2005), pp. 1307–1313.

[4] S. Childress, *Alpha-effect in flux ropes and sheets*, Phys. Earth Planet Int., 20 (1979), pp. 172–180.

[5] J. Choi, D. Margetis, T. M. Squires, and M. Z. Bazant, *Steady advection-diffusion around finite absorbers in two-dimensional potential flows*, J. Fluid Mech., 536 (2005), pp. 155–184.

[6] J. Cronin and R. E. O'Malley Jr., *Analyzing multiscale phenomena using singular perturbation methods : American Mathematical Society short course, January 5-6, 1998, Baltimore, Maryland.*, American Mathematical Society, Providence, 1999.

[7] G. Dal Maso and A. Defranceschi, *Correctors for the homogenization of monotone operators*, Differential Integral Equations, 3 (1990), pp. 1151–1166.

[8] Y. Efendiev, V. Ginting, T. Hou, and R. Ewing, *Accurate multiscale finite element methods for two-phase flow simulations*, J. Comput. Phys., 220 (2006), pp. 155–174.

[9] Y. Efendiev, T. Hou, and V. Ginting, *Multiscale finite element methods for nonlinear problems and their applications*, Commun. Math. Sci., 2 (2004), pp. 553–589.

[10] Y. Efendiev and A. Pankov, *Numerical homogenization of nonlinear random parabolic operators*, Multiscale Model. Simul., 2 (2004), pp. 237–268.

[11] ——, *Homogenization of nonlinear random parabolic operators*, Adv. Differential Equations, 10 (2005), pp. 1235–1260.

[12] Y. Efendiev and A. Pankov, *Meyers type estimates for approximate solutions of nonlinear parabolic equations and their applications*, J. Numer. Math., 13 (2005), pp. 105–118.

[13] L. C. Evans, *Partial differential equations*, American Mathematical Society, Providence, 1998.

[14] R. Eymard, T. Gallouët, and R. Herbin, *Finite volume methods*, vol. VII of Handbook of Numerical Analysis, North-Holland, Amsterdam, 2000, pp. 713–1020.

[15] A. Fannjiang and G. Papanicolaou, *Convection enhanced diffusion for periodic flows*, SIAM J. Appl. Math., 54 (1994), pp. 333–408.

[16] ——, *Convection-enhanced diffusion for random flows*, J. Statist. Phys., 88 (1997), pp. 1033–1076.

[17] D. Funaro, *A new scheme for the approximation of advection-diffusion equations by collocation*, SIAM J. Numer. Anal., 30 (1993), pp. 1664–1676.

[18] D. Funaro and O. Kavian, *Approximation of some diffusion evolution equations in unbounded domains by Hermite functions*, Math. Comp., 57 (1991), pp. 597–619.

[19] S. Heinze, *Diffusion-advection in cellular flows with large Péclet numbers*, Arch. Ration. Mech. Anal., 168 (2003), pp. 329–342.

[20] T. Y. Hou and X. H. Wu, *A multiscale finite element method for elliptic problems in composite materials and porous media*, J. Comput. Phys., 134 (1997), pp. 169–189.

[21] L. Jiang, Y. Efendiev, and V. Ginting, *Multiscale methods for parabolic equations with continuum spatial scales*, Discrete Contin. Dyn. Syst. Ser. B, 8 (2007), pp. 833–859.

[22] V. V. Jikov, S. M. Kozlov, and O. A. Oleinik, *Homogenization of differential operators and integral functionals*, Springer-Verlag, New York, 1994.

[23] L. Koralov, *Random perturbations of 2-dimensional hamiltonian flows*, Probab. Theory Related Fields, 129 (2004), pp. 37–62.

[24] A. Novikov, G. Papanicolaou, and L. Ryzhik, *Boundary layers for cellular flows at high Péclet numbers*, Comm. Pure Appl. Math., 58 (2005), pp. 867–922.

[25] F. Padilla, Y. Secretan, and M. Leclerc, *On open boundaries in the finite element approximation of two-dimensional advection-diffusion flows*, Internat. J. Numer. Methods Engrg., 40 (1997), pp. 2493–2516.

[26] A. Pankov, *G-convergence and homogenization of nonlinear partial differential operators*, Kluwer Academic Publishers, Dordrecht, 1997.

[27] M. N. Rosenbluth, H. L. Berk, I. Doxas, and W. Horton, *Effective diffusion in laminar convective flows*, Phys. Fluids, 30 (1987), pp. 2636–2647.

[28] J. Shen, *Stable and efficient spectral methods in unbounded domains using Laguerre functions*, SIAM J. Numer. Anal., 38 (2000), pp. 1113–1133.

[29] R. E. Showalter, *Monotone operators in Banach space and nonlinear partial differential equations*, American Mathematical Society, Providence, 1997.

[30] B. I. Shraiman, *Diffusive transport in a rayleigh-bénard convection cell*, Phys. Rev. A, 36 (1987), pp. 261–267.

[31] N. Svanstedt, *Correctors for the homogenization of monotone parabolic operators*, J. Nonlinear Math. Phys., 7 (2000), pp. 268–283.

VITA

Dukjin Nam was born in Seoul, Republic of Korea. He received his B.S. degree in mathematics from Hanyang University in Seoul, Korea in 1997. He received his M.S. degree in mathematics from the same university in 1999. He started his Ph.D. degree at Texas A&M University in September 2000 and received it in the area of numerical analysis in August 2008. He can be reached at: Department of Mathematics, Texas A&M University, College Station, TX 77843-3368. e-mail: dnam@math.tamu.edu.

The typist for this dissertation was Dukjin Nam.